TECHNISCHE UNIVERSITÄT WIEN

DISSERTATION

Synthesis and Reactivity of Nickel, Cobalt, and Molybdenum PCP Pincer Complexes

Ausgeführt zum Zwecke der Erlangung des akademischen Grades eines Doktors der technischen Naturwissenschaften unter der Leitung von

Prof. Dr. Karl Kirchner

Institut für Angewandte Synthesechemie

eingereicht an der Technischen Universität Wien

von

Sathiyamoorthy Murugesan M.Sc.

Matr. Nr. 1228756

Geboren am 17 März 1988 in Kadukkathurai, Manachanallur, Trichy, India

Datum   Unterschrift

Murugesan, Sathiyamoorthy

Title: Synthesis and Reactivity of Nickel, Cobalt, and Molybdenum PCP Pincer Complexes

Institute of Applied Synthetic Chemistry, Technical University of Vienna, Austria.

This Ph.D. thesis work was carried out at the Organometallic Chemistry and Homogeneous Catalysis Group, Institute of Applied Synthetic Chemistry, Vienna University of Technology, Vienna, Austria.

Contents

Aim and scope of this Thesis

In the literature reports on base metals bearing PCP ligands are very rare, only nickel, iron, cobalt and molybdenum PCP complexes were described. The objective of this thesis is to develop novel pincer complexes based on the non-precious transition-metals nickel, cobalt and molybdenum featuring anionic PCP pincer ligands. We focus on synthesis, structural characterization, and reactivity studies.

$$M = Ni, Co \text{ and } Mo$$
$$R = H, Me$$
$$PR_2 = PiPr_2, PtBu_2$$
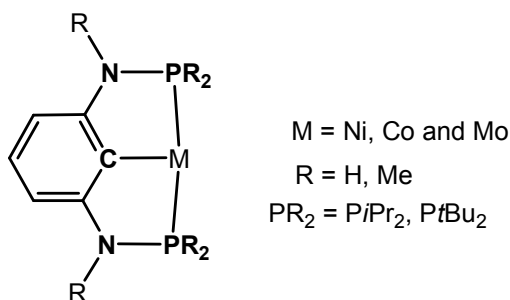
First we focus on the synthesis and characterization of PCP ligands based on the 1,3-diaminobenzene scaffold, which can be utilized in simple way to alter base metal pincer complexes starting from inexpensive base metal precursors. Pincer complexes will be useful for the activation of small molecules such as CO, CO_2, O_2, H_2, or N_2. In this respect we will gain insight into of fundamental organometallic reaction mechanism such as oxidation, reduction, oxidative addition, reductive elimination, non-oxidative addition, non-reductive elimination and ligand exchange processes. Most of the new compounds will be characterized by a combination of X-ray, NMR, IR, ESI MS, elemental analysis and magnetic measurements. These studies underline that the combination of cheap and abundant metals such as nickel and cobalt with PCP pincer ligands may result in the development of novel, versatile, and efficient catalysts for atom-efficient catalytic reactions. In **chapter 1**, In general development of nickel, cobalt and molybdenum metal complexes with PCP pincer ligands and their reactivities in order to understand that how non-precious metals is bearing with pincer PCP ligands. Within this context, we gained new ideas for further developments of base metal PCP pincer complexes. In **chapter 2**, a new PCP ligand is designed which is suitable to react with cobalt and nickel precursor forming new four coordinate PCP cobalt and nickel pincer complexes. These are further explored in terms of unique chemical properties. Some of the cobalt pincer complexes are compared with analogous of nickel pincer complexes in terms of structure and reactivity also with the aid of density functional theory. In **chapter 3**, a novel synthetic protocol is developed for the formation of cobalt PCP pincer borohydride complexes, which are compared with analogous nickel PCP pincer borohydride complex. A new synthetic protocol is established for the preparation of Co(I) PCP *bis*-carbonyl and *bis* CNtBu complexes from the reaction of Co(II) borohydride complex with CO ligand, and CNtBu, respectively. In **chapter 4**, the reactivity difference between the strong π-accepting, but weak σ-donor carbonyl ligand is compared with the strong π-acceptor and σ-donor CNtBu. An unusual transformation is described leading to the formation of a cobalt compex with an

agostic C-H arene bond. Finally, in **Chapter 5**, novel molybdenum pincer complexes are synthesized from molybdenum precursors $Mo(Br)_3(thf)_3$ and $[Mo(Br)_2(CO)_4]_2$.

Non-Precious Metal (Ni, Co and Mo) Complexes with an Aromatic Anionic PCP Architecture

This chapter provides an overview of the advancements in the field of non-precious metal (Ni, Co and Mo) complexes featuring anionic PCP pincer ligands where the (CH$_2$, O and NH) linkers between aromatic ring and phosphine moieties. While the research in nickel PCP complexes is already quite extensive, the chemistry of cobalt and molybdenum PCP complexes is comparatively sparse. In the case of nickel PCP complexes already many catalytic applications such as Suzuki–Miyaura coupling, C-S cross coupling, Michael additions, Alcoholysis of acrylonitrile, hydrosilylation of aldehyde and cyanomethylation of aldehydes were reported. Cobalt and molybdenum PCP complexes were not applied to any catalytic reactions. Surprisingly, only one molybdenum PCP complex is reported, which was capable of cleaving dinitrogen to give a nitride complex. This chapter underlines that the combination of cheap and abundant metals such as nickel, cobalt and molybdenum with PCP pincer ligands may result in the development of novel, versatile, and efficient catalysts for atom-efficient catalytic reactions.

1.1 Introduction

Transition metal complexes are indispensable tools for every chemist engaged in synthesis. Ideally, any metal-mediated catalytic process should be fast, clean, efficient, and selective. These criteria are especially important when one considers that many of the transition metals employed in catalysis are rare and/or expensive. One of the ways of modifying and controlling the properties of transition metal complexes is the use of appropriate ligand systems. Among the many ligand systems that can be found in the chemical literature pincer ligands play an important role and their complexes have attracted tremendous interest due to their high stability, activity and variability.[1,2] These tridentate ligands are often planar scaffolds consisting of an anionic or neutral central aromatic backbone tethered to two, mostly bulky, two-electron donor groups by different spacers. In recent years, pincers with aliphatic backbones have also received considerable attention. In this family of ligands steric, electronic, and also stereochemical parameters can be manipulated by modifications of the substituents at the donor sites and/or the spacers allowing the possibility of a rational and modular design enabling the generation of highly active catalysts for a range of chemical transformations with high selectivity. Most common are still pincer systems with phosphine donors tethered to an aromatic benzene backbone, so called PCP pincer ligands. The first PCP pincer complexes were already synthesized in the mid-1970s by Shaw and co-workers.[3] They prepared PCP pincers with bulky tertiary phosphines which were linked with a CH$_2$ spacer to a deprotonated anionic benzene unit and, in fact, also reported the synthesis of the first nickel PCP pincer complex. However, this area remained comparatively unexplored until in the late 1990s several applications of mostly precious second and third row transition metal pincer complexes in the fields of catalysis, molecular recognition and supramolecular chemistry were discovered turning this area into an intensively investigated subject in organometallic chemistry.

X = CH$_2$, O, NH, NMe
M = Ni, Co and Mo
R = electron withdrawing or donating group
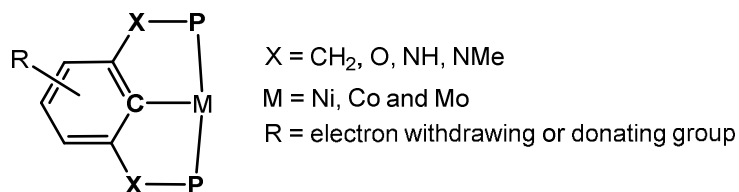
Scheme 1. The aromatic and aliphatic PCP pincer platforms with PCP frameworks connecting the phosphine donors with various linkers X.

This chapter provides an overview of the advancements in the field of non-precious metal pincer complexes featuring anionic PCP pincer ligands with aromatic systems as shown in Scheme 1. An overview of all PCP motifs found in the literature in conjunction with non-precious metals is provided in Chart 1.
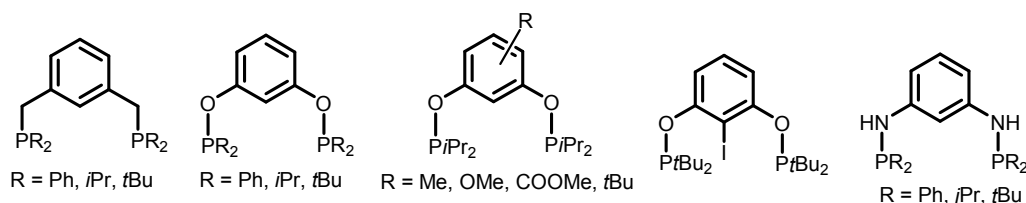

R = Ph, *i*Pr, *t*Bu   R = Ph, *i*Pr, *t*Bu   R = Me, OMe, COOMe, *t*Bu   R = Ph, *i*Pr, *t*Bu

Chart 1 Overview of PCP ligand motifs which are applied to non-precious metals

Kirchner and co-workers synthesized a series of chiral and achiral PCP pincer ligands from the reaction of 1,3-diaminobenzene with phosphine chloride in presence of strong base or week base. These PCP ligands contain amine spacers between aromatic ring and phosphine moieties.[4]
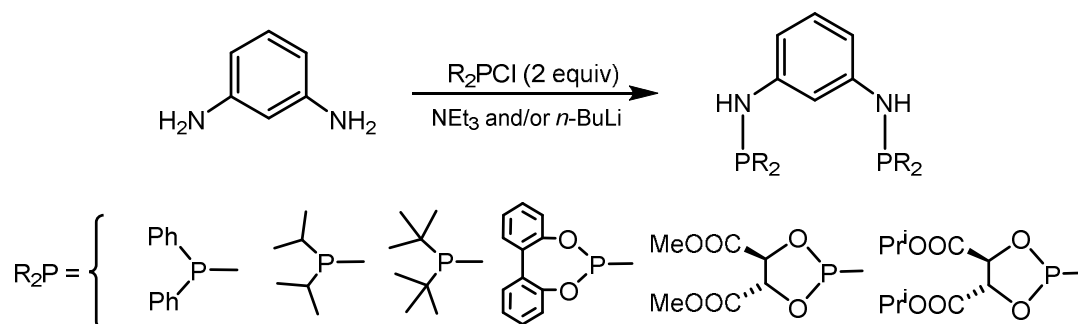
Scheme 2 Synthesis of PCP ligands

1.2 Nickel PCP Pincer Complexes

The first PCP nickel complexes were prepared and characterized by Shaw[3] in 1976. Since then the chemistry of nickel PCP complexes increased significantly particularly in the last decade.[4,5,6,7] Several [Ni(PCsp^2P)(X)] and [Ni(PCsp^3P)(X)] (X= Cl, Br, I) complexes, which are the most common synthetic entries into nickel PCP chemistry, were prepared by treating simple nickel halides with the respective pincer ligands in the presence of base. This led to the synthesis of many new nickel complexes as shown in Chart 2.[3,4,5,6,8,9,10,11,12]
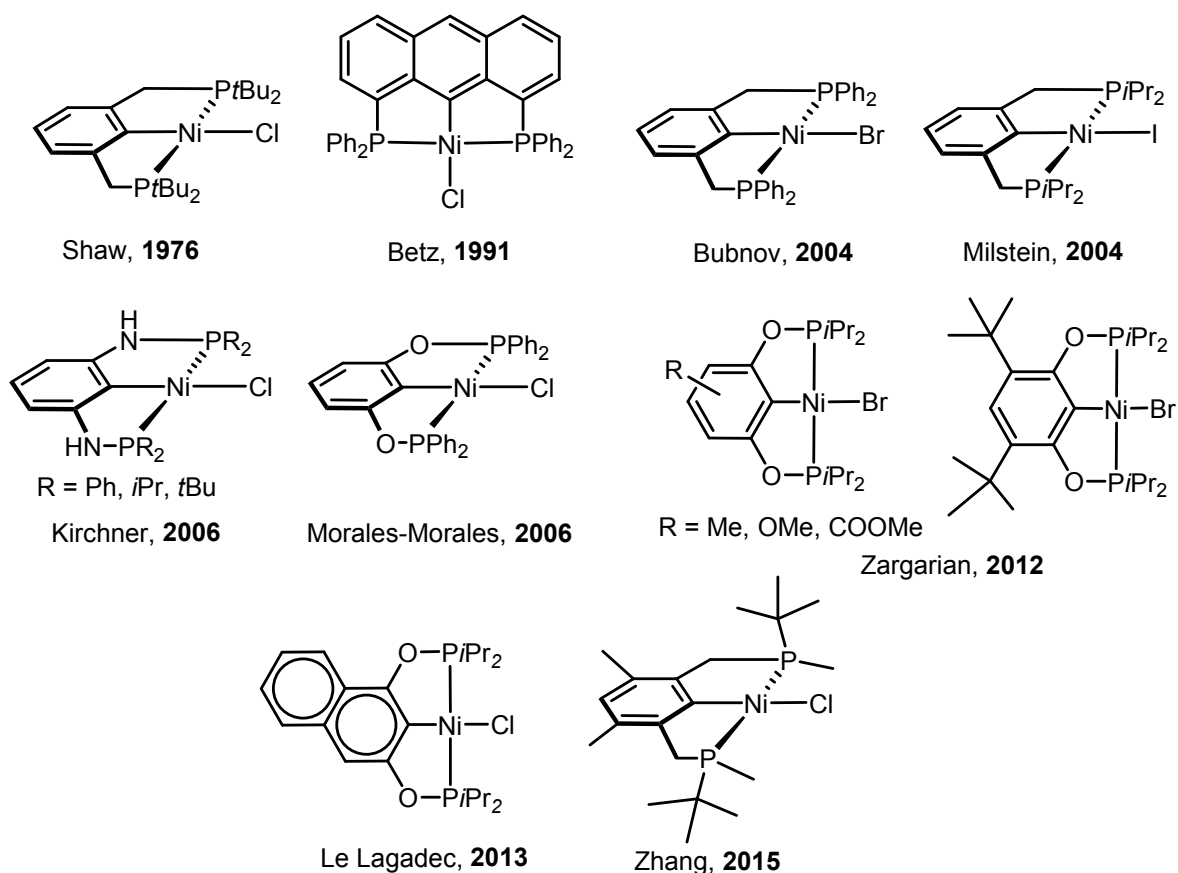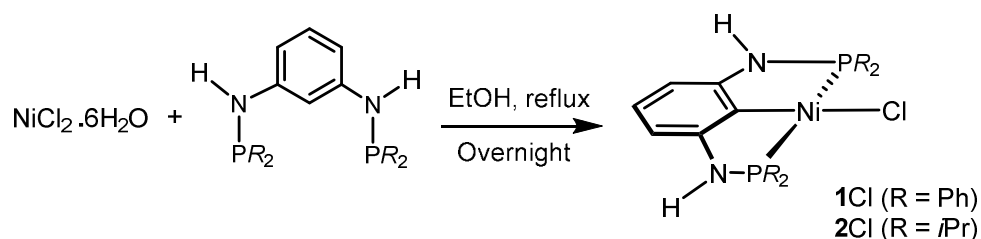

Chart 2 Overview of common Ni(II) PCP pincer precursors

Our research group was reported that the treatment of PCP ligands with hydrated Ni(II) chloride at reflux temperature in ethanol affords Ni(II) PCP pincer complex.[4]

Scheme 3 preparation of Ni(II) PCP complexes

Complex **3**Cl is a very efficient and robust catalyst which exhibits a comparable performance in the Suzuki–Miyaura cross coupling reactions as that of similar Pd(II) pincer systems albeit with longer reaction periods and larger catalytic amounts of catalysts (1.0% Ni *versus* 0.1% Pd). The cross-coupling of different *para*-substituted bromobenzenes with phenylboronic acid produced high yields of the corresponding biphenyl derivatives (Scheme 4).[13] Another attractive characteristic of the present system is the easy synthesis from cheap commercially available starting materials and the use of considerable cheaper and biocompatible Ni(II), thus making this system attractive for its potential application in organic synthesis.
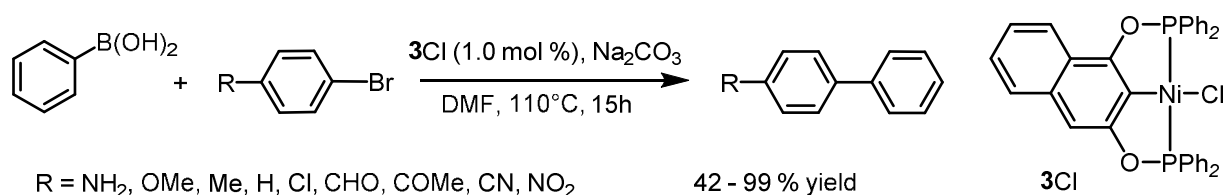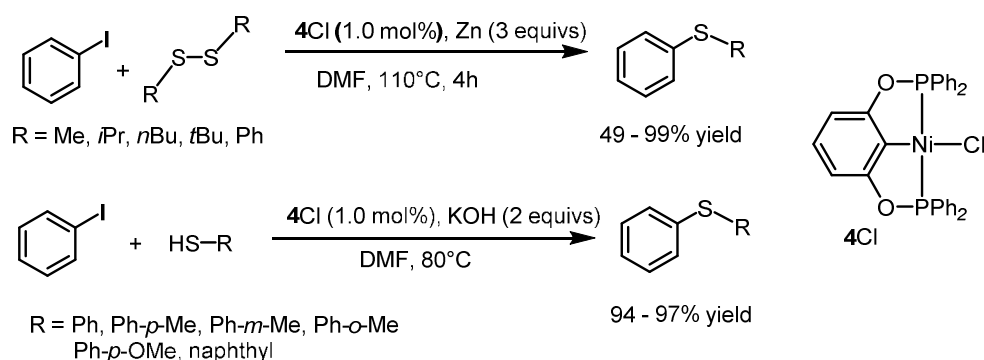

Scheme 4 Synthesis [Ni(PCsp^2P)Cl] (**5**) and its catalytic activity in the Suzuki-Miyaura cross coupling

Interestingly, the closely related complex **4**Cl featuring a benzene rather than a naphthalene backbone reacted with *para*-substituted benzyl bromides in the presence of Zn as reducing agent to afford only homo coupling products (Scheme 5).[14] The scope of the homo coupling reaction was explored with a variety of functionalized benzyl bromides. Excellent GC yields (75 - 99%) were achieved in most cases. Benzylbromides with electron-donating substituents on the phenyl ring tend to offer slightly better yields than those with electron-withdrawing groups. It was proposed that the Ni(II) PCP complex **4**Cl was reduced to a Ni(I) species which promotes C-Br bond cleavage thereby forming a Ni(II) pincer bromide intermediate along with the benzyl radicals, which underwent dimerization to afford homo coupling products.
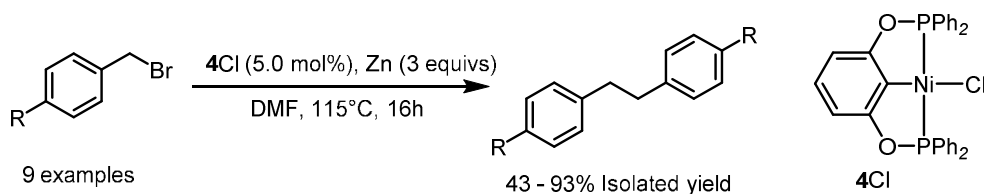
Scheme 5 Homocoupling of *para*-substituted benzylbromides catalyzed by complex **4**Cl

Moreover, complex **4**Cl also efficiently catalyzes the thiolation (C-S cross coupling) of iodobenzene with a broad scope of disulfides in the presence of Zn as reducing agent in DMF at 110°C (Scheme 6).[10] The coupled products were obtained in excellent and, in many cases, nearly quantitative yields. Another interesting direct C-S bond formation was discovered by Guan *et al.*[15] They were able to obtain thioethers in good to excellent yields (49-97%) from the reaction of iodobenzene with different aryl substituted thiols in the presence of **4**Cl (1.0 mol%) and KOH in DMF at 80°C (Scheme 6).


R = Me, *i*Pr, *n*Bu, *t*Bu, Ph

49 - 99% yield

R = Ph, Ph-*p*-Me, Ph-*m*-Me, Ph-*o*-Me
Ph-*p*-OMe, naphthyl

94 - 97% yield

4Cl

Scheme 6 C-S bond forming reactions catalyzed by the Ni(II) PCsp^2P complex **4**Cl

A series of complexes of the type [Ni(PCsp^2P)(L)] containing the 2,6-bis-(diisopropyl-phosphinomethyl)phenyl pincer ligand and simple monoanionic ligands L (L = F, Br, H, Me, Ph, NO$_3$, CF$_3$SO$_3$) were synthesized and characterized. The fluoride derivatives were prepared from bromide complexes (**5**Br) by exchange reactions with AgF or, by protonolysis of the methyl complexes [Ni(PCsp^2P)(Me)] (**6**) with NEt$_3$·3HF affording complex **5**F. Upon treatment of complex **5**Br with MeI halogen exchange took place to yield complex **5**I (Scheme 7).[16]
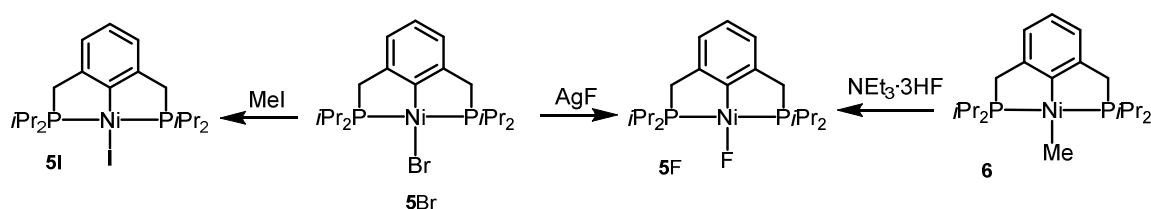
Scheme 7 Formation of halide complexes [Ni(PCsp^2P)(X)] (X = F, Br, I) (**5**F, **5**Br, **5**I)

Transmetalation reactions of the halide complex **5**Br with methyl or phenyllithium also proceeded easily affording the corresponding derivatives [Ni[(PCsp^2P)(R)] (R = Me, Ph) **6** and **7** in good yields. These complexes are thermally stable, and they resist exposure to air for some time in the solid state. However, during one of the attempts to crystallize the nickel methyl complex colorless crystals were isolated. These

were identified as the diphosphine oxide 1-Me-2,6-(iPr$_2$P(O)CH$_2$)$_2$C$_6$H$_3$, where the methyl group saturated the *ipso* position originally bound to nickel, suggesting that the reaction with oxygen induces the reductive coupling of the methyl and the pincer ligand (Scheme 8).[16]
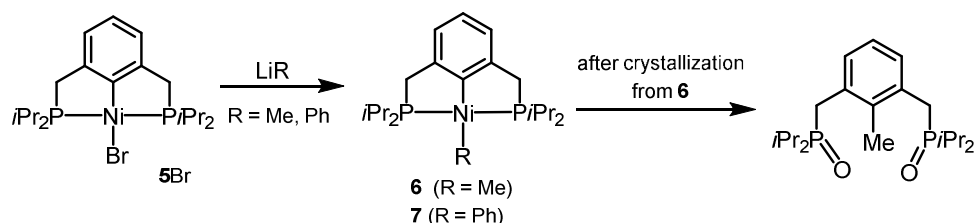
Scheme 8 Synthesis of [Ni(PCsp^2P)(Me)] (**6**) and [Ni(PCsp^2P)(Ph)] (**7**) *via* transmetallation

It is interesting to note that related nickel complexes with PCsp^2P backbones based on the bis-2,6-di-*tert*-butylphosphinomethyl- and bis-2,6-di-*iso*-propylphosphinomethylbenzene scaffolds (**5**Br, **8**Cl) reacted with an excess of sodium amide to afford complexes [Ni(PCsp^2P)(NH$_2$)] (**9**, **10**) (Scheme 9).[16,17,18]
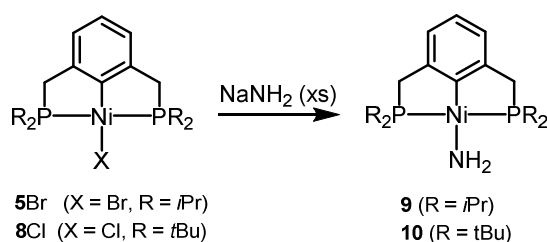
Scheme 9 Synthesis of [Ni(PCsp^2P)(NH$_2$)] complexes **9** and **10**

Complex [Ni(PCsp^2P)(NH$_2$)] (**10**) reacted with several substrates bearing acidic C-H bonds such as phenyl acetylene, imidazole, dimethyl malonate and oxazole to form complexes **11-14**. In the course of this reaction NH$_3$ is liberated (Scheme 10).[18] These complexes are able to insert carbon dioxide into the nickel-ligand bonds, which is a thermodynamically very favorable process. An example is depicted in Scheme 10. This was shown both experimentally and by means of DFT calculations.[18]
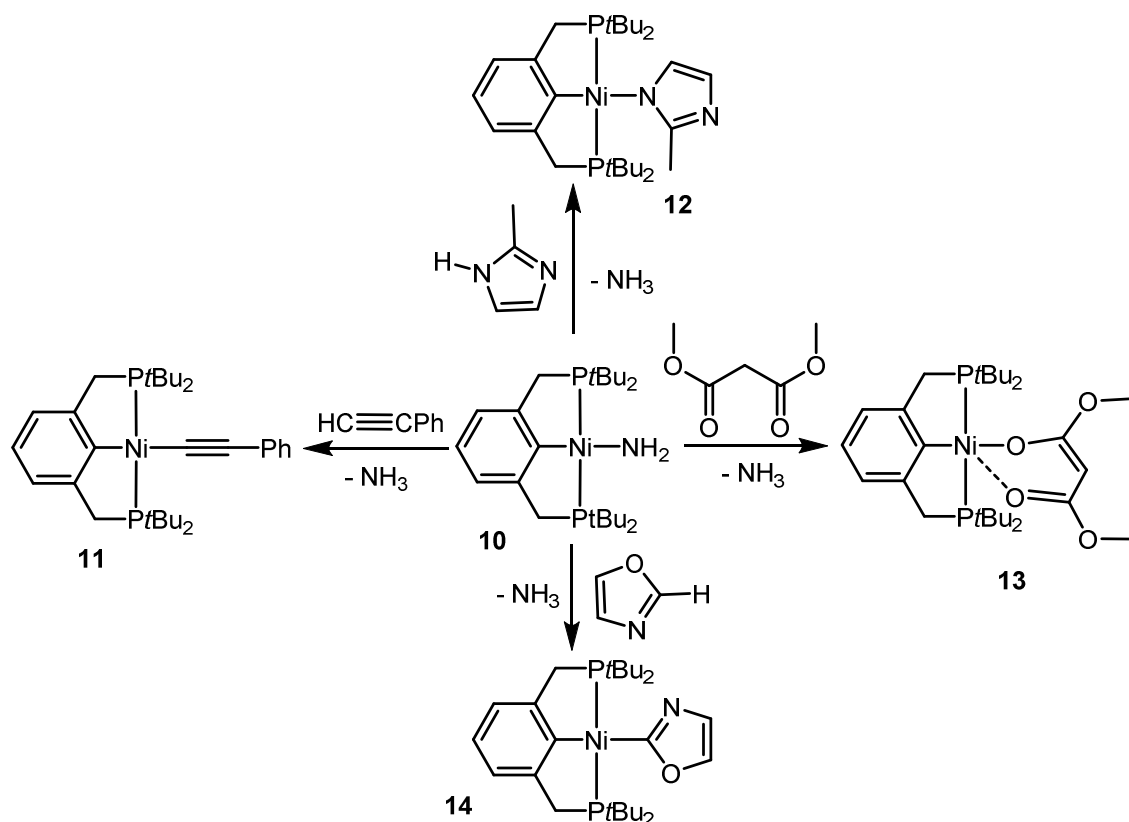
Scheme 10 Liberation of NH_3 gas from [Ni(PCsp^2P)(NH$_2$)] (**10**) upon treatment with C-H and N-H acidic compounds
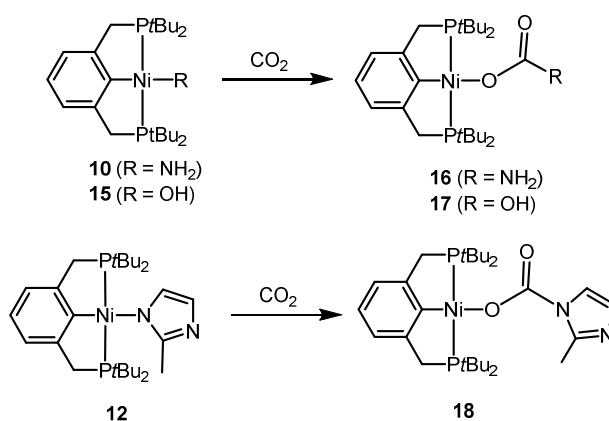
Scheme 11 Carbon dioxide insertion into the nickel-ligand bonds of [Ni(PCsp^2P)] complexes

Complexes **35** and **36** were prepared by reacting complex [Ni(PCsp^2P)(OH)] (**12**) with trimethylsilyl cyanide and trimethylsilyl azide, respectively. These two complexes are also able to insert carbon dioxide into the nickel-ligand bond (Scheme 12).[18] The synthesis of complex **19** was also described in an earlier

report[3] by the reaction of nickel complex **8**Cl with sodium cyanide in acetone. This complex was, however, not fully characterized.
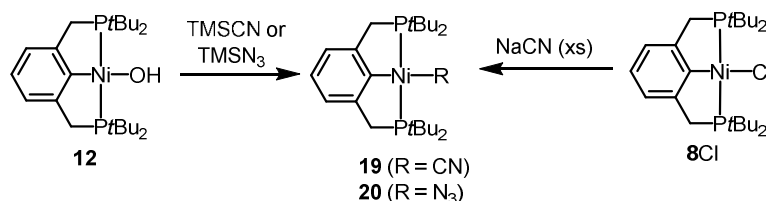
Scheme 12 Synthesis of [Ni(PCsp^2P)(CN)] (**19**) and [Ni(PCsp^2P)(N$_3$)] (**20**)

Guan and co-workers treated Zargarian's complex **21**Cl[7c] with LiCH$_2$CN to obtain the nickel cyanomethyl complex **22** in good isolated yield (Scheme 13).[19] Complex **22** turned out to be an incredibly robust nickel catalyst for the cyanomethylation of aldehydes under base free conditions with unprecedentedly high turnover numbers and frequencies. This was achieved in the presence of merely 0.01 mol % of **22** as catalyst in acetonitrile as solvent (Scheme 14).[19] The reaction was performed at room temperature with a reaction time of 72h. In some cases TONs of 82000 and TOFs of 1139 h^{-1} were achieved. Mechanistic studies suggested reversible insertion of aldehydes into the nickel-carbon bond of the cyanomethyl complex and subsequent C-H bond activation of acetonitrile by the nickel alkoxide intermediate **23**.
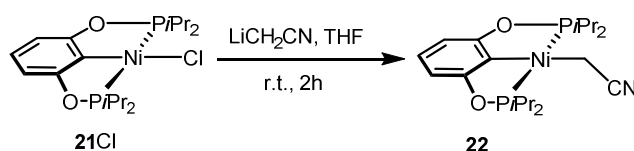
Scheme 13 Synthesis of [Ni(P*C*sp^2P)(CH$_2$CN)] (**22**)
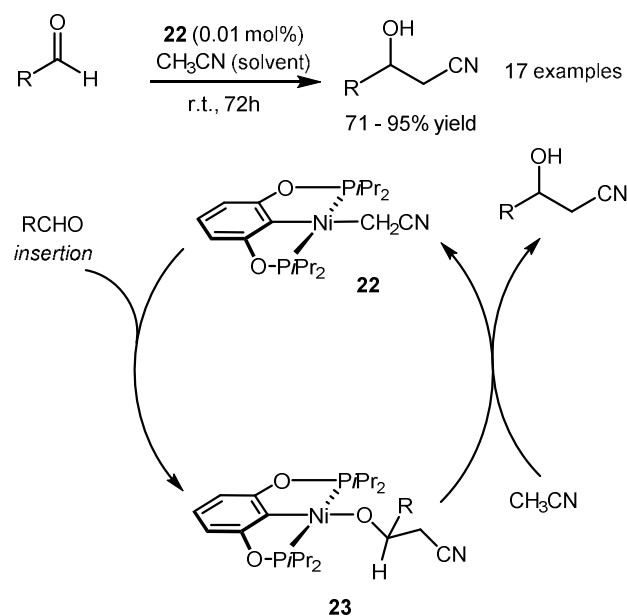
Scheme 14 Cyanomethylation of aldehydes catalyzed by [Ni(PCsp^2P)(CH$_2$CN)] (**22**)

Kemp and co-workers originally reported[20] the synthesis of the chloro complex [Ni(PCsp^2P)(Cl)] (**8**Cl). The chemistry of this compound was further investigated by Heinekey and co-workers who prepared several cationic Ni(II) complexes.[21] Upon treatment of complex **8**Cl with {[(Et$_3$Si)$_2$H][B(C$_6$F$_5$)$_4$]} as chloride scavenger, the coordinatively unsaturated intermediate **24** was formed, which reacted readily with both H$_2$ and HD to form complexes **25** and **26**, respectively. Complex **25** is the first isolated and structurally characterized nickel–dihydrogen complex. The H$_2$ ligand is heterolytically cleaved in the presence of base to form mono hydride complex **27**. The dihydrogen ligand is also easily displaced by carbon monoxide to yield the carbonyl complex **28** or by dinitrogen to form complex **29** which is a rare example of a Ni(II) terminal dinitrogen complex (Scheme 15).
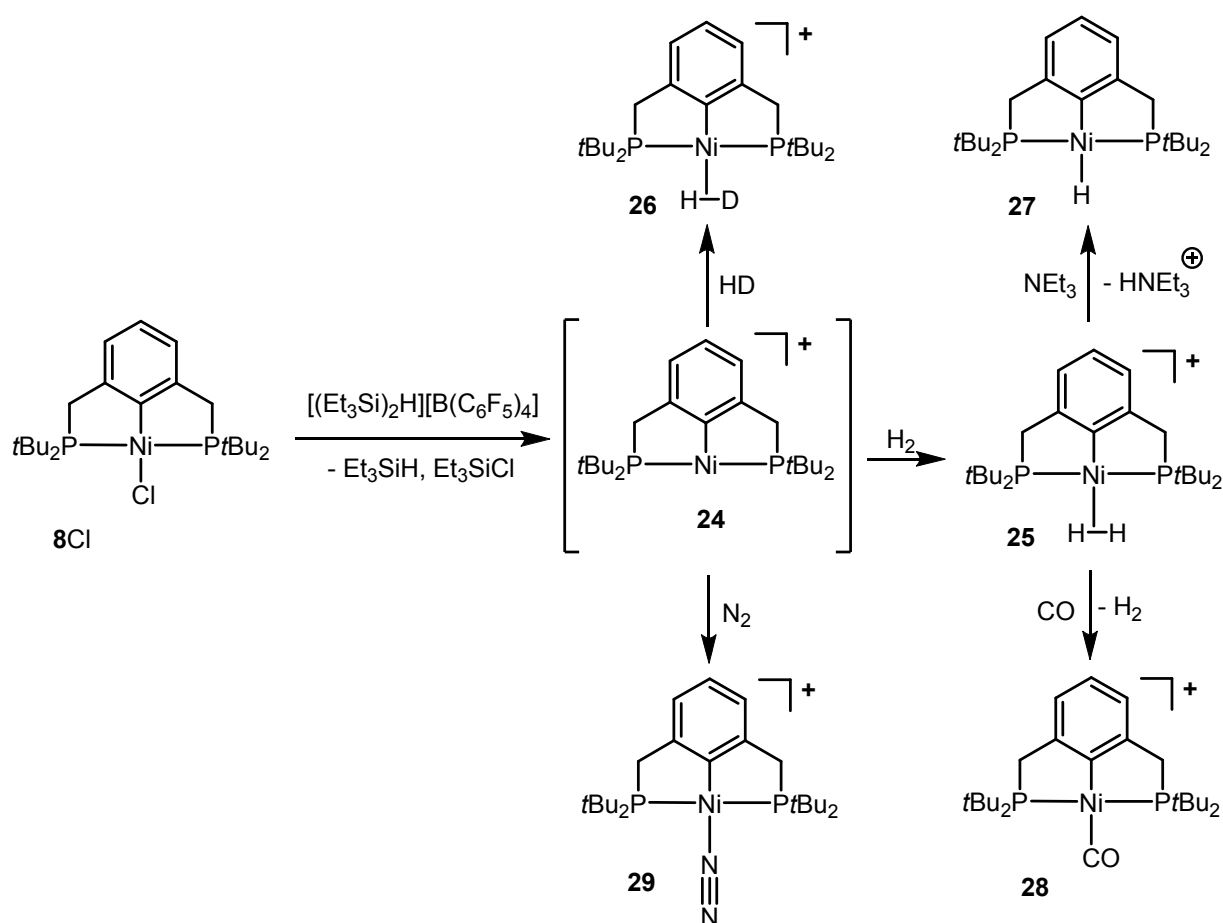
Scheme 15 Synthesis of several cationic Ni(II) PCsp^2P complexes after halide abstraction from **15**Cl.

Zargarian and co-workers were exploring some reactivities of neutral [Ni(PCP)(Br)] complexes which contain PCsp^2P ligands. Treatment of complexes **5**Br and **21**Br with sodium or silver tetraphenyl borate in the presence of acetonitrile as coordinating solvent afforded cationic complexes of the types **30** and **31** (Scheme 16).[22] These complexes adopt a distorted square-planar geometry around the nickel center.
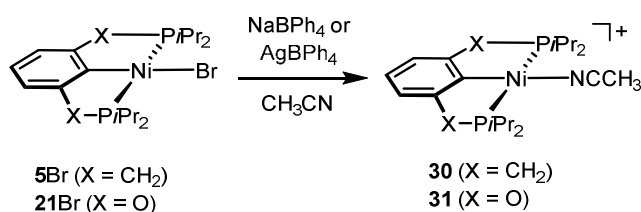
Scheme 16 Synthesis of the cationic complexes [Ni(PCsp^2P)(CH$_3$CN)] (**30, 31**)

Bromide abstraction from complex **4**Br with AgCF$_3$SO$_3$ in presence of CH$_2$Cl$_2$ at room temperature for 3h afforded the air sensitive compound **32**, which was readily converted by addition of acetonitrile to complex **33** which interestingly was resistant towards hydrolysis and/or oxidation (Scheme 17).[23]
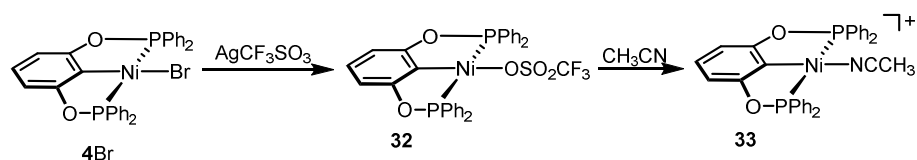
Scheme 17 Synthesis of [Ni(PC*sp*^{2}P)(CF$_3$SO$_3$)] (**32**) and [Ni(PC*sp*^{2}P)(CH$_3$CN)]$^+$ (**33**)

A variety of alcohols were treated with acrylonitrile in the presence of the Ni(II) diphosphinito PCP pincer catalyst **32** and NEt$_3$, which led to the formation of a C-O bond containing product (Scheme 18).[7c,24] Among these alcohols, only with 3-methyl phenol complete conversion could be achieved. Notably, without the addition of NEt$_3$ no reaction took place. Moreover, this reaction did not succeed with more nucleophilic alcohols such as methanol, ethanol, and isopropanol, due to decomposition of the catalyst.

Scheme 18 Alcoholysis of acrylonitrile catalyzed by the neutral Ni(II) catalyst **32**

The pincer complex **31** served also as a precatalyst for the regioselective anti-Markovnikov addition of nucleophiles to activated olefins.[24] The catalyzed additions of aliphatic amines to acrylonitrile, methacrylonitrile, and crotonitrile proceed at room temperature and give quantitative yields 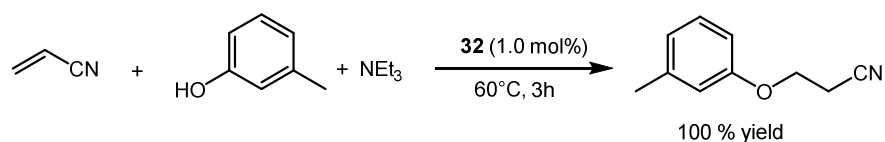of products resulting from the formation of C–N bonds. On the other hand, aromatic amines or alcohols are completely inert toward methacrylonitrile and crotonitrile, and much less reactive toward acrylonitrile, requiring added base, heating, and extended reaction times to give good yields. The catalytic reactivities of **31** seem to arise from the substitutional lability of the coordinated acetonitrile that allows competitive coordination of the nitrile moiety in the olefinic substrates. Zargarian and co-workers[7c,22,23,24] also described in an earlier report that a series of Ni(II) pincer complexes were evaluated as catalysts for the regioselective hydroamination of acrylonitrile. This Michael addition is favored when the generation of cationic Ni(II) species, therefore, α,β-unsaturated nitrile could coordinate to the Ni(II) center, followed by nucleophilic addition of free amine substrate to the activated double bond, then non-reductive elimination of aza-Michael addition product.

Very recently, Zhang and co-workers showed that the P-stereogenic pincer nickel complex **34** is an active catalysts for the asymmetric aza-Michael addition of α,β-unsaturated nitriles providing the products in good to excellent yields (up to 99%) and moderate enantiomeric excesses (up to 46% ee).

With 2-phenylacrylonitrile the desired product was obtained in quantitative yield, but without any enantiomeric excess (Scheme 19).[8]
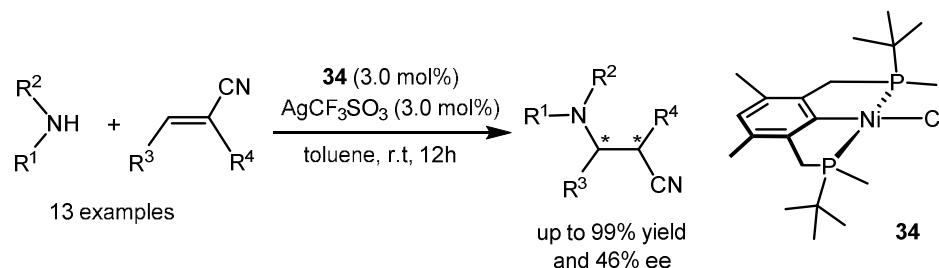
Scheme 19 Hydroamination of crotonitrile catalyzed by the chiral cationic Ni(II) pincer complex **34**

Hydrolytic decomposition[23] of complex **32** at the ambient room temperature in presence toluene as solvent for 2 days resulted the formation of a stable octahedral complex **35**. The formation of this compound presumably proceeds via initial protonation of aryl ring of PCP ligand reforming the aromatic C-H bond followed by oxidation of the phosphine moieties and coordination of water molecules (Scheme 20).
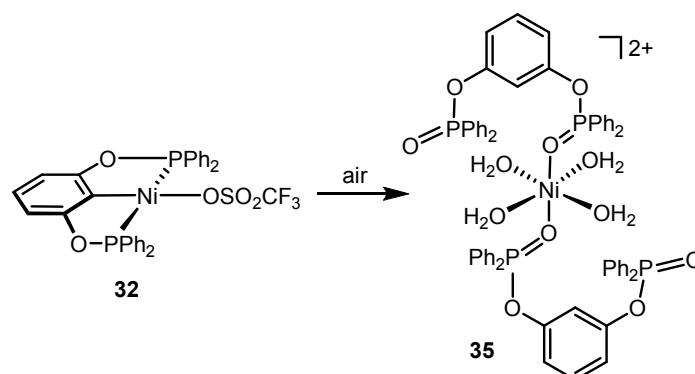
Scheme 20 Synthesis of stable dicationic octahedral Ni(II) complex (**35**) involving protonation and oxidation of the PCsp^2P ligand

Treatment of complexes **5**Br with stoichiometric amounts of silver salts such as CH_3COOAg and $AgNO_3$ resulted in the formation of complexes **36** and **37**, respectively (Scheme 21). Excess of silver salts caused oxidation of the metal center to give a stable Ni(III) complexes.[16]
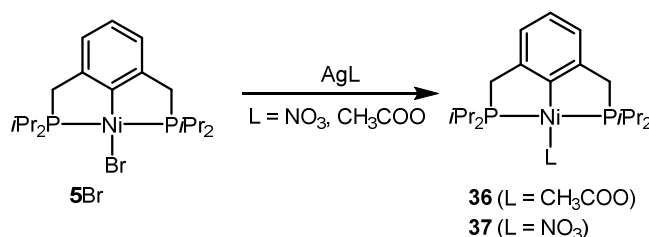
Scheme 21 Synthesis of [Ni(PCsp^2P)(CH$_3$OO)] (**36**) and [Ni(PCsp^2P)(NO$_3$)] (**37**) by halide displacement

An important class of compounds are hydrides. In 2009, nickel PCsp^2P pincer hydride complexes were synthesized.[20] The typical synthetic route starts from halide complexes. Treatment of **21**Cl and **38**Cl with LiAlH$_4$ in toluene at room temperature for 24h to yield nickel hydride complexes **39** and **40**, respectively (Scheme 39).[25] An alternative synthetic method utilized the nickel methoxy complex **41** and triethoxylsilane to prepare the hydride complex **42** (Scheme 22).[16] Complex [Ni(PCsp^2P)(OMe)] (**41**)[16] was synthesized from the amine complex (**9**) and methanol.[16]

21Cl (R = *i*Pr)
38Cl (R = *t*Bu)

39 (R = *i*Pr)
40 (R = *t*Bu)

41

42
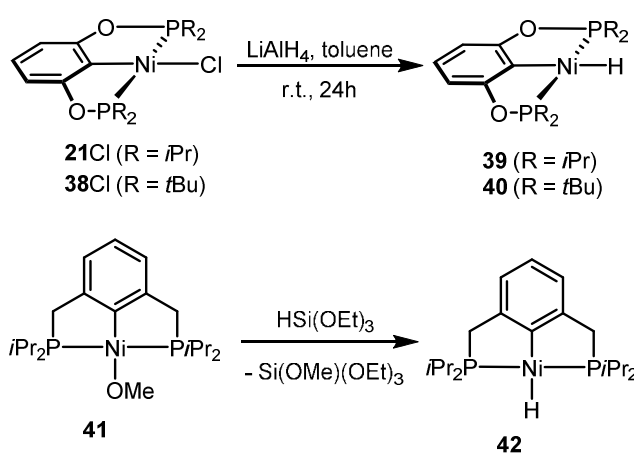
Scheme 22 Synthesis of [Ni(PCsp^2P)(H)] complexes **39**, **40** and **42**.

The hydride Ni(II) PCP pincer complex **39** was tested as catalysts the chemoselective hydrosilylation of C=O bonds of aldehydes and ketones in the presence of other functional groups.[25,26,27] Aldehydes were converted to primary alcohols with 0.2 mol% of catalyst **39** and a slight excess of hydrogen source of phenylsilane followed by basic hydrolysis good to excellent yields (Scheme 23). The mechanism involves C=O insertion into a nickel-hydrogen bond, followed by cleavage of the newly formed Ni-O bond **43** with a silane. It has to be noted that this catalyst did not work well for the hydrosilylation of ketones. For instance, substrates such as acetophenone, cyclohexanone, benzophenone afforded the corresponding alcohols in 18%, 6%, and 60%, respectively, in the presence of 1.0 mol% catalyst at 70°C for 24h.
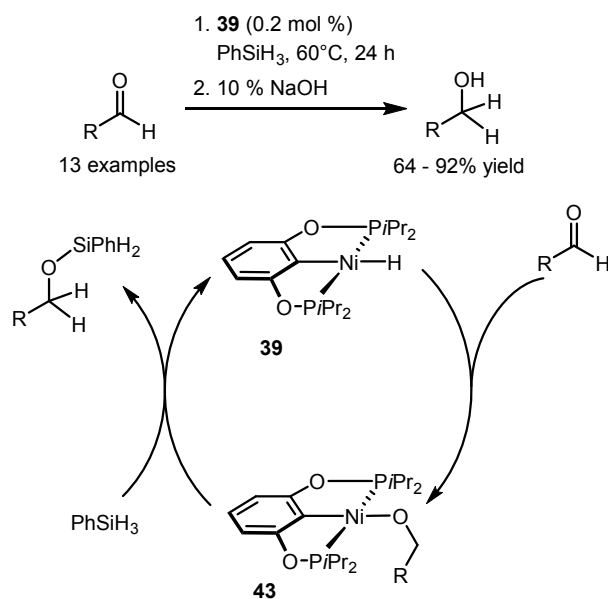
Scheme 23 Hydrosilylation of aldehydes catalyzed by the Ni(II) PCP pincer hydride complex **39**

Prior to our findings, Guan and co-workers[28] discovered that nickel hydride complexes react with BH$_3$·THF irreversibly at room temperature to yield BH$_4$-complexes. Reversing the reactions is possible at higher temperatures if there is a trapping agent available, or under a dynamic vacuum. Other boranes such as 9-Borabicyclo(3.3.1)nonane (9-BBN) and catecholborane (HBcat) are also capable of reacting with nickel hydride complexes such as **39** and **45** to form the corresponding nickel dihydridoborate complexes **44**, **46** and **47**, unless the hydride moiety is sterically inaccessible (Scheme 45).[28] In these cases, the reactions are reversible at room temperature, allowing nickel hydride species to reform. Under catalytic conditions reduction of CO$_2$ led to the methoxide level when 9-BBN or HBcat was employed as the reducing agent. The best catalyst involved bulky substituents on the phosphorus donor atoms such as in **39**. Catalytic reactions involving **44** were less efficient because of the formation of dihydridoborate complexes as the dormant species as well as partial decomposition of the catalyst by the boranes (Scheme 24).
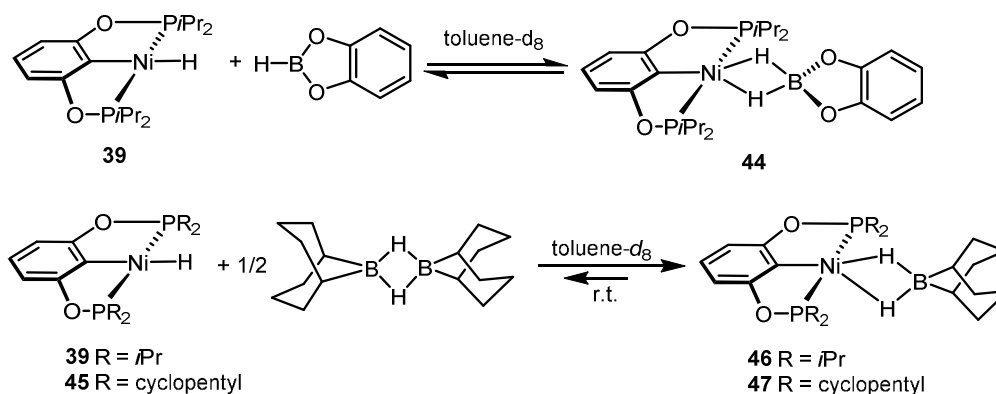
Scheme 24 Synthesis of [Ni(PCsp^2P)(borohydride)] derivatives

Both nickel hydride and borohydride complexes were able to reduce carbon dioxide to form the respective formate complexes (Scheme 25).[28,29] It has to be mentioned that several pincer complexes of the type [Ni(PCP)(R)] (R = H, OH, Me, allyl) were reported[30,31,32,33] to undergo insertion reactions with CO_2.
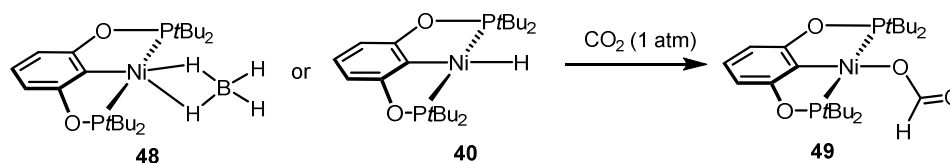
Scheme 25 Reduction of CO_2 by [Ni(PCsp^2P)(η^2-BH$_4$)] and [Ni(PCsp^2P)(H)] to give formate complexes

Dihydrogen bond interactions where transition metal hydride complexes serve as both proton acceptor and proton donor in a hydrogen bond are very rare. Peruzzini and co-workers studied the reaction of the stable electron-rich Ni(II) PCP pincer hydride [Ni(PCsp^2P)(H)] (**27**) with the acidic tungsten(II) complex [WCp(H)(CO)$_3$] (**50**).[34] Stoichiometric amounts of the acid hydride complex [WCp(H)(CO)$_3$] (**50**) and basic hydride complex [Ni(PCsp^2P)(H)] (**27**) reacted in THF or toluene at room temperature to give the bimetallic ion pair complex **52**. In this complex one carbonyl ligand bridges the two metal centers in a rather unconventional "isocarbonylic" mode (Scheme 26). The structure of complex **52** was confirmed by X-ray diffraction analysis. Deuterium exchange H/D was also studied with the isotopomeres [CpW(D)(CO)$_3$] and [Ni(PCsp^2P)(D)]. Complex **51** was an intermediate as suggested by DFT calculations (Scheme 27). Complex **52** dissociates in acetonitrile to produce the adduct [Ni(PCsp^2P)(CH$_3$CN)][CpW(CO)$_3$] that comprises a square-planar nickel(II) PCP cation binding one CH$_3$CN molecule and the piano stool tungsten(II) anion.[34]
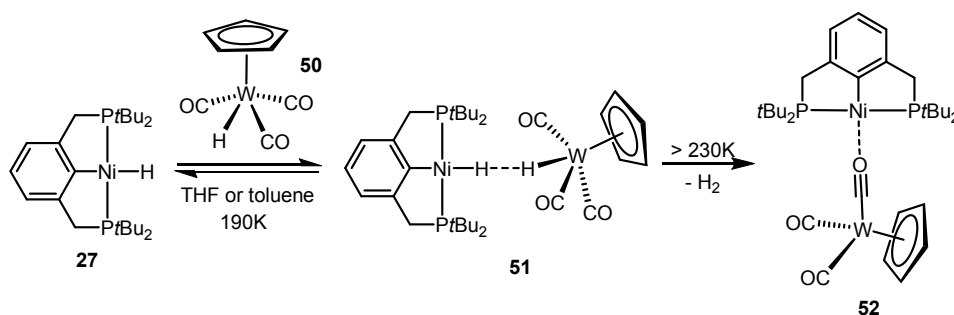
Scheme 26 Dihydrogen evolution upon reacting acidic and basic metal hydride complexes

It was shown that water plays an important role in the activation of Ni-F and W-H bonds. The reaction between the nickel(II) PCP pincer fluoride complex **8F** and the tungsten(II) carbonyl hydride **50** led to hydrofluoric acid evolution and formation of the bimetallic isocarbonylic species **52** (Scheme 27). The process was monitored through multinuclear ^{1}H, ^{19}F{^{1}H}, and ^{31}P{^{1}H} variable-temperature NMR spectroscopy.[35] According to DFT calculations four water molecules are involved in the Ni-F and W-H cleavage steps.
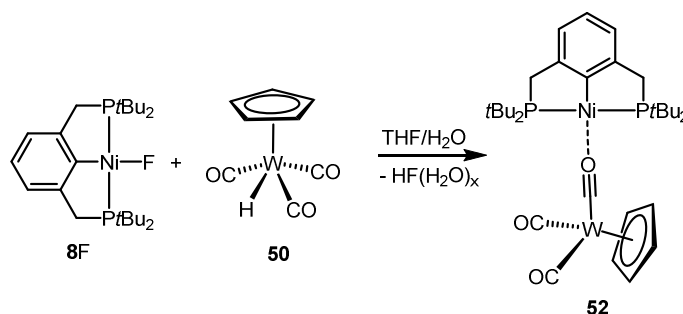
Scheme 27 Water assisted hydrofluoric acid evolution upon interaction of complexes **8F** and **50** and formation of **52**

1.3 Cobalt PCP Pincer Complexes

An overview of all cobalt PC*sp*^{2}P and PC*sp*^{3}P pincer complexes, which serve as synthetic entries into Co PCP chemistry are depicted in Chart 3.[36,37,38] These are typically derived from simple Co(0), Co(I) and Co(II) precursors such as Co(PMe$_3$)$_4$, Co(Cl)(PMe$_3$)$_3$, Co(Me)(PMe$_3$)$_4$, and CoX$_2$ (X = Cl, Br, I).

Li, **2010**   Heinekey, **2011**   Wass, **2014**
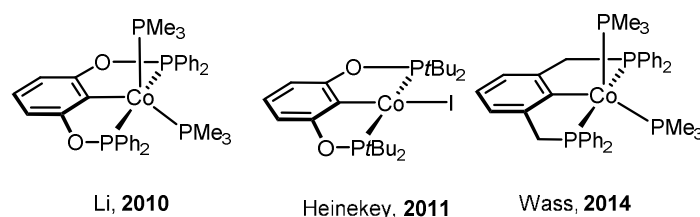
Chart 3 Overview of cobalt PC*sp*^{2}P and PC*sp*^{3}P pincer complexes

Pringle and co-workers reported the synthesis of the Co(I) PC*sp*^{2}P complex **53** by a transmetalation reaction between 1-lithio-2,6-bis((diphenylphosphino)methyl)benzene and CoCl(PMe$_3$)$_3$. Subsequent exposure of **53** to CO gave the dicarbonyl complex **54**. The synthesis of this complex proceeds via monophosphine intermediate **54**, which was identified by ^{31}P{^{1}H} NMR spectroscopy from the reaction mixture. The conversion of **54** to **55** was shown to be reversible (Scheme 28).[37]
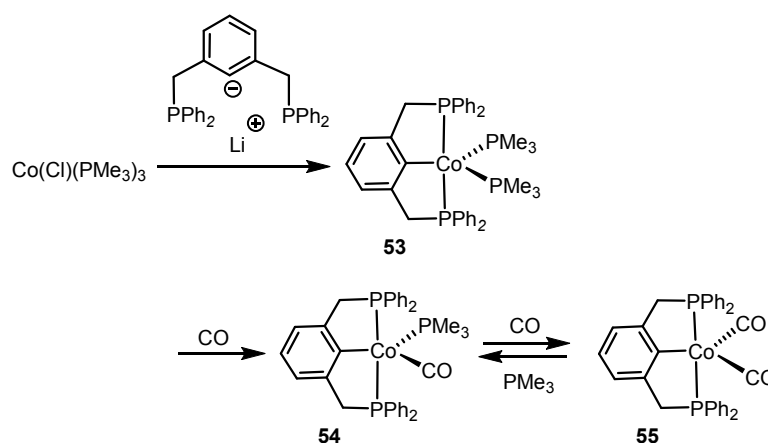
Scheme 28 Synthesis of the Co(I) PC*sp*^{2}P complex **53** and stepwise substitution of PMe$_3$ by CO

Heinekey and co-workers reported[38] the synthesis of the Co(II) iodo PCP complex [Co(PC*sp*^{2}P)(I)] (**122**). This compound was prepared in good yield by activation of the ligand with *n*BuLi and the addition of CoI$_2$·THF (Scheme 29). The magnetic moment of **56** was measured using the Evans method (μ_{eff} = 2.38 μ_B) and is consistent with a paramagnetic complex that contains one unpaired electron. Reduction of **56** was accomplished using sodium amalgam. The isolated product was a mercury-bridged dicobalt species [{Co(PC*sp*^{2}P)}$_2$Hg] (**57**). Introduction of H$_2$ gas to a solution of **57** at 195 K resulted in the formation of a new diamagnetic species. The ^{1}H NMR spectrum in the high-field region exhibited a new resonance (with an integration of two versus other ligand resonances) at δ = -11.6 ppm and was identified as the first cobalt-dihydrogen complex [Co(PC*sp*^{2}P)(η^2-H$_2$)] (**58**) (Scheme 30). Studying solutions of **58** under increased hydrogen pressure allowed observation of a new diamagnetic product identified as [Co(PC*sp*^{2}P)(η^2-H$_2$)(H)$_2$] (**59**). In addition to NMR spectroscopy, the identity of the dihydrogen and hydride species were confirmed by means of theoretical calculations.
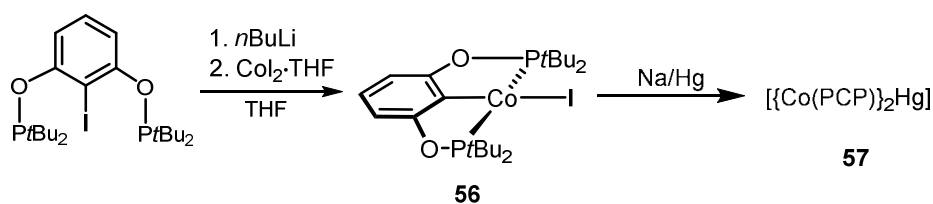
Scheme 29 Synthesis of complexes [Co(PC*sp*^{2}P)I] (**56**) and reduction to the mercury-bridged dicobalt species [{Co(PC*sp*^{2}P)}$_2$Hg] (**57**)
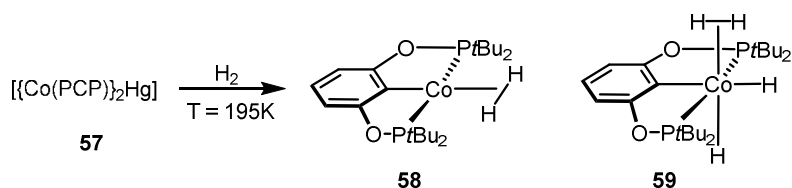
Scheme 30 Synthesis of [Co(PC*sp*^{2}P)(η^2-H$_2$)] (**58**) and [Co(PC*sp*^{2}P)(η^2-H$_2$)(H)$_2$] (**59**).

1.4 Molybdenum PCP Pincer Complexes

The chemistry of molybdenum PCP complexes is hardly developed. The first molybdenum PCP complex was prepared through lithiation of 1-iodo-2,6-[OP(t-Bu)$_2$]$_2$C$_6$H$_3$ and reaction of that lithium reagent with MoI$_3$(THF)$_3$ to give [Mo(PC*sp*^{2}P)(I)$_2$] (**60**) (Scheme 73),[39] a procedure similar to that employed to prepare the cobalt PCP complex **56** (Scheme 29).[38] Compound **60** was obtained in modest yield (46%). However, a diamagnetic impurity was present (10 -15%), which was proposed to be the Mo(IV) oxo complex (**61**). However, this was merely based on NMR spectroscopy and the fact that MoI$_3$(THF)$_3$ is known to decompose to give Mo=O species and 1,4-di-iodobutane. On the other hand, the lithiation of 1-iodo-2,6-[OP(t-Bu)$_2$]$_2$C$_6$H$_3$ and reaction of that lithium reagent with MoCl$_3$(THF)$_3$ and MoBrI$_3$(THF)$_3$ yielded a mixture of several products.[39]
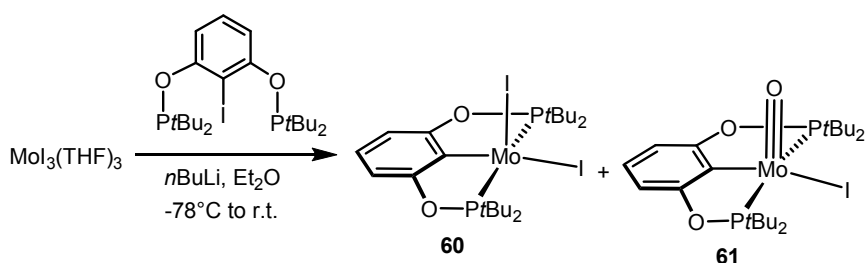
Scheme 31 Synthesis of Mo(III) and Mo(IV) PCP pincer complexes starting from MoI$_3$(THF)$_3$

When a THF solution of **60** (contaminated with **61**) was reduced with NaHg in the presence of 15-crown-5 under N$_2$, the anionic Mo(IV) nitride complex [Mo(PC*sp*^{2}P)(N)(I)]$^-$ (**62**) was obtained as a dark brown solid in 57% yield. This compound was also formed when two or more equivalents of KC$_8$ or Na naphthalenide were used as reducing agents. Upon protonation of **62** by [Et$_3$NH][BAr'$_4$] a diamagnetic compound, presumably **63**, was isolated in 64% yield. Based on NMR data it was proposed that proton addition occurred across the Mo-P bond (Scheme 32).[39]
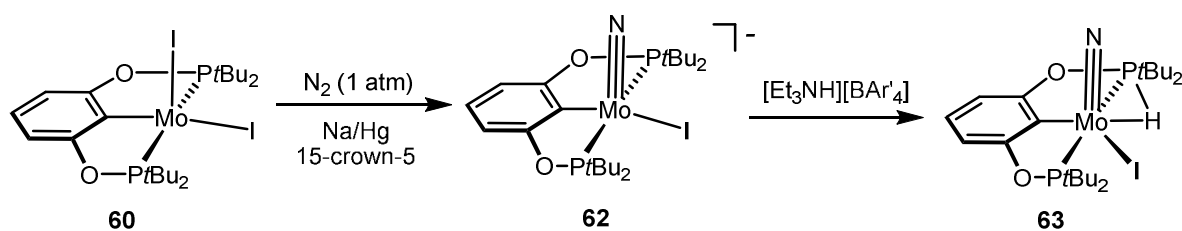
Scheme 32 Synthesis and reactivity of the anionic Mo(IV) complex [Mo(PCsp^2P)(N)(I)]⁻ (**62**)

1.5 Conclusion

This chapter provides an overview of the advancements in the field of non-precious metal (Ni, Co and Mo) complexes featuring anionic PCP pincer ligands where the (CH_2, O and NH) linkers between aromatic ring and phosphine moieties. While the research in nickel PCP complexes is already quite extensive, the chemistry of cobalt and molybdenum PCP complexes is comparatively sparse. In the case of nickel PCP complexes already many catalytic applications such as Suzuki–Miyaura coupling, C-S cross coupling, Michael additions, Alcoholysis of acrylonitrile, hydrosilylation of aldehyde and cyanomethylation of aldehydes were reported. Cobalt and molybdenum PCP complexes were not applied to any catalytic reactions. Surprisingly, only one molybdenum PCP complex is reported, which was capable of cleaving dinitrogen to give a nitride complex. This literature survey is motivated us to find and develop the combination of cheap and abundant metals such as nickel, cobalt and molybdenum with PCP pincer ligands may result in the development of novel, versatile, and efficient catalysts for atom-efficient catalytic reactions.

References

1   Coining of the name "pincer": G. van Koten, *Pure App. Chem.* 1989, **61**, 1681.

2   For reviews on pincer complexes, see: (a) R. A. Gossage, L. A. van de Kuil, G. van Koten, *Acc. Chem. Res.* 1998, **31,** 423. (b) M. Albrecht, G. van Koten, *Angew. Chem., Int. Ed.* 2001, **40**, 3750. (c) M. E. van der Boom, D. Milstein, *Chem. Rev.* 2003, **103,** 1759. (d) J. T. Singleton, *Tetrahedron* 2003, **59**, 1837. (e) L. C. Liang, *Coord. Chem. Rev.* 2006, **250,** 1152. (f) The Chemistry of Pincer Compounds; D. Morales-Morales, C. M. Jensen, Eds.; Elsevier: Amsterdam, 2007. (g) H. Nishiyama, *Chem. Soc. Rev.* 2007, **36,** 1133. (h) D. Benito-Garagorri, K. Kirchner, *Acc. Chem.* Res. 2008, **41,** 201. (i) J. Choi, A. H. R. MacArthur, M. Brookhart, A. S. Goldman, *Chem. Rev.* 2011, **111,** 1761. (j) N. Selander, K. J. Szabo, *J. Chem. Rev.* 2011, **111,** 2048. (k) P. Bhattacharya, H. Guan, *Comment Inorg. Chem.* 2011, **32**, 88. (l) S. Schneider, J. Meiners, B. Askevold, *Eur. J. Inorg. Chem.* 2012, 412. (m) G. van Koten, D. Milstein, Eds.; Organometallic Pincer Chemistry; Springer: Berlin, 2013; *Top. Organomet. Chem.* Vol. 40. (n) K. J. Szabo and O. F. Wendt, Pincer and Pincer-Type

Complexes: Applications in Organic Synthesis and Catalysis, Wiley-VCH, Germany, 2014. (o) M. Asay, D. Morales-Morales, *Dalton Trans.* 2015, **44**, 17432.

3   C. J. Moulton, B. L. Shaw, *J. Chem. Soc., Dalton. Trans.* 1976, 1020.

4   D. Benito-Garagorri, V. Bocokic, K. Mereiter, K. Kirchner, *Organometallics,* 2006, **25,** 3817.

5   W. M. Haenel, D. Jakubik, C. Krueger, P. Betz, *Chemische Berichte,* 1991, **124,** 333.

6   K. A. Kozhanov, M. P. Bubnov, V. K. Cherkasov, G. K. Fukin, G. A. Abakumov, *Dalton Trans.,* 2004, **18,** 2957.

7   a) X. Lefevre, D. M. Spasyuk, D. Zargarian, *J. Organomet. Chem.,* 2011, **696,** 864. b) V. Boris, L. Fabien, D. Zargarian, *Green Chem.,* 2013, **15,** 3188. c) V. Pandarus, D. Zargarian, *Organometallics,* 2007, **26,** 4321.

8   Z. Yang, D. Liu, Y. Liu, M. Sugiya, T. Imamoto, W. Zhang, *Organometallics,* 2015, **34**, 1228.

9   M. E. Van der Boom, S. Liou, L. J. W. Shimon, Y. Ben-David, D. Milstein, *Inorg. Chim. Acta.,* 2004, **357,** 4015.

10   V. Gomez-Benitez, O. Baldovino-Pantaleon, C. Herrera-Alvarez, R. A. Toscano, D. Morales-Morales, *Tetrahedron Lett.,* 2006, **47,** 5059.

11   N. A. Espinosa-Jalapa, S. Hernandez-Ortega, X. Le Goff, D. Morales-Morales, J. Djukic, R. Le Lagadec, *Organometallics*, 2013, **32,** 2661.

12   B. Vabre, D. M. Spasyuk, D. Zargarian, *Organometallics,* 2012, **31,** 8561.

13   F. Estudiante-Negrete, S. Hernandez-Ortega, D. Morales-Morales, *Inorg. Chim. Acta,* 2012, **387,** 58.

14   T. Chen, L. Yang, L. Li, K. Huang, *Tetrahedron* 2012, **68,** 6152.

15   J. Zhang, C. M. Medley, J. A. Krause, H. Guan, *Organometallics,* 2010, **29,** 6393.

16   L. M. Martinez-Prieto, C. Melero, D. Del Rio, P. Palma, J. Campora, E. Alvarez, *Organometallics,* 2012, **31,** 1425.

17   J. Campora, P. Palma, D. Del Rio, M. Mar Caonejo, E. Alvarez, *Organometallics,* 2004, **23**, 5653.

18   T. J. Schmeier, A. Nova, N. Hazari, F. Maseras, *Chem. Eur. J.* 2012, **18**, 6915.

19   S. Chakraborty, Y. J. Patel, J. A. Krause, H. Guan, *Angew. Chem. Int. Ed.,* 2013, **52**, 7523.

20   B. J. Boro, E. N. Duesler, K. I. Goldberg, R. A. Kemp, *Inorg. Chem.* 2009, **48**, 5081.

21   S. J. Connelly, A. C. Zimmerman, W. Kaminsky, D. M. Heinekey, *Chem. Eur. J.,* 2012, **18**, 15932.

22   A. Castonguay, D. M. Spasyuk, N. Madern, A. L. Beauchamp, D. Zargarian, *Organometallics,* 2009, **28,** 2134.

23   A. B. Salah, C. Offenstein, D. Zargarian, *Organometallics,* 2011, **30**, 5352.

24   X. Lefèvre, G. Durieux, S. Lesturgez, D. Zargarian, *J. Mol. Catal. A,* 2011, **335**, 1.

25   S. Chakraborty, J. A. Krause, H. Guan, *Organometallics* 2009, **28**, 582.

26   S. Chakraborty, H. Guan, *Dalton Trans.,* 2010, **39,** 7427.

27   S. Chakraborty, P. Bhattacharya, H. Dai, H. Guan, *Acc. Chem. Res.* 2015, **48**, 1995.

28   S. Chakraborty, J. Zhang, Y. J. Patel, J. A. Krause, H. Guan, *Inorg. Chem.,* 2013, **52,** 37.

29   S. Chakraborty, J. Zhang, J. A. Krause, H. Guan, *J. Am. Chem. Soc.* 2010, **132**, 8872.

30   T. J. Schmeier, N. Hazari, C. D. Incarvito, J. A. Raskatov, *Chem. Commun.,* 2011, **47**, 1824.

31   S. Chakraborty, Y. J. Patel, J. A. Krause, H. Guan, *Polyhedron,* 2012, **32,** 30.

32   L. M. Martinez-Prieto, C. Real, E. Avila, E. Alvarez, P. Palma, J. Campora, *Eur. J. Inorg. Chem.,* 2013, 5555.

33   H. Suh, T. J. Schmeier, N. Hazari, R. A. Kemp, M. K. Takase, *Organometallics,* 2012, **31,** 8225.

34   A. Vladislava, A. Rossin, N. V. Belkova, M. R. Chierotti, L. M. Epstein, O. A. Filippov, R. Gobetto, L. Gonsalvi, A. Lledos, E. S. Shubina, F. Zanobini, M. Peruzzini, *Angew. Chem. Int. Ed.,* 2011, **50,** 1367.

35   M. R. Chierotti, A. Rossin, R. Gobetto, M. Peruzzini, *Inorg. Chem.,* 2013, **52,** 12616.

36   Z. Lian, G. Xu, X. Li, *Acta Crystallogr. Sect. E: Struct. Rep. Online* 2010, **E66**, m636.

37   M. A. Kent, C. H. Woodall, M. F. Haddow, C. L. McMullin, P. G. Pringle, D. F. Wass, *Organometallics,* 2014, **33,** 5686.

38   T. J. Hebden, A. J. St. John, D. G. Gusev, W. Kaminsky, K. I. Goldberg, D. M. Heinekey, *Angew. Chem. Int. Ed.,* 2011, **50,** 1873.

39   T. J. Hebden, R. R. Schrock, M. K. Takase, P. Mueller, *Chem. Comm.,* 2012, **48,** 1851.

Synthesis and Reactivity of Four and Five Coordinate Low-spin Co(II) PCP Pincer Complexes and some Ni(II) Analogs

Anhydrous $CoCl_2$ react with the ligand PCP-*iPr* (**1a**) in the absense of base to afford the 15e square planar complex [Co(PCP^{Me}-*iPr*)Cl] (**2a**) with moderate yield, whereas anhydrous $CoCl_2$ or [NiCl$_2$(DME)] react with the ligand PCP^{Me}-*iPr* (**1b**) in the presence of *n*BuLi to afford the high yield of 15e and 16e square planar complexes [Co(PCP^{Me}-*iPr*)Cl] (**2b**) or [Ni(PCP^{Me}-*iPr*)Cl] (**3**), respectively. Complex **2b** is a paramagnetic d^7 low-spin complex, which is a useful precursor for a series of Co(I), Co(II), and Co(III) PCP complexes. Complex **2b** reacts readily with CO and pyridine to afford the five-coordinate square-pyramidal 17e complexes [Co(PCP^{Me}-*iPr*)(CO)Cl] (**4**) and [Co(PCP^{Me}-*iPr*)(py)Cl] (**5**), respectively, while in the presence of Ag^+ and CO the cationic complex [Co(PCP^{Me}-*iPr*)(CO)$_2$]$^+$ (**6**) is afforded. The effective magnetic moments μ_{eff} of all Co(II) complexes were derived from the temperature dependence of the inverse molar magnetic susceptibility by SQUID measurements and are in the range of 1.9 to 2.4μ_B. This is consistent with a d^7 low spin configuration with some degree of spin orbit coupling. Oxidation of **2b** with $CuCl_2$ affords the paramagnetic Co(III) PCP complex [Co(PCP^{Me}-*iPr*)Cl$_2$] (**7**), while the synthesis of the diamagnetic Co(I) complex [Co(PCP^{Me}-*iPr*)(CO)$_2$] (**8**) was achieved by stirring **2** in toluene with KC_8 in the presence of CO. Finally, the cationic 16e Ni(II) PCP complex [Ni(PCP^{Me}-*iPr*)(CO)]$^+$ (**10**) was obtained by reacting complex **3** with 1 equiv of $AgSbF_6$ in the presence of CO. The reactivity of CO addition to Co(I), Co(II) and Ni(II) PCP square planar complexes of the type [M(PCP^{Me}-*iPr*)(CO)]^n (n = +1, 0) was investigated by DFT calculations showing that formation of the Co species, **6** and **8**, is thermodynamically favorable, while Ni(II) maintains the 16e configuration since CO addition is unfavorable in this case. X-ray structures of most complexes are provided and discussed. A structural feature of interest is that the apical CO ligand in **4** deviates significantly from linearity with a Co-C-O angle of 170.0(1)°. The DFT calculated value is 172° clearly showing that this is not a packing but an electronic effect.

2.1 Introduction

One of the ways of modifying and controlling the properties of transition metal complexes is the use of appropriate ligand systems such as pincer ligands, i.e., tridentate ligands that are coordinated in meridional fashion. Usually consisting of a central aromatic backbone tethered to two two-electron donor groups by different spacers, this class of tridentate ligands has found numerous applications in various areas of chemistry, including catalysis, due to their combination of stability, activity and variability.[1] We are currently focusing on the synthesis and reactivity of transition metal PNP and PCP pincer complexes where the pincer ligands contain amine (NH and NR) linkers between the aromatic ring and the phosphine moieties.[2] These type of PNP and PCP ligands are readily available *via* condensation reactions between various 2,6-diaminopyridines and 1,3-diaminobenzenes and electrophilic chlorophosphines R_2PCl. These ligands can be designed in modular fashion and are thus very versatile ligand platforms. This has resulted in the preparation of a series of square-planar group 10 metal PCP complexes,[3] as well as numerous iron[4] and molybdenum PNP systems.[5]

Surprisingly, as cobalt is concerned only a few PCP pincer complexes featuring a direct cobalt-carbon single bond have been reported in the literature. An overview of cobalt PCP pincer systems (**A−E**), mostly based on the Co(I)/Co(III) oxidation states, is depicted in Scheme 1.[6,7,8,9,10] It has to be noted that several related cobalt complexes containing anionic pincer-type PNP, PSiP, NCN, and NNN frameworks are described.[11,12,13,14,15,16,17,18,19]
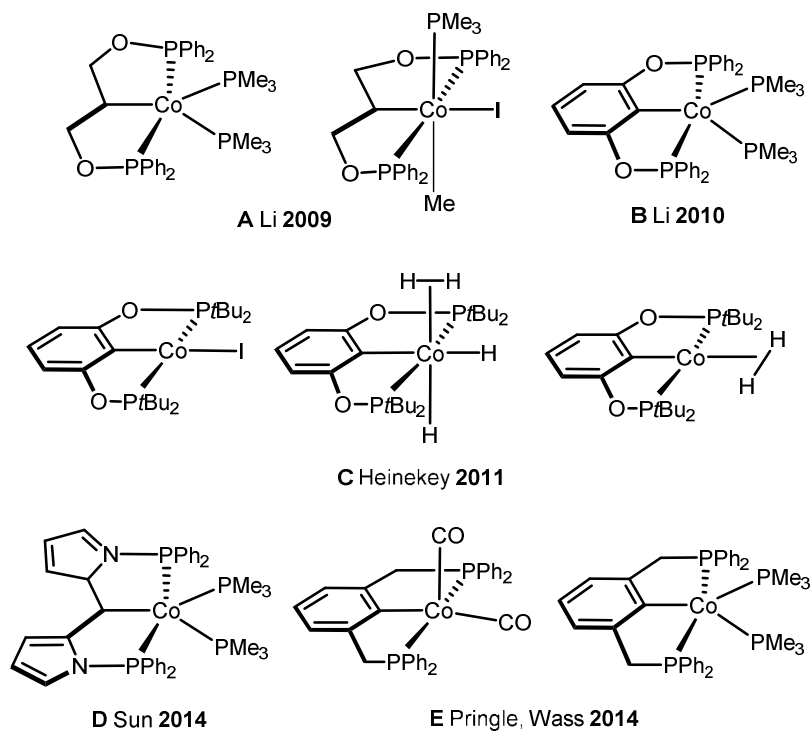
Scheme 1 Overview of Co PCP complexes reported in the literature

Here we report on the synthesis, characterization and reactivity of a series of new cobalt PCP pincer complexes in oxidation states +I, +II, and +III based on the d^7 low-spin Co(II) complex [Co(PCP^{Me}-*i*Pr)Cl] where the P*i*Pr$_2$ moieties of the PCP ligand are connected to the benzene ring via NMe linkers. For comparison, the syntheses of some analogous low-spin d^8 Ni(II) PCP complexes are also reported.

2.2 Results and Discussion

The complex [Co(PCP-*t*Bu)Cl] (**2a**) where the PCP ligand features acidic NH protons, had to be prepared via a slightly modified snynthetic procedure to that employed to prepare nickel PCP complex (Scheme 3, Chapter 1). Refluxing a solution of anhydrous CoCl$_2$ with the ligand PCP-*t*Bu (**1a**) in THF afforded directly **2a** albeit in moderate isolated yield (32%) (Scheme 2). In analogy to **2a**, [Co(PCP-*t*Bu)Cl] (**2a**) is a d^7 low spin complex with a solution magnetic moment μ_{eff} of 1.8(1)μ_B (Evans method). The solid state structure of this complex was determined by X-ray diffraction and a representation of the molecule is shown in Figure 1 with selected metrical parameters given in the caption. The

molecular structure shows the metal in a typical slightly distorted-square planar configuration. The C1-Co1-Cl1 angle deviates slight from linearity being 176.80(7)°. The P(1)-Co1-P2 angle is 165.92(3)°.
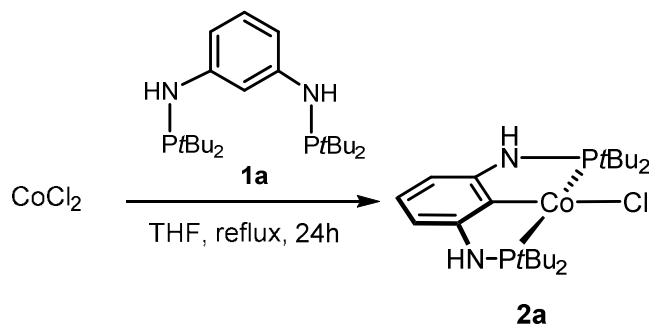
Scheme 2 Synthesis of complex [Co(PCP-*t*Bu)Cl] (**2a**)

is shown in Figure 1 with selected metrical parameters given in the caption. The molecular structure shows the metal in a typical slightly distorted-square planar configuration. The C1-Co1-Cl1 angle deviates slight from linearity being 176.80(7)°. The P(1)-Co1-P2 angle is 165.92(3)°.
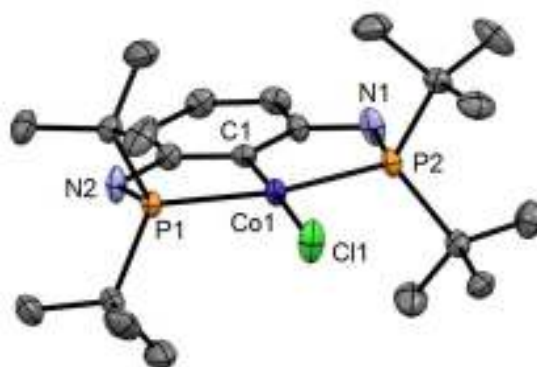
Figure 1. Structural view of [Co(PCP-*t*Bu)Cl] (**2a**) showing 50% thermal ellipsoids (H atoms omitted for clarity). Selected bond lengths (Å) and bond angles (°): Co1-Cl1 2.260(1), Co1-P1 2.2209(7), Co1-P2 2.2343(7), Co1-C1 1.935(2), Cl1-Co1-P1 96.67(3), Cl1-Co1-P2 97.12(3), Cl1 Co1-C1 176.80(7), P1-Co1-P2 165.92(3), P1-Co1-C1 82.90(7), P2-Co1-C1 83.48(7).

In this section, our aim is to improve the yield for the formation of type of cobalt pincer complex **2a** and we therefore designed the ligand **1b** (Scheme 3) starting from the N^1,N^3-dimethylbenzene-1,3-diamine as ligand precursor, a procedure similar to that employed to prepare the PCP ligands (Scheme 2, Chapter 1). In other hand the preparation of **1c** ligand was not succeded *via* nucleophilic substitution because of bulkyness of di-tert-butylphosphine chloride reagent.

1b (R = *i*Pr)
1c (R = *t*Bu), *not formed*
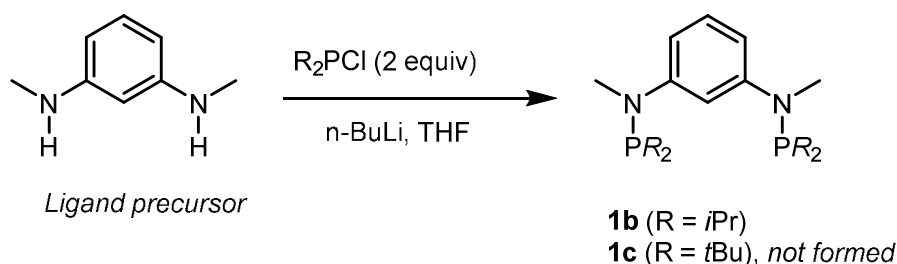
Scheme 3 Synthesis of complex (PCP^Me-*i*Pr) (**1b**)

And the treatment of anhydrous $CoCl_2$ or [NiCl_2(DME)] (DME = 1,2-dimethoxyethane) with the ligand PCP^Me-*i*Pr (**1b**) in the presence of *n*BuLi in THF affords the 15e and 16e complexes [Co(PCP^Me-*i*Pr)Cl] (**2b**) and [Ni(PCP^Me-*i*Pr)Cl] (**3**) in 96 and 97% isolated yields, respectively (Scheme 4). The Co(II) complex displays large paramagnetic shifted and very broad ^1H NMR signals and were thus not very informative. $^{13}C\{^1H\}$ and $^{31}P\{^1H\}$ NMR could not be detected at all. The magnetic moment

2b M = Co, S = 1/2
3 M = Ni, S = 0

M = Co, S = 3/2
not observed
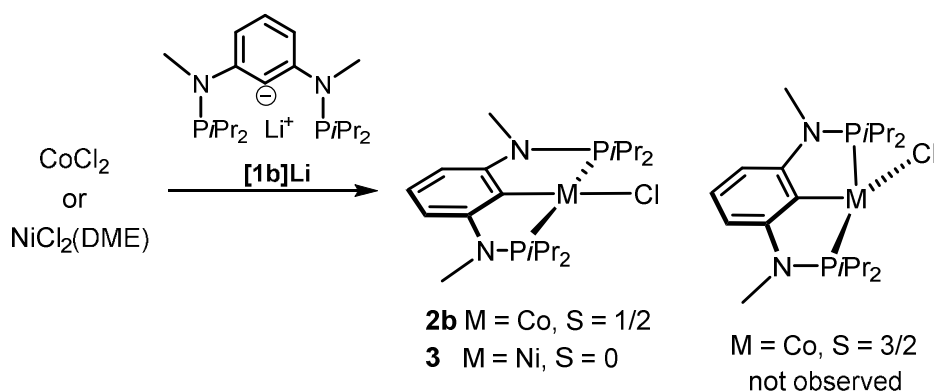
Scheme 4 Synthesis of complexes [Co(PCP^Me-*i*Pr)Cl] (**2b**) and [Ni(PCP^Me-*i*Pr)Cl] (**3**)

of μ_{eff} = 2.3(1)μ_B was derived from the temperature dependence of the inverse molar magnetic susceptibility, which is well described by a Curie law above 10 K (one unpaired electron). This value is higher than the one expected for the spin-only approximation and is explained by a spin orbit coupling contribution, being consistent with a low-spin square planar complex.[20] DFT calculations[21] reveal that the corresponding high-spin Co(II) complex with S = 3/2, which adopts a pseudo-tetrahedral geometry, is 19.5 kcal/mol less stable[22] than the square planar low-spin state with S = ½ and was not observed experimentally (Figure 2). Solution equilibria between square planar low-spin and tetrahedral high-spin species, which are also accompanied by color changes, were observed for the related Co(II) pincer-type complexes [Co(PNP)Cl], where PNP are anionic disilylamido PNP ligands [N(SiMe_2CH_2PPh_2)_2]⁻
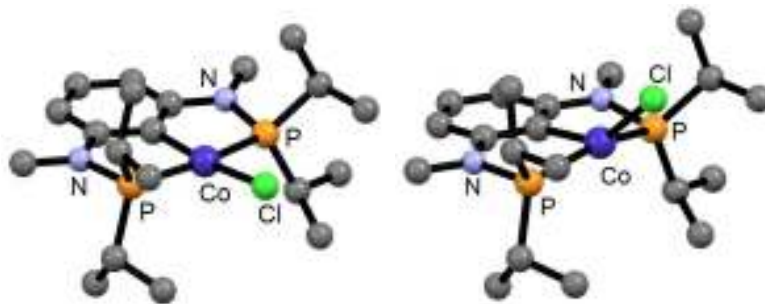
Figure 2. Optimized B3LYP geometries of the low-spin (left) and high-spin (right) isomers [Co(PCP^Me-*i*Pr)Cl] (**2b**). Hydrogen atoms are omitted for clarity.

and [N(SiMe$_2$CH$_2$P*t*Bu$_2$)$_2$]$^-$.[11,12d] The Ni(II) complex, as expected, is diamagnetic and was fully characterized by NMR spectroscopy and elemental analysis.

The solid state structures of these complexes were determined by X-ray diffraction and representations of the molecules are presented in Figures 3 and 4. Selected metrical parameters for **2b** and **3** are given in Table 1 and in the figure captions, respectively. It has to be noted that structurally characterized square planar complexes of Co(II)-Cl are rare, generally requiring strong-field ligands.[12e] The molecular structures of all these compounds show the metal in a typical slightly distorted-square planar conformation with the PCP ligands coordinated to the metal center in a tridentate meridional mode. In both complexes the C1-metal-Cl1 angles deviate slight from linearity being 171.40(9)$^\circ$ and 175.30(7)$^\circ$, respectively. The P(1)-M-P2 angles are 167.00(3) and 159.06(1)$^\circ$, respectively.
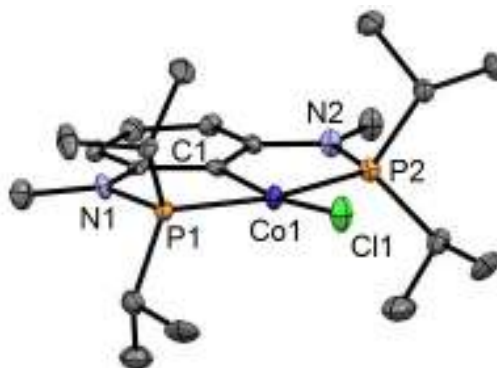
Figure 3. Structural view of [Co(PCP^Me-*i*Pr)Cl] (**2b**) showing 50% thermal ellipsoids (H atoms and a second independent complex omitted for clarity).

Figure 4. Structural view of [Ni(PCP^Me-*i*Pr)Cl] (**4**) showing 50% thermal ellipsoids (H atoms and three other independent complexes omitted for clarity). Selected bond lengths (Å) and bond angles (°): Ni1-P1 2.1811(5), Ni1-P2 2.1800(5), Ni1-C1 1.915(2), Ni1-Cl1 1.785(2), P1-Ni1-P2 165.79(2), C1-Ni1-Cl1 175.30(7).
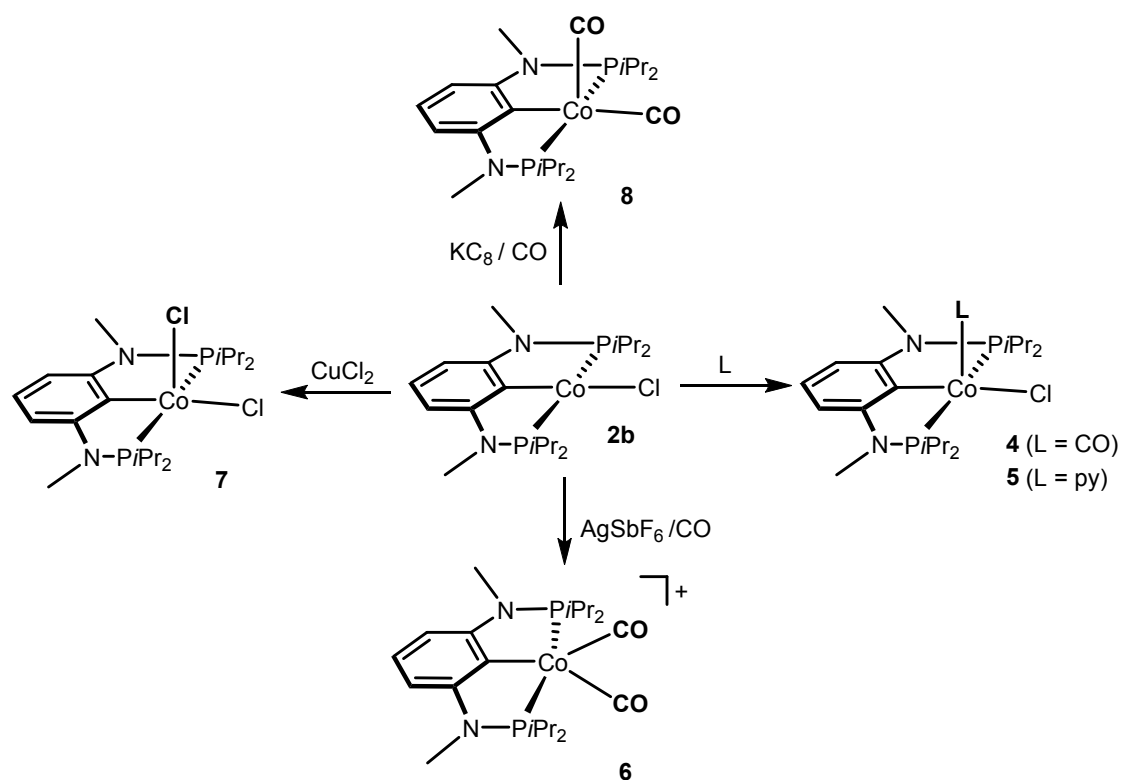
Scheme 5 Synthesis of Co(I), Co(II), and Co(III) PCP complexes based on [Co(PCP^Me-*i*Pr)Cl] (**2b**)

Complex **2b** reacts readily with the simple ligands CO and pyridine to afford the five-coordinate square-pyramidal 17e complexes [Co(PCP^Me-*i*Pr)(CO)Cl] (**4**) and [Co(PCP^Me-*i*Pr)(py)Cl] (**5**) in 94 and 95% isolated yields (Scheme 5). These complexes are paramagnetic and ^1H NMR spectra gave rise to broad and featureless signals and were not very informative. ^13C{^1H} and ^31P{^1H} NMR signals could again not be detected at all. The magnetic properties of **4** and **5** were studied by SQUID magnetometry. The cobalt effective magnetic moments extracted from a Curie law fitting to inverse

molar susceptibility data were 2.0(1) and 2.4(1)μ_B, respectively, consistent with a low-spin d^7 center (one unpaired electron) again with some degree of second-order spin orbit coupling. Moreover, the CO ligand in **4** gives rise to a strong absorption at 1948 cm^{-1} indicating strong π-back-bonding from the metal center (*cf* 2143 cm^{-1} in free CO). This is also in accordance with the fact that the CO ligand is not removable under vacuum at 25°C within several days. Complex **3**, on the other hand, does not react with CO or pyridine to give five-coordinate 18e complexes but maintains its square planar geometry.

The solid state structures of **4** and **5** were determined by single-crystal X-ray diffraction. Structural diagrams are depicted in Figures 5 and 6 with selected bond distances given in Table 1. Both complexes exhibit a distorted square-pyramidal coordination with CO and py in the apical position. The C-Co-Cl angles of **4** and **5** are 151.49(3) and 166.89(3)°, respectively, thus strongly deviating from linearity. The P-Co-P angles are 159.06(1)and 158.44(1)°, respectively. A structural feature of interest is that the apical CO ligand in **4** deviates significantly from linearity with a Co-C-O angle of 170.0(1)°. The DFT calculated value is 172° clearly showing that this is not a packing but an electronic effect. Similar structural peculiarities have been observed for square pyramidal Fe(0) complexes of the type [Fe(PNP-*t*Bu)(CO)$_2$] (PNP = di-*tert*-butylphosphinomethyl)pyridine) where this issue has been discussed in detail.[23] The bending of the apical CO ligand in **4** may be also rationalized by the theoretical investigations of Hoffmann on five-coordinate metal nitrosyl complexes.[24]

(a) (b)
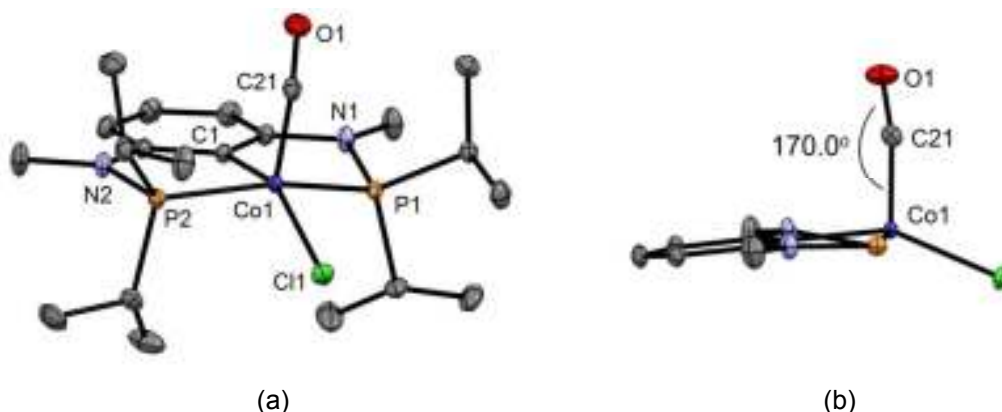
Figure 5. (a) Structural view of [Co(PCP^{Me}-*i*Pr)(CO)Cl] (**4**) showing 50% thermal ellipsoids (H atoms omitted for clarity). (b) Inner part of **4** showing the square pyramidal structure as well as the significant bending of the apical CO ligand.
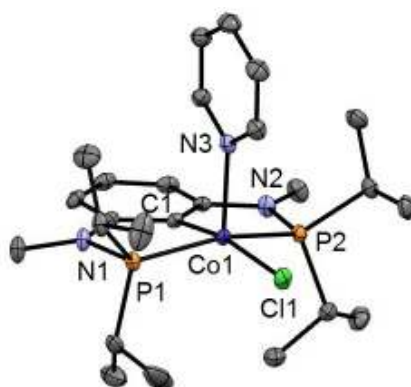
Figure 6. Structural view of [Co(PCP^{Me}-*i*Pr)(py)Cl] (**5**) showing 50% thermal ellipsoids (H atoms omitted for clarity).

The electronic structures of complexes **2b** and **4** was evaluated by DFT calculations. Representations of the frontier molecular orbitals and spin density plots are presented in Figure 7. The electronic structures correspond to low spin Co(II) complexes with the SOMO centered in the d$_{z2}$ orbital of the metal. The spin density plots confirm this view of the electronic structure with practically all the unpaired spin located on the cobalt center. There is an important participation of the PCP ligand in the second occupied molecular orbital of each complex, but no significant unpaired spin density is observed in the ligands.

(a)

(b)
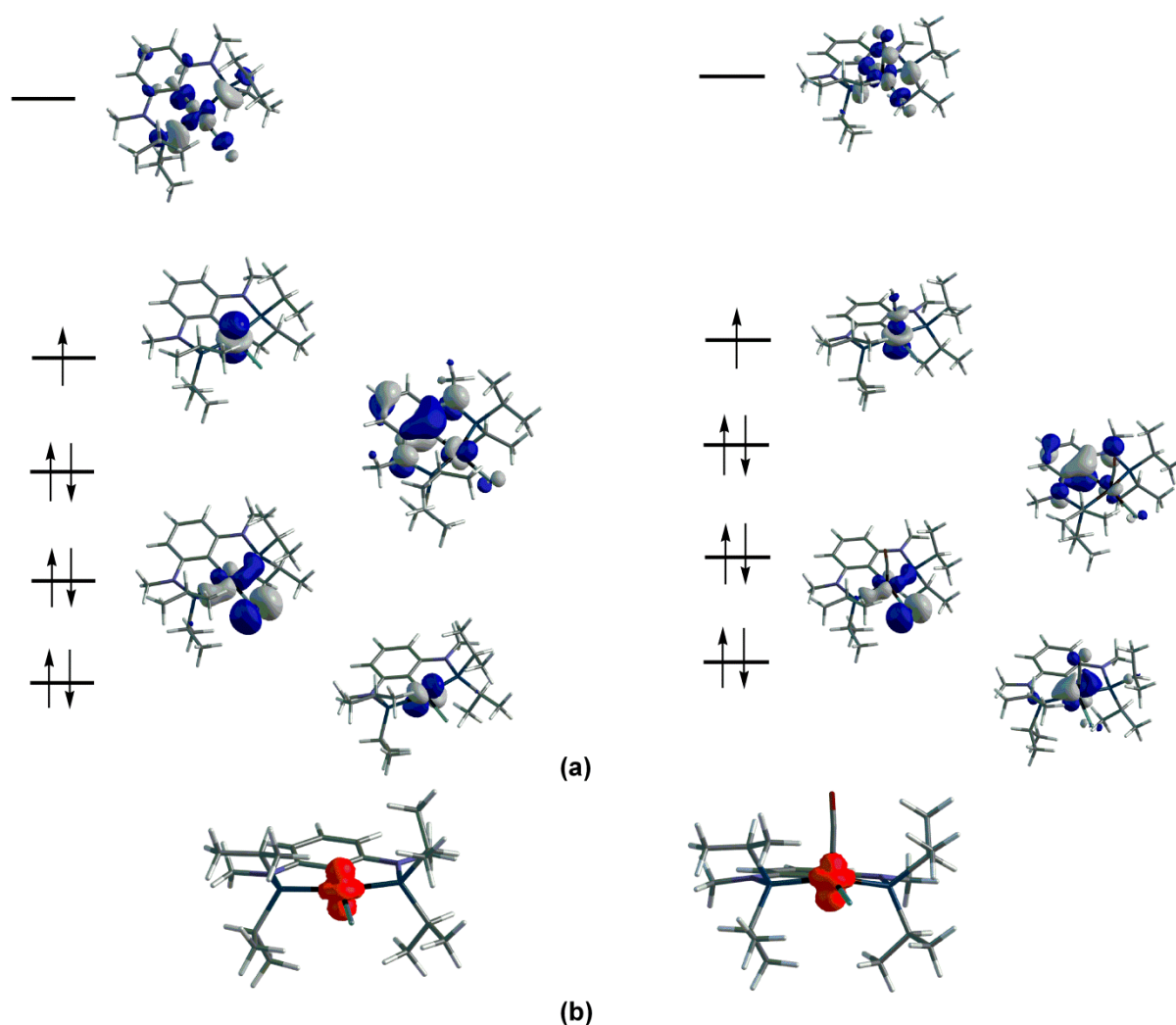
Figure 7. (a) DFT-computed frontier orbitals (*d*-splitting) and (b) spin density for [Co(PCP^{Me}-*i*Pr)Cl] (**2**) (left) and for [Co(PCP^{Me}-*i*Pr)(CO)Cl] (**4**) (right).

Under a CO atmosphere in the presence of 1 equiv of AgSbF$_6$ complex **2b** reacts readily to give the cationic dicarbonyl complex [Co(PCP^{Me}-*i*Pr)(CO)$_2$]$^+$ (**6**) in 93% yield (Scheme 5). This complex

exhibits an effective magnetic moment of $1.9(1)\mu_B$ in agreement with a d^7 low-spin electron configuration. Complex **6** exhibits two bands at 2013 and 2046 cm^{-1} in the IR spectrum for the mutually *cis* CO ligands assignable to the symmetric and asymmetric CO stretching frequencies, respectively. Moreover, complex **6** was also investigated by means of ESI-MS in the positive ion mode in a CH_3CN solution. Under so called "soft ionization" conditions, only one signal was observed at m/z 454.2 which corresponds to the mono CO fragment [Co(PCP^{Me}-*i*Pr)(CO)]$^+$ [M-CO]$^+$. This clearly suggests that one CO ligand in **6** is labile. An X-ray structure of **6** is shown in Figure 8 with selected bond distances and angles provided in Table 1. In contrast to complexes **4** and **5**, the overall geometry of **6** about the cobalt center is better described as distorted trigonal bipyramidal. The two carbonyl ligands and the benzene carbon C1 define the equatorial plane with bond angles of 93.3(1), 143.6(1), and 123.0(1)° for C21-Co1-C22, C1-Co1-C21, C1-Co1-C22, respectively. A significant distortion is also observed in the axial phosphine ligands where the P1-Co1-P2 bond angle of 162.32(2)° is contracted toward the benzene ring. The CO ligands exhibit some bending with Co1-C21-O1 and Co1-C22-O2 angles of 176.6(3) and 176.7(2)°, respectively, and is thus not as pronounced as in complex **4** where the Co1-C21-O1 angle is only 170.0(1)°.

Table 1. Selected Bond Distances (Å) and Angles (Deg) for the Co(II) PCP Complexes [Co(PCP^{Me}-*i*Pr)Cl] (**2b**), [Co(PCP^{Me}-*i*Pr)(CO)Cl] (**4**), [Co(PCP^{Me}-*i*Pr)(py)Cl] (**5**), and [Co(PCP^{Me}-*i*Pr)(CO)$_2$]SbF$_6$ (**6**).

	2b	**4**	**5**	**6**
Co1-C1	1.919(2)	1.950(1)	1.946(1)	1.953(2)
Co1-P1	2.192(1)	2.2066(4)	2.2206(3)	2.2270(6)
Co1-P2	2.184(1)	2.2134(4)	2.2057(4)	2.2154(6)
Co1-Cl1	2.234(1)	2.2743(4)	2.3103(4)	
Co1-C21		1.800(1)		1.821(2)
Co1-C22				1.833(2)
Co1-N3			2.1417(8)	
P1-Co1-P2	167.00(3)	159.06(1)	158.44(1)	162.32(2)
C1-Co1-Cl1	171.40(9)	151.49(3)	166.89(3)	
Co1-C21-O1		170.0(1)		176.6(3)
Co1-C22-O2				176.7(2)
C1-Co1-N3			96.28(3)	
C1-Co1-C21				143.62(8)
C1-Co1-C22				123.0(1)
C21-Co1-C22				93.3(1)

The metal-ligand bond lengths are generally sensitive to spin state. With respect to low-spin Co(II), a typical Co(II)-C(sp^2) bond distance is 1.994(3) Å as in the low-spin square planar cobalt(II) aryl complex [Co(PEt$_2$Ph)$_2$(mesityl)$_2$].[25] In complexes **2b**, **4**, **5**, and **6** the Co-C(sp^2) distances are in the range of 1.919 to 1.953 Å. Typical low-spin Co(II)-P bond distances are 2.2127(8) and 2.2162(8) Å

such as in [Co(CH$_2$Ph){N(SiMe$_2$CH$_2$PPh$_2$)$_2$}].[11] The Co(II)-P bond distances of complexes **2b**, **4**, **5**, and **6** are in range of 2.184 to 2.227 Å. Accordingly, both Co-C and Co-P bond distances are fully consistent with the low-spin nature of these complexes.
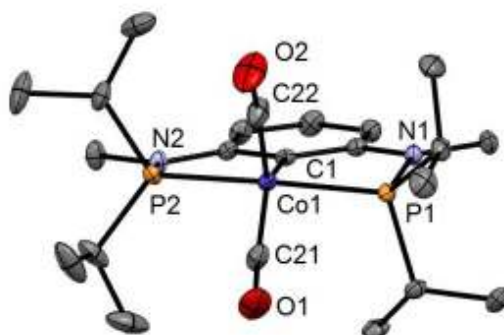
Figure 8. Structural view of [Co(PCP^{Me}-*i*Pr)(CO)$_2$]SbF$_6$ (**6**) showing 50% thermal ellipsoids (H atoms and SbF$_6^-$ counterion omitted for clarity).

Oxidation of **2b** with CuCl$_2$ cleanly affords the paramagnetic five coordinate Co(III) PCP complex [Co(PCP^{Me}-*i*Pr)Cl$_2$] (**7**) in 93% isolated yield (Scheme 5). The solution magnetic moment of 3.1μ_B (Evans method)[26] is consistent with a d^6 intermediate spin system, corresponding to two unpaired electrons, and is within the observed range of other five-coordinate Co(III) complexes known.[11] This complex displays a large paramagnetic shifted ^{1}H NMR spectrum. At room temperature the line widths are relatively narrow in this particular case and, thus, some ligand resonances could be assigned on the basis of integration. ^{13}C{^{1}H} and ^{31}P{^{1}H} NMR signals could not be detected at all. A structural view of this complex is shown in Figure 9 with selected bond distances and angles reported in the caption. The molecular structure shows the metal in a distorted-square pyramidal conformation which is not uncommon for five-coordinate Co(III) complexes.[11]

Treatment of **7** with AgSbF$_6$ in CH$_3$CN affords, on workup, the diamagnetic tris-acetonitrile complex [Co(PCP^{Me}-*i*Pr)(CH$_3$CN)$_3$](SbF$_6$)$_2$ (**9**) (Scheme 6). This complex was characterized by a combination of elemental analysis and ^{1}H, ^{13}C{^{1}H}, and ^{31}P{^{1}H} NMR spectroscopy.
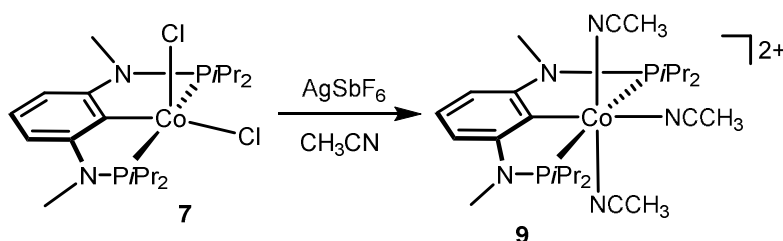
Scheme 6 Synthesis of [Co(PCP^{Me}-*i*Pr)(CH$_3$CN)$_3$]$^{2+}$ (**9**)
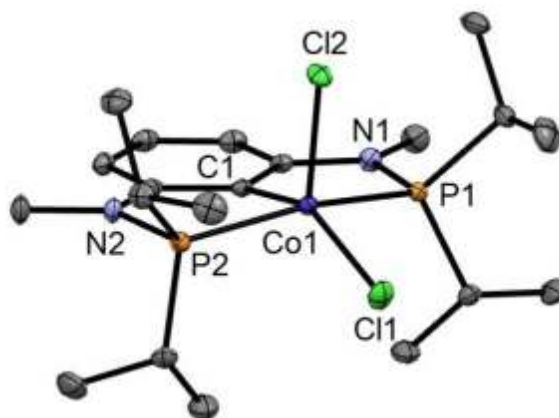
Figure 9. Structural view of [Co(PCP^{Me}-*i*Pr)Cl$_2$] (**7**) showing 50% thermal ellipsoids (H atoms omitted for clarity). Selected bond lengths (Å) and bond angles (°): Co1-P1 2.2549(4), Co1-P2 2.2602(4), Co1-C1 1.937(1), Co1-Cl1 2.2635(4), Co1-Cl2 2.2918(3), P1-Co1-P2 161.16(1), C1-Co1-Cl1 148.87(3), C1-Co1-Cl2 106.77(3), Cl1-Co1-Cl2 104.36(1).

The synthesis of the Co(I) complex [Co(PCP^{Me}-*i*Pr)(CO)$_2$] (**8**) was achieved by stirring **2b** in toluene with stoichiometric amounts of the strong reducing agent KC$_8$ in the presence of carbon monoxide (Scheme 5). This compound was obtained in 90% isolated yield as an air-sensitive but thermally stable yellow solid. The identity of this complex was unequivocally established by ^{1}H, ^{13}C{^{1}H} and ^{31}P{^{1}H} NMR, IR spectroscopy, and elemental analysis. Complex **8** exhibits two bands at 1906 and 1963 cm^{-1} in the IR spectrum for the mutually *cis* CO ligands assignable to the symmetric and asymmetric CO stretching frequencies, respectively. For comparison, the IR spectrum of the related Co(I) complex [Co(PCP-Ph)(CO)$_2$][10] (PCP-Ph = 1,3-bis(diphenylphosphinomethyl)benzene) shows two bands at 1929 and 1982 cm^{-1} slightly shifted to higher wave numbers indicating that PCP-*i*Pr is a stronger donor than PCP-Ph. In the cationic Co(II) complex [Co(PCP^{Me}-*i*Pr)(CO)$_2$]$^+$ (**6**) these bands were found at 2013 and 2046 cm^{-1}. The shift of the CO bands to even higher wave numbers is consistent with the more electron rich Co(I) center in **8**. In the ^{13}C{^{1}H} NMR spectrum the CO ligand gives rise to a low-field resonance as poorly resolved triplet centered at 207.6 ppm. In the ^{31}P{^{1}H} NMR spectrum a singlet at 170.7 ppm is observed.

The molecular structure of **8** was determined by X-ray crystallography. A structural view is depicted in Figure 10 with selected bond distances and angles reported in the caption. This complex adopts basically a distorted square-pyramidal geometry with C1-Co1-C21 and C1-Co1-C22 angles of 99.94(8) and 154.76(7)°, respectively. The P1-Co1-P1 angle is comparatively small being 147.69(2)° (cf 167.0, 159.1, 158.4 and 162.3° in **2**, **4**, **5**, and **6**, respectively). In this case, in contrast to **4**, the CO ligands do not deviate significantly from linearity with Co1-C21-O1 and Co1-C22-O2 angles of 178.0(1) and 175.1(2)°, respectively. The structure of **8** is very different from the structure of the related complex [Co(PCP-Ph)(CO)$_2$],[10] which adopts a distorted trigonal bipyramidal geometry, with an unusually small P−Co−P angle of 134.6(1)°.
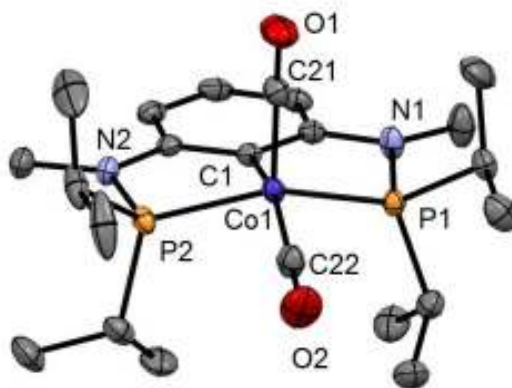
Figure 10. Structural view of [Co(PCP^{Me}-*i*Pr)(CO)$_2$] (**8**) showing 50% thermal ellipsoids (H atoms and a second independent complex omitted for clarity). Selected bond lengths (Å) and bond angles (°): Co1-P1 2.1710(5), Co1-P2 2.1740(5), Co1-C1 1.998(2), Co1-C21 1.799(2), Co1-C22 1.743(2), P1-Co1-P2 147.69(2), C1-Co1-C21 99.94(8), C1-Co1-C22 154.76(7), C21-Co1-C22 105.28(8), Co1-C21-O1 175.1(2), Co1-C22-O2 178.0(1).

Finally, the cationic 16e Ni(II) PCP complex [Ni(PCP^{Me}-*i*Pr)(CO)]$^+$ (**10**) was obtained by reacting complex **3** with 1 equiv of AgSbF$_6$ in the presence of CO (Scheme 7). The formation of a dicarbonyl complex was not observed. Complex **10** is diamagnetic and has been characterized by a combination of ^{1}H, ^{13}C{^{1}H} and ^{31}P{^{1}H} NMR, IR spectroscopy, and elemental analysis. In the IR
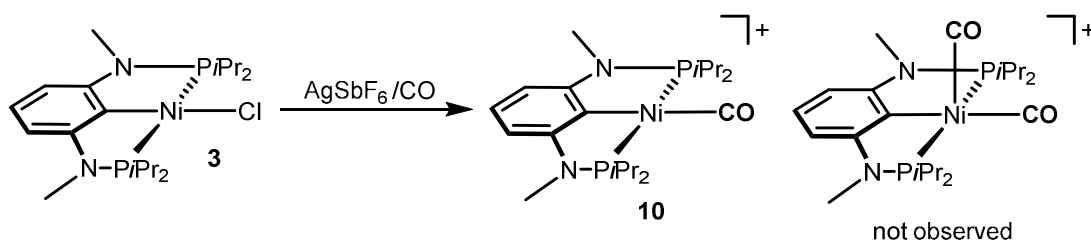
Scheme 7 Synthesis of [Ni(PCP^{Me}-*i*Pr)(CO)]$^+$ (**10**)

spectrum an intense carbonyl band was observed at 2051 cm^{-1}. In the ^{13}C{^{1}H} NMR spectrum the CO ligand gives rise to a low-field resonance triplet centered at 189.9 ppm with a coupling constant J_{CP} of 13.7 Hz. A singlet at 148.6 ppm is observed in the ^{31}P{^{1}H} NMR spectrum. In the full scan ESI-MS of **10** in the positive ion mode in CH$_3$CN only signals at m/z 453.2 and 425.2 were detected corresponding to the intact complex [Ni(PCP^{Me}-*i*Pr)(CO)]$^+$ (**10**) [M]$^+$ and the fragment [Ni(PCP^{Me}-*i*Pr)]$^+$ [M-CO]$^+$. This clearly shows that **10** is more labile than the corresponding cationic mono CO fragment of Co(II) *viz* [Co(PCP^{Me}-*i*Pr)(CO)]$^+$ where CO dissociation was not observed in the full scan ESI MS.
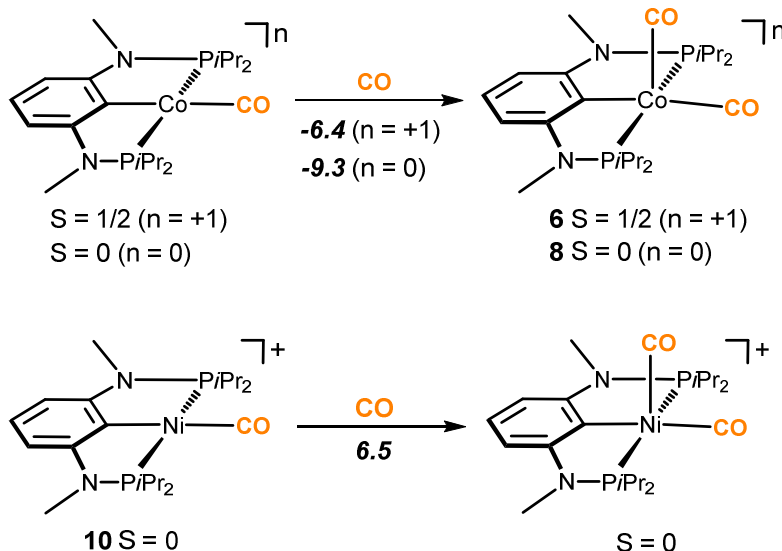
Scheme 8 Free energies (kcal/mol) calculated for the addition of CO to the 15e and 16e square planar complexes [Co(PCP^{Me}-iPr)(CO)]^n (n = +1, 0) and [Ni(PCP^{Me}-iPr)(CO)]$^+$.

The addition of CO to the 15e and 16e complexes [Co(PCP^{Me}-iPr)(CO)]^n (n = +1, 0) and to [Ni(PCP^{Me}-iPr)(CO)]$^+$ was also studied by means of DFT calculations showing that the reaction is exergonic by -6.4 and by -9.3 kcal/mol for the cationic and the neutral Co complexes, respectively, while it is endergonic by 6.5 kcal/mol in the case of [Ni(PCP^{Me}-iPr)(CO)]$^+$ (**10**) (Scheme 8).[27] This indicates that four-coordinate Co complexes are able to add a fifth ligand forming either square pyramidal or trigonal bipyramidal complexes, while Ni(II) typically remains in the 16e configuration. This, of course, may also have significant implications to catalysis with respect to substrate binding and activation.

The reactions of [Co(PCP^{Me}-iPr)Cl] (**2b**) with NaNH$_2$ and LiCH$_2$CN did not afford the desired complexes and only intractable materials were obtained (Scheme 9). Treatment of **2b** complex with methyl lithium or phenyllithium led to the formation of the four coordinate complexes [Co(PCP^{Me}-iPr)(Me)] and [Co(PCP^{Me}-iPr)(Ph)], respectively. These two complexes are paramagnetic, very air sensitive, and could not be isolated in pure form. Though, these complexes were able to form a single crystal for the X-ray measurement but these crystals were superimposed in crystal structure where we could also see the alkyl group (R = Me, Ph) with the cobalt centre (Scheme 10).
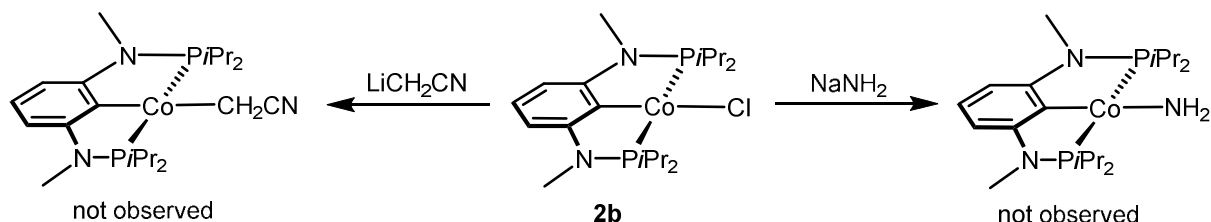
Scheme 9 Reaction of [Co(PCP^{Me}-iPr)Cl] (**2b**) with NaNH$_2$ and LiCH$_2$CN
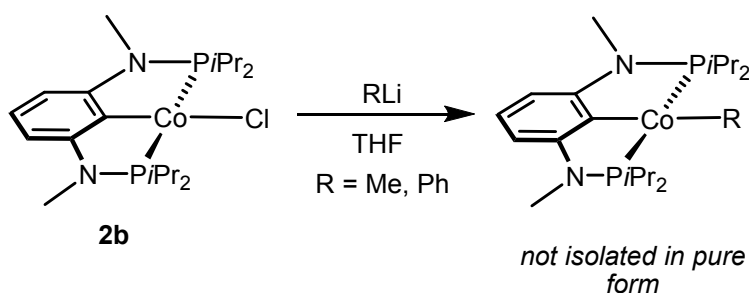
Scheme 10 Synthesis of cobalt alkyl and aryl pincer complexes [Co(PCP^{Me}-iPr)(R)] (R = Me, Ph)

2.3 Conclusion

We have shown here that a PCP pincer ligand based on 1,3-diaminobenzene acts as versatile supporting scaffold in cobalt chemistry. The PCP moiety provides access to a range of Co complexes in formal oxidation states +I, +II, and +III by utilizing the 15e square planar d^7 complex [Co(PCP^{Me}-iPr)Cl] (**2b**) as synthetic precursor. In contrast to the analogous Ni(II) complex [Ni(PCP^{Me}-iPr)Cl] (**3**), **2b** is able to form stable pentacoordinate square pyramidal or trigonal bipyramidal 17e complexes. For instance, **2b** readily adds CO and pyridine to afford the five-coordinate square-pyramidal complexes [Co(PCP^{Me}-iPr)(CO)Cl] (**4**) and [Co(PCP^{Me}-iPr)(py)Cl] (**5**), respectively, while in the presence of Ag$^+$ and CO the cationic bipyramidal complex [Co(PCP^{Me}-iPr)(CO)$_2$]$^+$ (**6**) is formed. The effective magnetic moments μ_{eff} of all Co(II) complexes derived from the temperature dependence of the inverse molar magnetic susceptibility by SQUID measurements are in the range of 1.9 to 2.4μ_B. This is consistent with a d^7 low spin configuration with a contribution from the second-order spin orbit coupling. Oxidation of **2** with CuCl$_2$ yields the Co(III) PCP complex [Co(PCP^{Me}-iPr)Cl$_2$] (**7**), while the synthesis of the Co(I) complex [Co(PCP^{Me}-iPr)(CO)$_2$] (**8**) was achieved by reducing **2b** with KC$_8$ in the presence of CO. Complex **7** exhibits a solution magnetic moment of 3.1μ_B which is consistent with a d^6 intermediate spin system. The tendency of Co(I), Co(II) and Ni(II) PCP complexes of the type [M(PCP^{Me}-iPr)(CO)]^n (n = +1, 0) to add CO was investigated by DFT calculations showing that the Co species readily form the five-coordinate complexes **6** and **8** which are thermodynamically favorable, while Ni(II) maintains the 16e configuration since CO addition is thermodynamically unfavorable in this case. X-ray structures of most complexes are provided and discussed. A structural feature of interest is that the CO ligand in **4** deviates significantly from linearity with a Co-C-O angle of 170.0(1)°. The DFT calculated value is 172° clearly showing that this is not a packing but an electronic effect.

2.4 Experimental Section

All manipulations were performed under an inert atmosphere of argon by using Schlenk techniques or in a MBraun inert-gas glovebox. The solvents were purified according to standard procedures.[28] The deuterated solvents were purchased from Aldrich and dried over 4 Å molecular sieves. [NiCl$_2$(DME)][29] and potassium graphite (KC$_8$)[30] were prepared according to the literature. ^{1}H,

^{13}C{^{1}H}, and ^{31}P{^{1}H} NMR spectra were recorded on Bruker AVANCE-250 and AVANCE-300 DPX spectrometers. ^{1}H and ^{13}C{^{1}H} NMR spectra were referenced internally to residual protio-solvent, and solvent resonances, respectively, and are reported relative to tetramethylsilane (δ = 0 ppm). ^{31}P{^{1}H} NMR spectra were referenced externally to H$_3$PO$_4$ (85%) (δ = 0 ppm.

Magnetization measurements as a function of temperature were performed on powder samples using a SQUID magnetometer (Quantum Design MPMS). The curves were obtained at 0.1 T for temperatures ranging from 5 to 300 K. The susceptibilities values were corrected for diamagnetism of the constituent atoms using Pascal constants.

All mass spectrometric measurements were performed on an Esquire 3000^{plus} 3D-quadrupole ion trap mass spectrometer (Bruker Daltonics, Bremen, Germany) in positive-ion mode electrospray ionization (ESI-MS). Mass calibration was done with a commercial mixture of perfluorinated trialkyl-triazines (ES Tuning Mix, Agilent Technologies, Santa Clara, CA, USA). All analytes were dissolved in MeOH "Lichrosolv" quality (Merck, Darmstadt, Germany) to a concentration of roughly 1 mg/mL. Direct infusion experiments were carried out using a Cole Parmer model 74900 syringe pump (Cole Parmer Instruments, Vernon Hills, IL, USA) at a flow rate of 2 μl/min. Full scan MS-scans were measured in the range m/z 100-1000 with the target mass set to m/z 800. Further experimental conditions include: drying gas temperature: 150°C; capillary voltage: -4 kV; skimmer voltage: 40 V; octapole and lens voltages: according to the target mass set. Helium was used as buffer gas for full scans. All mass calculations are based on the lowest mass cobalt and nickel isotopes (^{59}Co and ^{58}Ni-isotope). Mass spectra were averaged during data acquisition time of 1 to 2 min and one analytical scan consisted of five successive micro scans resulting in 50 and 100 analytical scans, respectively, for the final mass spectrum.

N,N'-bis(di-*iso*-propylphosphino)-N,N'-dimethyl-1,3-diaminobenzene (PCP^{Me}-*i*Pr) (1b). A suspension of N,N'-dimethyl-1,3-benzenediamine (4.9 g, 36.1 mmol) in THF (250 mL) was cooled to -78°C and *n*BuLi (73.98 mmol, 29.6 mL of a 2.5 M solution in hexane) was added in a dropwise fashion. The mixture was allowed to reach room temperature and stirred for additional 3h. Upon cooling to 0°C P*i*Pr$_2$Cl (72.18 mmol, 10.97 mL) was added slowly via a syringe and the reaction mixture was allowed to reach room temperature and stirred for 20 h. After that, the solvent was removed under reduced pressure and the crude product was dissolved in toluene (150 mL) and stirred well at 60°C for 20 min. A precipitate of lithium chloride was removed by filtration, the solvent was evaporated, and the oily residue dried under vacuum. Colorless crystals of the pure product were obtain from a saturated acetonitrile solution after cooling to -30°C for 24 hours. Yield: 12.5 g (94%). Anal. Calcd. for C$_{20}$H$_{38}$N$_2$P$_2$ (368.49): C, 65.19; H, 10.39; N, 7.60. Found: C, 65.01; H, 10.45; N, 7.68. ^{1}H NMR (δ, CDCl$_3$, 20 °C): 7.09 (t, $^3J_{HH}$= 2.5 Hz, 1H, Ph), 7.06 (d, $^4J_{HP}$ = 7.5 Hz, 1H, Ph), 6.71 (dt, $^3J_{HH}$= 2.4 Hz, $^4J_{HP}$= 8.2 Hz, 2H, Ph), 2.97 (d, $^3J_{HP}$= 1.5 Hz, 6H, NCH_3), 2.01-2.13 (m, 4H, CH), 1.00-1.17 (m, 24H, CH_3). ^{13}C{^{1}H} NMR (δ, CDCl$_3$, 20 °C): 153.2 (d, $^2J_{CP}$= 19.5 Hz, Ph), 128.1 (py), 107.4 (d, $^3J_{CP}$= 16.6 Hz, Ph), 105.3 (vt, $^4J_{CP}$= 16.1 Hz, Ph), 34.6 (d, $^2J_{CP}$= 7.5 Hz, NCH_3), 26.6 (d, $^1J_{CP}$= 16.0 Hz, CH), 19.4 (m, CH_3). ^{31}P{^{1}H} NMR (δ, CDCl$_3$, 20 °C): 71.1.

[Co(PCP-*t*Bu)Cl] (2a). A suspension of N,N'-bis(di-*tert*-butylphosphino)-1,3-diaminobenzene (PCP-*t*Bu) (**1a**) (300 mg, 0.758 mmol) and anhydrous CoCl$_2$ (104 mg, 0.796 mmol) in THF (40mL) was

refluxed for 24h. After that the solvent was removed under vacuum. The resulting crude product was dissolved in toluene, insoluble materials were removed by filtration, and the solvent was evaporated under vacuum to afford **2a** as an orange solid. Yield: 118 mg (32%). Anal. Calcd. for $C_{22}H_{41}ClCoN_2P_2$ (489.91): C, 53.94; H, 8.44; N, 5.72. Found: C, 53.89; H, 8.51; N, 5.78. μ_{eff} = 1.81(1) μ_B (CH_2Cl_2, Evans method).

[Co(PCP^{Me}-*i*Pr)Cl] (2b). A suspension of **1b** (1.0 g, 2.72 mmol) in THF (10 mL) was cooled to -78°C and *n*-BuLi (2.86 mmol, 1.14 mL of a 2.5 M solution in *n*-hexane) was slowly added in a dropwise fashion and the mixture was then allowed to reach room temperature and stirred for 2h. After that, 1.1 equivs of anhydrous $CoCl_2$ (390 mg, 2.99 mmol) were added whereupon the solution rapidly turned to deep red. After the mixture was stirred for 24h and the solvent was removed under vacuum. The resulting crude product was redissolved in CH_2Cl_2, insoluble materials were removed by filtration, and the solvent was evaporated under vacuum to afford the product as red solid. Yield: 1.2 g (96%). Anal. Calcd. for $C_{20}H_{37}ClCoN_2P_2$ (461.86): C, 52.01; H, 8.08; N, 6.07. Found: C, 52.15; H, 8.14; N, 6.15. μ_{eff} = 2.3(1)μ_B.

[Ni(PCP^{Me}-*i*Pr)Cl] (3). This complex was prepared in analogous fashion to **2b** with $NiCl_2$(DME) (327 mg, 1.50 mmol), **1b** (500mg, 1.36 mmol), and *n*-BuLi (1.43 mmol, 571 μL of a 2.5 M solution in *n*-hexane). Yield: 97% (610 mg). Anal. Calcd. for $C_{20}H_{37}ClN_2NiP_2$ (461.62): C, 52.04; H, 8.08; N, 6.07. Found: C, 51.91; H, 8.13; N, 6.13. ^{1}H NMR (δ, CD_2Cl_2, 20°C): 6.91 (t, $^3J_{HH}$= 8.4 Hz,1H, Ph), 5.86 (d, $^3J_{HH}$ = 7.9 Hz, 2H, Ph), 2.87 (vt, $^3J_{HP}$= 2.5 Hz, 6H, NCH_3), 2.46-2.60 (m, 4H, CH), 1.37-1.46 (dd, $^3J_{HH}$= 7.5 Hz, $^3J_{HP}$= 15 Hz, 12H, CH_3), 1.25-1.33 (dd, $^3J_{HH}$= 7.5 Hz, $^3J_{HP}$= 15 Hz, 12H, CH_3). ^{13}C{^{1}H} NMR (δ, CD_2Cl_2, 20°C): 161.6 (t, $^2J_{CP}$= 16.8 Hz, Ph), 126.9 (Ph), 120.9 (vt, $^2J_{CP}$= 19.8 Hz, Ph), 100.4 (vt, $^3J_{CP}$= 5.9 Hz, Ph), 31.9 (s, NMe), 25.4 (t, $^1J_{CP}$= 11.1 Hz, CH), 17.8 (CH_3). ^{31}P{^{1}H} NMR (δ,CD_2Cl_2, 20°C): 120.4.

[Co(PCP^{Me}-*i*Pr)(CO)Cl] (4). A suspension of **2b** (200 mg, 0.43 mmol) in toluene was stirred und a CO atmosphere and the solution immediately turned from red to brown. After removal of the solvent under vacuum complex **4** was obtained as a brown solid. Yield: 94% (200 mg). Anal. Calcd. for $C_{21}H_{37}ClCoN_2OP_2$ (489.87): C, 51.49; H, 7.61; N, 5.72. Found: C, 51.65; H, 7.69; N, 5.65. μ_{eff} = 2.0(1)μ_B. IR (ATR, cm^{-1}): 1948 (ν_{CO}).

[Co(PCP^{Me}-*i*Pr)(py)Cl] (5). To a suspension of **2b** (200 mg, 0.43 mmol) in toluene (5 mL) excess of pyridine (0.5 mL) was added and stirred for 2h. After removal of the solvent under reduced pressure, complex **5** was obtained in analytically pure form as a yellow solid. Yield: 222 mg (95%). Anal. Calcd. for $C_{25}H_{42}ClCoN_3P_2$ (540.96): C, 55.51; H, 7.83; N, 7.77. Found: C, 55.66; H, 7.79; N, 7.82. μ_{eff} = 2.4(1)μ_B.

[Co(PCP^{Me}-*i*Pr)(CO)$_2$]SbF$_6$ (6). A suspension of **2b** (100 mg, 0.216 mmol) in CH_2Cl_2 was treated with AgSbF$_6$ (75 mg, 0.217 mmol) under a CO atmosphere and stirred for 1h. After that, the solution was filtered through Celite, and the solvent was removed under reduced pressure to afford a blue-green solid. Yield: 147 mg (93%). Anal. Calcd. for $C_{22}H_{37}CoF_6N_2O_2P_2Sb$ (717.18): C, 36.79; H, 5.19; N, 3.90. Found: C, 36.85; H, 5.23; N, 3.88. IR (ATR, cm^{-1}): 2013 (ν_{CO}), 2046 (ν_{CO}). μ_{eff} = 1.9(1)μ_B. ESI-MS (*m/z,* CH_3CN) positive ion: 454.2 [M-CO]$^+$.

[Co(PCP^{Me}-*iPr*)Cl$_2$] (7). A suspension of **2b** (200 mg, 0.43 mmol) in THF was reacted with CuCl$_2$ (64 mg, 0.47 mmol) and stirred for 30 min. After that, the solvent was evaporated and CH$_2$Cl$_2$ was added and stirred for 15 min. After that, the solution was filtered through Celite, and the solvent was removed under reduced pressure to afford a green solid. Yield: 93% (200 mg). Anal. Calcd. for C$_{20}$H$_{37}$Cl$_2$CoN$_2$P$_2$ (497.31): C, 48.30; H, 7.50; N, 5.63. Found: C, 48.35; H, 7.49; N, 5.67. ^{1}HNMR (δ, C$_6$D$_6$, 20°C): 37.22 (br, 1H), 29.63 (br, 2H), 3.63 (br, 6H), 0.31-2.35 (br, 22H), -6.37 (br, 6H). μ_{eff} = 3.1μ_B (CH$_2$Cl$_2$, Evans method).

[Co(PCP^{Me}-*iPr*)(CO)$_2$] (8). A suspension of **2b** (100 mg, 0.23 mmol) in toluene was treated with 1.1 equivs of freshly prepared KC$_8$ under a CO atmosphere and was stirred for 30 min. After that, the product was filtered through Celite, the solvent was removed under vacuum and an analytically pure yellow solid was obtained. Yield: 90% (100 mg). Anal. Calcd. for C$_{22}$H$_{37}$CoN$_2$O$_2$P$_2$ (482.43): C, 54.77; H, 7.73; N, 5.81. Found: C, 54.75; H, 7.79; N, 5.72. ^{1}HNMR (δ, C$_6$D$_6$, 20°C): 7.19 (t, $^3J_{HH}$= 9.2 Hz, 1H, Ph), 6.17 (d, $^3J_{HH}$= 7.5 Hz, 2H, Ph), 2.61 (s, 6H, NCH$_3$), 2.11-2.26 (m, 4H, C*H*), 1.27 (dd, $^3J_{HH}$= 7.5 Hz, $^3J_{HP}$= 17.5 Hz, 12H, C*H*$_3$), 1.09 (dd, $^3J_{HH}$= 7.5 Hz, $^3J_{HP}$= 12.5 Hz, 12H, C*H*$_3$). ^{13}C{^{1}H} NMR (δ, C$_6$D$_6$, 20°C): 207.6 (br, CO), 157.3 (t, $^4J_{CP}$ = 15.0 Hz, Ph), 129.0 (Ph), 124.3 (Ph), 100.6 (vt, $^3J_{CP}$ = 5.9 Hz, Ph), 31.9 (NCH$_3$), 31.4 (vt, $^1J_{CP}$= 11.8 Hz, CH), 18.2 (d, $^2J_{CP}$= 10.6 Hz, CH$_3$), the C$_{ipso}$ carbon atom was not detected. ^{31}P{^{1}H} NMR (δ, C$_6$D$_6$, 20°C): 170.6. IR (ATR, cm^{-1}): 1906 (ν_{CO}), 1963 (ν_{CO}).

[Co(PCP^{Me}-*iPr*)(CH$_3$CN)$_3$](SbF$_6$)$_2$ (9). A suspension of **8** (200 mg, 0.43 mmol) in CH$_3$CN (5 mL) was treated with AgSbF$_6$ (274 mg, 0.80 mmol) and the mixture was stirred for 30 min. After that, the solvent was evaporated and the crude product redissolved in CH$_2$Cl$_2$. Insoluble materials were removed by filtration and upon removal of the solvent a brown solid was obtained. Yield: 265 mg (93%). Anal. Calcd. for C$_{26}$H$_{46}$CoF$_{12}$N$_5$P$_2$Sb$_2$ (1021.07): C, 30.58; H, 4.54; N, 6.86. Found: C, 30.65; H, 4.69; N, 6.52. ^{1}HNMR (δ, CD$_2$Cl$_2$, 20°C): 7.18 (t, $^3J_{HH}$= 15.0 Hz, 1H, Ph), 6.29 (d, $^3J_{HH}$ = 10.0 *Hz*, 1H, Ph), 3.18 (s, 6H, NC*H*$_3$), 2.90-3.07 (m, 4H, C*H*), 2.59 (s, 3H, C*H*$_3$CN), 2.27 (s, 6H, C*H*$_3$CN), 1.38-1.51 (m, 24H, C*H*$_3$). ^{13}C{^{1}H} NMR (δ, CD$_2$Cl$_2$, 20°C): 158.2 (t, $^2J_{CP}$= 11.6 Hz, Ph), 135.3 (CN), 131.5 (*C*N), 129.0 (Ph), 111.5 (d, $^2J_{CP}$= 5.6 Hz, Ph), 104.8 (d, $^3J_{CP}$= 3.9 Hz, Ph), 34.1 (NCH$_3$), 28.4 (*C*H), 18.7 (*C*H$_3$), 17.8 (*C*H$_3$), 5.4 (*C*H$_3$CN), 3.4 (*C*H$_3$CN). ^{31}P{^{1}H} NMR (δ, CD$_2$Cl$_2$, 20°C): 133.2.

[Ni(PCP^{Me}-*iPr*)(CO)]SbF$_6$ (10). A suspension of **3** (100 mg, 0.217 mmol) in CH$_2$Cl$_2$ was treated with AgSbF$_6$ (89 mg, 0.26 mmol) under a CO atmosphere and stirred for 2h. After that, the solution was filtered through Celite, and the solvent was removed under reduced pressure to afford yellow solid. Yield: 130 mg (87%). Anal. Calcd. for C$_{21}$H$_{37}$NiF$_6$N$_2$OP$_2$Sb (689.93): C, 36.56; H, 5.41; N, 4.06. Found: C, 36.45; H, 5.40; N, 3.96. ^{1}H NMR (δ, CD$_2$Cl$_2$, 20°C): 7.21 (t, $^3J_{HH}$= 8.7 Hz, 1H, Ph), 6.18 (d, $^3J_{HH}$= 8.4, 2H, Ph), 2.81 (vt, $^3J_{HP}$= 2.5 Hz, 6H, NC*H*$_3$), 2.69-2.85 (m, 4H, C*H*), 1.24-1.43 (m, 24H, C*H*$_3$). ^{13}C{^{1}H} NMR (δ, CD$_2$Cl$_2$, 20°C): 189.9 (t, $^2J_{CP}$ = 13.7 Hz, CO), 161.9 (t, $^2J_{CP}$= 14.0 Hz, Ph), 133.0 (s, Ph), 102.7 (t, $^2J_{CP}$= 6.6 Hz, ^{4}Ph), 32.4 (NCH$_3$), 28.1 (vt, $^1J_{CP}$= 14.0 Hz, CH), 18.5 (*C*H$_3$), 18.0 (s, *C*H$_3$), the C$_{ipso}$ carbon atom was not detected. ^{31}P{^{1}H} NMR (δ, CD$_2$Cl$_2$, 20°C): 148.6. IR (ATR, cm^{-1}): 2051 (ν_{CO}). ESI-MS (*m/z*, CH$_3$CN) positive ion: 453.2 [M]$^+$, 425.2 [M-CO]$^+$.

X-ray Structure Determination. X-ray diffraction data for **2a**, **2b**, **3**, **4**, **5**, **6**, **7** and **10** were collected at *T* = 100 K on a Bruker Kappa APEX-2 CCD diffractometer with an Oxford Cryosystems

cooler using graphite-monochromatized Mo-$K\alpha$ radiation (λ = 0.71073 Å). For **8** a Bruker SMART APEX three-circle diffractometer was used instead. Redundant data sets were collected in φ- and ω-scan modes (**8**: only ω-scans) covering the whole reciprocal sphere. Automatic lattice parameter determination failed for **2b**. Inspection of the reflection data revealed the existence of two domains, which were separated using the RLATT tool of the Apex2 software suite.[31] The reflections of both domains could be assigned to two isometric monoclinic cells, related by a reflection at (100). Data of all crystals were reduced to intensity values with SAINT and an absorption correction was applied with the multi-scan approach implemented in SADABS (**2**: TWINABS).[30] The structures were solved by charge flipping using SUPERFLIP[32] and refined against F with JANA2006.[33] Non-hydrogen atoms were refined with anisotropic displacement parameters. Hydrogen atoms were placed at calculated positions and refined as riding on the parent C atom. Since **2b** crystallizes in the non-centrosymmetric space group *Pc*, it was refined as four domains with the twin-volume fractions of three domains as refineable parameter. The crystal was composed of two domains related by reflection at (100), whereas contributions of the inverted domains are negligible (Flack parameter 0.038(6)). In **5** significant albeit smeared out electron density was observed in channels of the structure around the three-fold rotoinversion axes. Attempts to model disordered pentane solvent molecules were unsuccessful and therefore the contribution of this electron cloud (65 e per channel and unit-cell, slightly less than one pentane molecule, 72 e) to the intensity data was removed using the SQUEEZE routine of PLATON.[34] Molecular graphics were generated with program MERCURY.[35] Crystal data and experimental details are given in Table S1 S2 and S3.

Table S1. Details for the crystal structure determinations of [Co(PCP-*t*Bu)Cl] **2a**

	2a
formula	$C_{22}H_{41}ClCoN_2P_2$
fw	489.9
cryst.size, mm	0.78 x 0.66 x 0.02
color, shape	red plate
crystal system	orthorhombic
space group	*Pna*2_1 (no. 33)
a, Å	22.7302(12)
b, Å	7.994(2)
c, Å	13.738(4)
α, °	90
β, °	90
γ, °	90
V, Å^3	2496.2(9)
T, K	100
Z,Z'	4,1
ρ_{calc}, g cm^{-3}	1.3032
μ, mm^{-1} (MoKα)	0.934
F(000)	1044
absorption corrections, T_{min}-T_{max}	multi-scan, 0.49–0.98
θ range, deg	2.33–30.16
no. of rflns measd	50010
R_{int}	0.0714
no. of rflns unique	7334
no. of observed rflns	5460
no. of params / restraints	262 / 0
R (obs) [a]	0.0359
R (all data)	0.0616
wR (obs)	0.0349
wR (all data)	0.0373
GooF	1.280
Diff.Four.peaks min/max, eÅ^{-3}	-0.31 / 0.35
Flack Parameter	0.030(11)
CCDC no.	1044983

[a] $R = \Sigma||F_o|-|F_c|| \,/\, \Sigma|F_o|$, $wR = \Sigma w(|F_o| - |F_c|) \,/\, \Sigma w|F_o|$, $GooF = \{\Sigma[w(F_o^2 - F_c^2)^2] \,/\, (n–p)\}^{\frac{1}{2}}$

Table S2. Details for the crystal structure determinations of compounds [Co(PCP^Me-*i*Pr)Cl] (**2b**), [Ni(PCP^Me-*i*Pr)Cl] (**3**), [Co(PCP^Me-*i*Pr)(CO)Cl] (**4**), and [Co(PCP^Me-*i*Pr)(py)Cl] (**5**).

	2b	3	4	5
formula	$C_{20}H_{37}ClCoN_2P_2$	$C_{20}H_{37}ClN_2NiP_2$	$C_{21}H_{37}ClCoN_2OP_2$	$C_{25}H_{42}ClCoN_3P_2$
fw	461.9	461.6	489.9	541.0
cryst.size, mm	0.63 x 0.38 x 0.30	0.44 x 0.34 x 0.03	0.67 x 0.53 x 0.20	0.76 x 0.53 x 0.12
color, shape	dark red block	yellow block	dark red plate	dark red trapezoidal
crystal system	monoclinic	monoclinic	orthorhombic	trigonal
space group	*Pc* (no. 7)	*P2/c* (no. 13)	*Pbca* (no. 61)	*R-3*
a, Å	14.566(3)	37.370(3)	14.6089(13)	38.9446(13)
b, Å	11.279(2)	8.0272(6)	17.1689(16)	38.9446(13)
c, Å	14.640(3)	34.986(3)	19.2961(18)	9.6467(7)
α, °	90	90	90	90
β, °	105.829(5)	116.886(4)	90	90
γ, °	90	90	90	120
V, Å^3	2314.1(7)	9360.5(13)	4839.8(8)	12670.8(11)
T, K	100	100	100	100
Z	4	16	8	18
ρ_{calc}, g cm^{-3}	1.3253	1.3098	1.3442	1.2757
μ, mm^{-1} (MoKα)	1.003	1.087	0.966	0.835
$F(000)$	980	3936	2072	5166
absorption corrections,	multi-scan, 0.64–0.74	multi-scan, 0.51–0.81	multi-scan, 0.54–0.82	multi-scan, 0.59–0.90
θ range, deg	1.45–33.06	1.16–28.08	2.11–32.61	1.05–32.59
no. of rflns measd	81191	289067	272647	168931
R_{int}	0.0704	0.0459	0.0521	0.0378
no. of rflns unique	81161	22543	8823	10278
no. of rflns $I>3\sigma(I)$	68052	18899	7050	8900
no. of params /	472 / 0	937 / 0	253 / 0	289 / 0
R ($I > 3\sigma(I)$)	0.0499	0.0629	0.0290	0.0270
R (all data)	0.0631	0.0766	0.0462	0.0334
wR ($I > 3\sigma(I)$)	0.0720	0.0770	0.0407	0.0428
wR (all data)	0.0743	0.0779	0.0424	0.0452
GooF	1.39	3.93	1.48	1.64
Diff.Four.peaks min/max, eÅ^{-3}	-0.52 / 0.69	-0.86 / 1.80	-0.31 / 0.44	-0.33 / 0.44
Twin operation	Reflection at (100)	-	-	-
Twin volume ratio	0.632:0.367(11)	-	-	-
Flack parameter	0.038(6)	-	-	-

Table S3. Details for the crystal structure determinations of compounds [Co(PCP^{Me}-*i*Pr)(CO)$_2$]SbF$_6$ (**6**), [Co(PCP^{Me}-*i*Pr)Cl$_2$] (**7**), [Co(PCP^{Me}-*i*Pr)(CO)$_2$] (**8**), and [Ni(PCP^{Me}-*i*Pr)(CO)]SbF$_6$ (**10**).

	6	7	8	10
formula	C$_{22}$H$_{37}$CoF$_6$N$_2$O$_2$P$_2$Sb	C$_{20}$H$_{37}$Cl$_2$CoN$_2$P$_2$	C$_{22}$H$_{37}$CoN$_2$O$_2$P$_2$	C$_{21}$H$_{37}$F$_6$N$_2$NiOP$_2$Sb
fw	718.2	497.3	482.4	689.9
cryst.size, mm	0.62 x 0.32 x 0.23	0.78 x 0.63 x 0.44	0.60 x 0.30 x 0.25	0.63 x 0.29 x 0.11
color, shape	dark blue rod	dark green block	translucent red /	yellow plate
crystal system	monoclinic	orthorhombic*Pbca* (no.	triclinic	monoclinic
space group	*P*2$_1$/*n* (no. 14)	*Pbca* (no. 61)	*P*-1 (no. 2)	*P*2$_1$/*n (no. 14)*
a, Å	14.7515(15)	11.4194(8)	8.0970(5)	14.6254(12)
b, Å	8.4907(9)	15.3929(11)	17.8216(11)	8.4029(7)
c, Å	23.347(2)	26.9717(18)	17.9396(11)	23.161(2)
α, °	90	90	70.854(3)	90
β, °	104.923(3)	90	80.438(3)	105.928(2)
γ, °	90	90	80.517(3)	90
V, Å^3	2825.6(5)	4741.0(6)	2394.6(3)	2737.2(4)
T, K	100	100	100	100
Z	4	8	4	4
ρ_{calc}, g cm^{-3}	1.6876	1.3930	1.3377	1.6737
μ, mm^{-1} (MoKα)	1.718	1.093	0.870	1.849
F(000)	1444	2096	1024	1392
absorption	multi-scan, 0.52–0.67	multi-scan, 0.44–0.61	multi-scan, 0.74–0.81	multi-scan, 0.54–0.89
θ range, deg	1.48–32.62	2.34–32.66	2.35–32.54	1.49–32.65
no. of rflns measd	81348	284978	30437	59202
R_{int}	0.0316	0.0378	0.0242	0.0317
no. of rflns unique	10289	8651	15986	10006
no. of rflns *I*>3σ(*I*)	9198	7707	13036	8336
no. of params /	330 / 0	244 / 0	523 / 0	327 / 0
R (*I* > 3σ(*I*))	0.0307	0.0244	0.0398	0.0264
R (all data)	0.0357	0.0300	0.0496	0.0355
wR (*I* > 3σ(*I*))	0.0464	0.0508	0.0489	0.0323
wR (all data)	0.0471	0.0525	0.0501	0.0332
GooF	2.70	1.46	2.00	1.70
Diff.Four.peaks min/max, eÅ^{-3}	-1.14 / 1.12	-0.19 / 0.27	-0.72 / 1.63	-0.67 / 1.26

Computational Details. All calculations were performed using the GAUSSIAN 09 software package[36] on the Phoenix Linux Cluster of the Vienna University of Technology. The optimized geometries were obtained with spin unrestricted calculations, using the B3LYP functional.[37] That functional includes a mixture of Hartree-Fock[38] exchange with DFT[21] exchange-correlation, given by Becke's three parameter functional with the Lee, Yang and Parr correlation functional, which includes both local and non-local terms.

The basis set used for the geometry optimizations (basis b1) consisted of the Stuttgart/Dresden ECP (SDD) basis set[39] to describe the electrons of Co and Ni, and a standard 6-31G(d,p) basis set[40] for all other atoms. Frequency calculations were performed to confirm the nature of the stationary points, yielding no imaginary frequency for the minima. The electronic energies (E_{b1}) obtained at the B3LYP/b1 level of theory were converted to free energy at 298.15 K and 1 atm (G_{b1}) by using zero point energy and thermal energy corrections based on structural and vibration frequency data calculated at the same level. The molecular orbitals presented in Figure 6a resulted from single point restricted open shell calculations performed on the optimized structures.

Single point energy calculations were performed using the M06 functional and a standard 6-311++G(d,p) basis set,[41] on the geometries optimized at the B3LYP/b1 level. The M06 functional is a hybrid meta-GGA functional developed by Truhlar and Zhao,[42] and it was shown to perform very well for transition metal systems, providing a good description of weak and long range interactions.[43] Solvent effects (benzene) were considered in the M06/6-311++G(d,p)//B3LYP/b1 energy calculations using the Polarizable Continuum Model (PCM) initially devised by Tomasi and coworkers[44] with radii and non-electrostatic terms of the SMD solvation model, developed by Truhler *et al.*[45]

The free energy values presented along the text (G_{b2}^{soln}) were derived from the electronic energy values obtained at the M06/6-311G(d,p)//B3LYP/b1 level, including solvent effects (E_{b2}^{soln}), according to the following expression: $G_{b2}^{soln} = E_{b2}^{soln} + G_{b1} - E_{b1}$. Three-dimensional representations of the orbitals were obtained with the program Chemcraft.[46]

References

1   For reviews on pincer complexes, see: (a) Albrecht, M.; van Koten, G. *Angew. Chem., Int. Ed.* **2001**, *40*, 3750-3781. (b) van der Boom, M. E.; Milstein, D. *Chem. Rev.* **2003**, *103*, 1759-1792. (c) Singleton, J. T. *Tetrahedron* **2003**, *59*, 1837. (d) Bhattacharya, P.; Guan, H. *Comment Inorg. Chem.* **2011**, *32*, 88. (e) Schneider, S.; Meiners, J.; Askevold, B. *Eur. J. Inorg. Chem.* **2012**, 412-429. (f) Morales-Morales, D.; Jensen, C. M. Eds. The Chemistry of Pincer Compounds; Elsevier: Amsterdam, **2007**. (g) van Koten, G., Milstein, D., Eds.; Organometallic Pincer Chemistry; Springer: Berlin, **2013**; *Top. Organomet. Chem.* Vol. 40.

2   Benito-Garagorri, D.; Kirchner, K. *Acc. Chem. Res.* **2008**, *41*, 201-213.

3   Benito-Garagorri, D., Bocokić, V.; Mereiter, K.; Kirchner, K. *Organometallics* **2006**, *25*, 3817-3823.

4   For recent examples of Fe PNP complexes based on the 2,6-diamonopyridine scaffold see: (a) Bichler, B.; Holzhacker, C.; Stöger, B.; Puchberger, M.; Veiros, L. F.; Kirchner, K. *Organometallics* **2013***, 32*, 4114-4121. (b) Benito-Garagorri, D.; Alves, L. G.; Veiros, L. F.; Standfest-Hauser, C. M.; Tanaka, S.; Mereiter, K.; Kirchner, K. *Organometallics* **2010**, *29*, 4932-4942. (c) Benito-Garagorri, D., Puchberger, M.; Mereiter, K.; Kirchner, K. *Angew. Chem., Int. Ed.*, **2008**, *47*, 9142-9145.

5   For recent examples of Mo PNP complexes based on the 2,6-diamonopyridine scaffold see: (a) Öztopcu, Ö.; Holzhacker, C.; Puchberger, M.; Weil, M.; Mereiter, K.; Veiros, L. F.; Kirchner, K. *Organometallics* **2013**, *32*, 3042-3052. (b) de Aguiar, S. R. M. M.; Stöger, B.; Pittenauer, E.; Allmaier, G.; Puchberger, M.; Veiros, L. F.; Kirchner, K. *J. Organomet. Chem.* **2014**, *760*, 74-83.

6   Xu, G. Q.; Sun, H. J.; Li, X. Y. *Organometallics* **2009**, *28*, 6090-6095.

7   Lian, Z.; Xu, G.; Li, X. *Acta Crystallogr., Sect. E:* Struct. Rep. Online **2010**, *E66*, m636.

8   Hebden, T. J.; St. John, A. J.; Gusev, D. G.; Kaminsky, W.; Goldberg, K. I.; Heinekey, D. M. *Angew. Chem. Int. Ed.* **2011,** *50,* 1873-1876.

9   Zhu, G.; Li, X.; Xu, G.; Wang, L.; Sun, H. *Dalton Trans.* **2014**, *43*, 8595-8598.

10   Kent, M. A.; Woodall, C. H.; Haddow, M. F.; McMullin, C. L.; Pringle, P. G.; Wass, D. F. *Organometallics* **2014**, *33,* 5686-5692.

11   Fryzuk, M. D.; Leznoff, D. B.; Thompson., R. C.; Rettig, S. J. *J. Am. Chem. Soc.* **1998**, *120,* 10126-10135.

12   (a) M. J. Ingleson, M. Pink, K. G. Caulton, *J. Am. Chem. Soc.* **2006**, *128*, 4248-4249. (b) M. Ingleson, H. Fan, M. Pink, J. Tomaszewski, K. G. Caulton, *J. Am. Chem. Soc.* **2006**, *128*, 1804-1805. (c) Ingleson, M. J.; Fullmer, B. C.; Buschhorn, D. T.; Fan, H.; Pink, M.; Huffman, J. C.; Caulton, K. G. *Inorg. Chem.* **2008**, *47*, 407-409. (d) M. J. Ingleson, M. Pink, H. Fan, K. G. Caulton, *J. Am. Chem. Soc.* **2008**, 130, 4262-4276. (e) M. J. Ingleson, M. Pink, H. Fan, K. G. Caulton, *Inorg. Chem.* **2007**, *46*, 10321-10334.

13   (a) Rozenel, S. S.; Padilla, R.; Arnold, J. *Inorg. Chem.* **2013**, 52, 11544−11550. (b) Rozenel, S. S.; Padilla, R.; Camp, C.; Arnold, J. *Chem. Commun.* **2014**, *50*, 2612-2614.

14   Fout, A. R.; Basuli, F.; Fan, H.; Tomaszewski, J.; Huffman, J. C.; Baik, M.-H.; Mindiola, D. J. *Angew. Chem. Int. Ed.* **2006**, *45*, 3291-3295.

15   Semproni, S. P.; Milsmann, C.; Chirik, P. J. *J. Am. Chem. Soc.* **2014**, *136*, 9211-9224.

16   Khaskin, E.; Diskin-Posner, Y.; Weiner, Leitus, L. G.; Milstein, D. *Chem. Commun.,* 2013, **49**, 2771-2773.

17   Wu, S.; Li, X.; Xiong, Z.; Xu, W.; Lu, Y.; Sun, H. *Organometallics* **2013**, *32*, 2327-2337.

18   Hosokawa, S.; Ito, J.; Nishiyama, H. *Organometallics* **2013**, *32*, 3980-3985.

19   Sauer, D. C.; Kruck, M.; Wadepohl, H.; Enders, M.; Gade, L. H. *Organometallics* **2013**, *32*, 885-892

20   (a) Carlin, R. L. *Magnetochemistry*; Springer-Verlag: Heidelberg, **1986**. (b) Orchard, A. F. *Magnetochemistry*; Oxford University Press, **2003**.

21   Parr, R. G.; Yang, W. *Density Functional Theory of Atoms and Molecules*, Oxford University Press, New York, 1989.

22   Obtained at the B3LYP/b1 level (see Computational Details).

23   For a discussion and references of bend CO ligands, see: Pelczar, E. M.; Emge, T. J.; Krogh-Jespersen, K.; Goldman, A. S. *Organometallics* **2008**, *27*, 5759-5767.

24   Hoffmann, R.; Chen, M. M. L.; Elian, M.; Rossi, A. R.; Mingos, D. M. P. *Inorg. Chem.* **1974**, *13*, 2666–2675.

25   Falvello, L.; Gerloch, M. *Acta Crystallogr. B* **1979**, *B35*, 2547.

26   Sur, S. K. *J. Magn. Reson.* **1989**, *82*, 169.

27   Free energy values including solvent effects (PCM model, see Computational Details).

28   Perrin, D. D.; Armarego, W. L. F. *Purification of Laboratory Chemicals*, 3rd ed.; Pergamon: New York, **1988**.

29   Kermagoret, A.; Braunstein, P. *Organometallics* **2008**, *27*, 88-99.

30   Weitr, I. S., Rabinovitz, M. *J. Chem. Soc., Perkin Trans. 1* **1993**, *1*, *117–120*.

31   Bruker computer programs: APEX2, SAINT, SADABS and TWINABS (Bruker AXS Inc., Madison, WI, 2012).

32   Palatinus, L.; Chapuis. G. *J. Appl. Cryst.* **2007,** *40*, 786–790.

33   Petříček, V.; Dušek, M.; Palatinus, L. *Z. Kristallogr.* **2014**, *229*, 345–352.

34   Spek, A. L., *J. Appl. Cryst.* **2003**, *36*, 7–3.

35   Macrae, C. F.; Edgington, P. R.; McCabe, P.; Pidcock, E.; Shields, G. P.; Taylor, R.; Towler, M.; van de Streek, J. *J. Appl. Cryst.* **2006**, *39*, 453-457.

36   Frisch, M. J. *et.al. Gaussian 09, Revision A.02*; Gaussian, Inc., Wallingford, CT, **2009**.

37   (a) Becke, A. D. *J. Chem. Phys.* **1993**, *98*, 5648-5652. (b) Miehlich, B.; Savin, A.; Stoll, H.; Preuss, H. *Chem. Phys. Lett* **1989**, *157*, 200-206. (c) Lee, C.; Yang, W.; Parr, G. *Phys. Rev. B* **1988**, *37*, 785-789.

38   Hehre, W. J.; Radom, L.; Schleyer, P. v. R.; Pople, J. A., *Ab Initio Molecular Orbital Theory*. John Wiley & Sons, New York, **1986**.

39   (a) Haeusermann, U.; Dolg, M.; Stoll, H.; Preuss, H. *Mol. Phys.* **1993**, *78*, 1211-1224. (b) Kuechle, W.; Dolg, M.; Stoll, H.; Preuss, H. *J. Chem. Phys.* **1994**, *100*, 7535-7542. (c) Leininger, T.; Nicklass, A.; Stoll, H.; Dolg, M.; Schwerdtfeger, P. *J. Chem. Phys.* **1996**, *105*, 1052-1059.

40   (a) McLean, A. D.; Chandler, G. S. *J. Chem. Phys.* **1980**, *72*, 5639-5648. (b) Krishnan, R.; Binkley, J. S.; Seeger, R.; Pople, J. A. *J. Chem. Phys.* **1980**, *72*, 650-654. (c) Wachters, A. J. H. *J. Chem. Phys.* **1970**, *52*, 1033-1036. (d) Hay, P. J. *J. Chem. Phys.* **1977**, *66*, 4377-4384. (e) Raghavachari, K.; Trucks, G. W. *J. Chem. Phys.* **1989**, *91*, 1062-1065. (f) Binning Jr., R. C.; Curtiss, L. A. *J. Comp. Chem.*, **1990**, *11*, 1206. (g) McGrath, M. P.; Radom, L. *J. Chem. Phys.* **1991**, *94*, 511-516.

41   (a) McClean, A. D.; Chandler, G. S. *J. Chem. Phys.* **1980**, *72*, 5639-5648. (b) Krishnan, R.; Binkley, J. S.; Seeger, R. Pople, J. A. *J. Chem. Phys.* **1980**, *72*, 650-654. (c) Wachters, A. J. H. *J. Chem. Phys.* **1970**, *52*, 1033-1036. (d) Hay, P. J. *J. Chem. Phys.* **1977**, *66*, 4377-4384. (e) Raghavachari, K.; Trucks, G. W. *J. Chem. Phys.* **1989**, *91*, 1062-1065. (f) Binning Jr., R. C.; Curtiss, L. A. *J. Comp. Chem.*, **1990**, *11*, 1206-1216. (g) McGrath, M. P.; Radom, L. *J. Chem. Phys.* **1991**, *94*, 511-516. (h) Clark, T.; Chandrasekhar, J.; Spitznagel, G. W.; Schleyer, P. v. R.

J. Comp. Chem. **1983**, *4*, 294-301. (i) Frisch, M. J.; Pople, J. A.; Binkley, J. S. *J. Chem. Phys.* **1984**, *80*, 3265-3269.

42   Zhao, Y.; Truhlar, D.G. *Theor. Chem. Acc.*, **2008**, *120*, 215-241.

43   (a) Zhao, Y.; Truhlar, D.G. *Acc, Chem. Res.*, **2008**, *41*, 157-167. (b) Zhao, Y.; Truhlar, D.G. *Chem. Phys. Lett.*, **2011**, *502*, 1-13.

44   (a) Cancès, M. T.; Mennucci, B.; Tomasi, J. *J. Chem. Phys.* **1997**, *107*, 3032-3041. (b) Cossi, M.; Barone, V.; Mennucci, B.; Tomasi, J. *Chem. Phys. Lett.* **1998**, *286*, 253-260. (c) Mennucci B.; Tomasi, J. *J. Chem. Phys.* **1997**, *106*, 5151-5158. (d) Tomasi, J.; Mennucci, B.; Cammi, R. *Chem. Rev.* **2005**, *105*, 2999-3094.

45   Marenich, A. V.; Cramer, C. J.; Truhlar, D. G. *J. Phys. Chem. B*, **2009**, *113*, 6378-6396.

46   http://www.chemcraftprog.com/

Synthesis, Structure, and Reactivity of Co(II) and Ni(II) PCP Pincer Borohydride Complexes

The 15e square planar complexes [Co(PCP-*t*Bu)Cl] (**1a**) and [Co(PCP^{Me}-*i*Pr)Cl] (**1b**), respectively, react readily with NaBH$_4$ to afford complexes [Co(PCP-*t*Bu)(η^2-BH$_4$)] (**2a**) and [Co(PCP^{Me}-*i*Pr)(η^2-BH$_4$)] (**2b**) in high yields as confirmed by IR spectroscopy, X-ray crystallography, and elemental analysis. The borohydride ligand is symmetrically bound to the cobalt center in η^2-fashion. These compounds are paramagnetic with effective magnetic moments of 2.1(1) and 2.0(1)μ_B consistent with a d^7 low spin system corresponding to one unpaired electron. None of these complexes reacted with CO$_2$ to give formate complexes. For structural and reactivity comparisons, we prepared the analogous Ni(II) borohydride complex [Ni(PCP^{Me}-*i*Pr)(η^2-BH$_4$)] (**4**) *via* two different synthetic routes. One utilizes [Ni(PCP^{Me}-*i*Pr)Cl] (**3**) and NaBH$_4$, the second one makes use of the hydride complex [Ni(PCP^{Me}-*i*Pr)H] (**5**) and BH$_3$·THF. In both cases, **4** is obtained in high yields. In contrast to **2a** and **2b**, the borohydride ligand is asymmetrically bound to the nickel center but still in an η^2-mode. [Ni(PCP^{Me}-*i*Pr)(η^2-BH$_4$)] (**4**) loses readily BH$_3$ at elevated temperatures in the presence of NEt$_3$ to form **5**. Complexes **4** and **5** are both diamagnetic and were characterized by a combination of ^{1}H, ^{13}C{^{1}H} and ^{31}P{^{1}H} NMR, IR spectroscopy, and elemental analysis. Additionally, the structure of these compounds was established by X-ray crystallography. Complexes **4** and **5** react with CO$_2$ to give the formate complex [Ni(PCP^{Me}-*i*Pr)(OC(C=O)H] (**6**). The extrusion of BH$_3$ from [Co(PCP^{Me}-*i*Pr)(η^2-BH$_4$)] (**2b**) and [Ni(PCP^{Me}-*i*Pr)(η^2-BH$_4$)] (**4**) with the aid of NH$_3$ to yield the respective hydride complexes [Co(PCP^{Me}-*i*Pr)H] and [Ni(PCP^{Me}-*i*Pr)H] (**5**) and BH$_3$NH$_3$ was investigated by DFT calculations showing that formation of the Ni hydride is thermodynamically favorable, while the formation of the Co(II) hydride, in agreement with the experiment, is unfavorable. The electronic structures and the bonding of the borohydride ligand in [Co(PCP-*t*Bu)(η^2-BH$_4$)] (**2a**) and [Co(PCP^{Me}-*i*Pr)(η^2-BH$_4$)] (**2b**) were established by DFT computations. A very rare bidentate and tridentate ligand containing pincer complex [Co(PCP^{Me}-*i*Pr)(NO)(NO$_2$)] (**7**) synthesized by the reacting substrate **2b** and NaNO$_2$. The cobalt borohydride complex [Co(PCP^{Me}-*i*Pr)(η^2-BH$_4$)] (**2b**) is readily reacted with CO and *t*BuNC to produce the diamagnetic Co(I) complexes [Co(PCP^{Me}-*i*Pr)(CO)$_2$] (**8**) and [Co(PCP^{Me}-*i*Pr)(CN*t*Bu)$_2$] (**9**), respectively.

3.1 Introduction

Complexes containing the borohydride anion BH$_4^-$ are known for almost all transition metals and are the focus of much research over the last decades.[1] They exhibit an extensive and diverse coordination chemistry where, in the case of mononuclear complexes, the BH$_4^-$ ligand is coordinated in η^1, η^2, or η^3-fashion featuring thus one, two, or three M-H-B bridges, respectively. Borohydride complexes are useful starting materials for the preparation of organometallic compounds, in particular hydride and dihydrogen complexes, and are active catalysts, for instance, in hydrogenation reactions.[2,3,4,5,6,7,8,9,10,11] Moreover, since BH$_4^-$ and CH$_4$ are isoelectronic, it has been suggested that borohydrides can serve as structural models for the activation of C-H bonds in saturated hydrocarbons.[12,13]

We are currently focusing on the chemistry of cobalt PCP pincer complexes based on the 1,3-diaminobenzene scaffold.[14] A few PCP pincer complexes featuring a direct cobalt-carbon single bond were reported in the literature,[15,16,17,18,19] but none of these contain a borohydride ligand. It has to be noted that, in general, cobalt borohydride complexes are very scarce. An overview of all complexes known to date (**A−F**),[20,21,22,23,24,25] mostly based on the Co(I) oxidation state, is depicted in Scheme 1. The borohydride hapticity in **A** was inferred only on the basis of electronic spectroscopy comparisons to [Co(PPh$_3$)$_3$X] (X = Cl, Br, I), while in the case of **B-F**, their molecular structures and thus the bonding mode of the BH$_4^-$ ligands were unequivocally established by X-ray crystallography or neutron diffraction. Noteworthy, the complex *trans*-[Co(H)(η^2-BH$_4$)(PCy$_3$)$_2$] (Cy = cyclohexyl) (**C**) is the only known Co(II) borohydride complex which adopts a d^7 low-spin configuration. In the dinuclear complex **F**, the mode of BH$_4^-$ coordination is unusual in that each BH$_4^-$ unit chelates to two adjacent Co atoms as well as directly bridges these two Co atoms with a shared hydrogen.
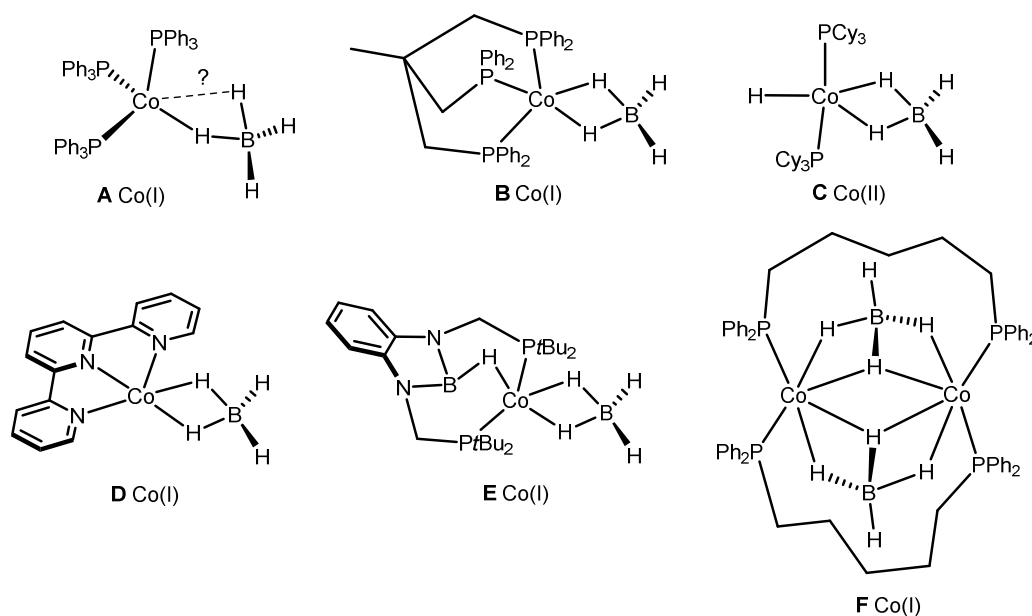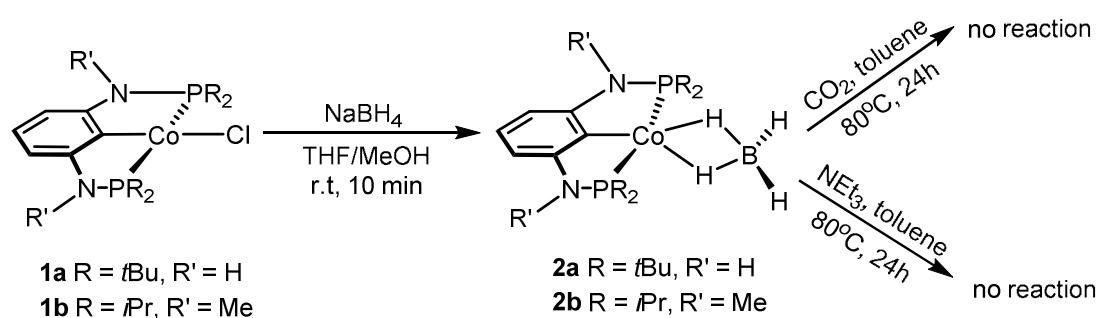

Scheme 1

In this chapter we show on the synthesis and reactivity of low-spin cobalt PCP pincer borohydride complexes in the oxidation state +II. For comparison, the synthesis and reactivity of an analogous low-spin Ni(II) PCP borohydride complex is also reported. A combination of structural, spectroscopic and computational methods is presented to address the bonding in these new complexes.

3.2 Results and Discussion

The starting material for the present study, [Co(PCP-*t*Bu)Cl] (**1a**)[14b] and [Co(PCP^{Me}-*i*Pr)Cl] (**1b**)[14a] complexes were prepared via different synthetic methodology in each other (Scheme 2 and 4, Chapter 2). Treatment of the 15e complexes [Co(PCP-*t*Bu)Cl] (**1a**) and [Co(PCP^{Me}-*i*Pr)Cl] (**1b**) with 2 equivs of NaBH$_4$ in THF/MeOH (1:1) for 5 min afforded the borohydride complexes [Co(PCP-*t*Bu)(η^2-

$BH_4)]$ (**2a**) and $[Co(PCP^{Me}-iPr)(\eta^2-BH_4)]$ (**2b**) in 91 and 94% isolated yields, respectively (Scheme 2). These Co(II) complexes display large paramagnetic shifted and very broad ^{1}H NMR signals and were thus not very informative. $^{13}C\{^1H\}$ and $^{31}P\{^1H\}$ NMR spectra could not be detected at all. The solution[26] magnetic moments of 2.0(1) and 2.1(1)μ_B are consistent with a d^7 low spin system corresponding to one unpaired electron. This value is higher than the one expected for the spin-only approximation and is explained by a spin orbit coupling contribution, being consistent with a low-spin square planar complex.[27] The η^2-coordination mode of BH_4^- ligand was first established by IR spectroscopy. Attenuated total reflectance IR spectra of the solid samples of **2a** and **2b** show two strong bands in the range of 2415-2312 cm^{-1}, which are attributed to terminal hydrogen-boron stretch ν_{B-Ht}. The bridging boron-hydrogen stretching bands ν_{B-Hb} are very broad and located in the region 1975-1825 cm^{-1}.

1a R = *t*Bu, R' = H
1b R = *i*Pr, R' = Me

2a R = *t*Bu, R' = H
2b R = *i*Pr, R' = Me

Scheme 2 Synthesis of Co(II) borohydride complexes $[Co(PCP-tBu)(\eta^2-BH_4)]$ (**2a**) $[Co(PCP^{Me}-iPr)(\eta^2-BH_4)]$ (**2b**)

The solid state structures of **2a** and **2b** were determined by X-ray diffraction unequivocally establishing the η^2-bonding mode of the BH_4^- ligand. Structural views are presented in Figures 1 and 2. Selected
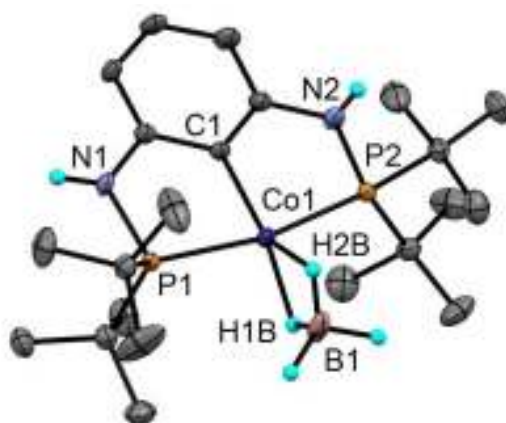

Figure 1. Structural view of $[Co(PCP-tBu)(\eta^2-BH_4)]$ (**2a**) showing 50% thermal ellipsoids (most H atoms omitted for clarity). Selected bond lengths (Å) and bond angles (°): Co1-C1 1.945(2), Co1-P1 2.2265(5), Co1-P2 2.2288(6), Co1···B1 2.157(3), Co1-H1B 1.66(3), Co1-H2B 1.78(3), P1-Co1-P2 165.24(2), P1-Co1-C1 82.72(6), P2-Co1-C1 82.93(6), C1-Co1-B1 174.0(1).
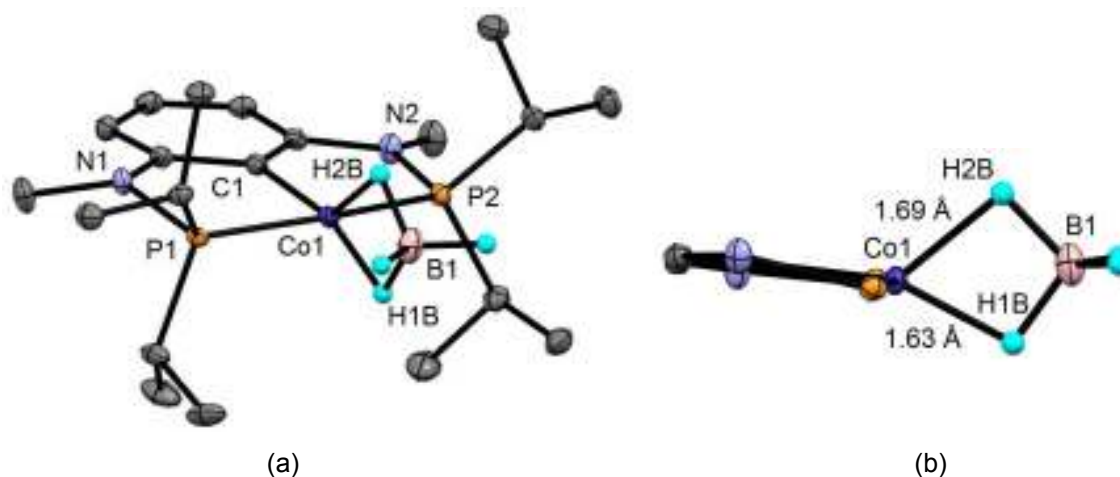
(a)	(b)

Figure 2. (a) Structural view of [Co(PCP^{Me}-*i*Pr)(η^2-BH$_4$)] (**2b**) showing 50% thermal ellipsoids (most H atoms omitted for clarity). (b) Inner part of **2b** showing the slightly asymmetric bonding of the BH$_4^-$ ligand. Selected bond lengths (Å) and bond angles (°): Co1-C1 1.933(1), Co1-P1 2.1752(5), Co1-P2 2.1860(5), Co1$\cdots$B1 2.149(2), Co1-H1B 1.63(2), Co1-H2B 1.69(2). C1-Co1-B1 167.73(7), C1-Co1-P1 83.12(4), C1-Co1-P2 83.57(4), P1-Co1-P2 165.67(2).

metrical parameters are given in the captions. Comparisons with related cobalt, nickel, and iron complexes are presented in Table 1. Cobalt borohydrides are rare and typically found for Co(I) rather than Co(II). In fact, there is as yet only one report of a Co(II) borohydride complex, *trans*-[Co(PCy$_3$)$_2$(H)(η^2-BH$_4$)], which was also structurally characterized.[22] In **2a** and **2b**, cobalt is in a five-fold coordination by one C, two P and two H atoms furnished by the η^3*P,C,P*-bonded pincer ligand and by the η^2-bonded BH$_4^-$ anion. The coordination sphere of the cobalt can be described as a strongly distorted square pyramid with P1, C1, P2, and H1B as the basal atoms and H2B as the apical atom. In pentacoordinated systems, the actual geometry of the complex can be described by the structural index parameter $\tau = (\beta - \alpha)/60$, where β and α are the two largest angles ($\beta > \alpha$). For an ideal square pyramidal geometry $\tau = 0$, while for an ideal trigonal bipyramidal geometry $\tau = 1$.[28] According to this [a]Neutron diffraction data, [c]cyclam = 1,4,8,11-tetraazacyclotetradecane, [d]Tp* = hydrotris(3,5-dimethylpyrazolyl)borate. BH$_4^-$ moiety is essentially symmetrically bound in η^2-fashion, which is in contrast to related Ni(II) PCP complexes (*vide infra*). Moreover, the Co$\cdots$B distances of 2.149(2) and 2.157(3)Å are also consistent with this binding mode. One of the few known compounds is the closely related terpyridine Co(I) complex [Co(terpy)(η^2-BH$_4$)], which displays Co-H$_b$ and Co$\cdots$B distances of 1.71(1), 1.74(1), and 2.162 Å, respectively.

Table 1. Selected bond distances (Å) for the Co(II) and Ni(II) PCP borohydride complexes **2a**, **2b**, **4** and comparisons with some related borohydride Co(I), Co(II), Ni(I), Ni(II), and Fe(II) complexes.

[a]Neutron diffraction data, [c]cyclam = 1,4,8,11-tetraazacyclotetradecane, [d]Tp* = hydrotris(3,5-

Metal	Spin state	Compound	M···B, Å	M-H$_b$, Å	Ref.
Co(II)	S = ½	[Co(PCP-tBu)(η^2-BH$_4$)] (**2a**)	2.156(3)	1.78(3), 1.66(3)	this work
Co(II)	S = ½	[Co(PCP^{Me}-iPr)(η^2-BH$_4$)] (**2b**)	2.149(2)	1.63(2), 1.69(2)	this work
Co(I)	S = 1	[Co(ppp)(η^2-BH$_4$)] (**B**)	2.21(3)	1.6(2), 1.5(2)	21
Co(II)	S = ½	*trans*-[Co(PCy$_3$)$_2$(H)(η^2-BH$_4$)] (**C**)	2.14(1)	1.87(9), 1.80(8)	22
Co(I)	S = 0	[Co(terpy)(η^2-BH$_4$)] (**D**)	2.162	1.81(5), 1.80(5)	23
				1.71(1), 1.74(1)[a]	
Co(I)	S = 0	[Co(^{tBu}DBP)(η^2-BH$_4$)] (**E**)	2.131(2)	1.66(2), 1.73(2)	24
Ni(II)	S = 0	[Ni(PCP^{Me}-iPr)(η^2-BH$_4$)] (**4**)	2.218(3)	1.70(3), 1.85(2)	this work
Ni(II)	S = 0	[Ni(POCOP-iPr)(η^2-BH$_4$)]	2.214(3)	1.78(3), 1.85(3)	5
Ni(II)	S = 0	[Ni(POCOP-tBu)(η^2-BH$_4$)]	2.187(5)	1.77(4), 1.87(4)	5
Ni(II)	S = 0	[Ni(POCOP-C$_5$H$_9$)(η^2-BH$_4$)]	2.189(5)	1.78(5), 1.87(5)	5
Ni(I)	S = ½	[Ni(ppp)(η^2-BH$_4$)]	2.24	1.59(5), 1.83(5)	29
Ni(II)	S = 0	[Ni(cyclam)(η^2-BH$_4$)]BH$_4$ [c]	2.202(6)	1.736, 1.800	30
Ni(II)	S = 0	*trans*-[Ni(PCy$_3$)$_2$(H)(η^2-BH$_4$)]	2.201(8)	1.73(5), 1.76(6)	31
Ni(II)	S = 0	[Ni(Tp*)(η^3-BH$_4$)][d]	2.048(5)	1.87(4) - 1.94(7)	32
Fe(II)	S = 0	[Fe(PNP^{CH2}-iPr)(H)(η^2-BH$_4$)]	2.095(3)	1.60(2), 1.68(2)	8

dimethylpyrazolyl)borate.

For structural and reactivity comparisons, we also prepared the analogous Ni(II) borohydride complex [Ni(PCP^{Me}-iPr)(η^2-BH$_4$)] (**4**) via two different routes. First, upon treatment of [Ni(PCP^{Me}-iPr)Cl] (**3**) with an excess of NaBH$_4$ in THF/MeOH (1:1) yields **4** in 91% isolated yield (Scheme 3). The second approach makes use of the hydride complex [Ni(PCP^{Me}-iPr)H] (**5**) which was obtained from the reaction of **3** with LiAlH$_4$. Treatment of **5** with BH$_3$·THF at room temperature led to the clean formation of **5** in 93% isolated yield. In contrast to the analogous cobalt complexes, [Ni(PCP^{Me}-iPr)(η^2-BH$_4$)] (**4**) loses readily BH$_3$ at elevated temperatures. Heating a toluene solution of **5** at 80°C for 24h in the presence of NEt$_3$ yields **5** in 93% isolated yield (Scheme 4). Complexes **4** and **5** are both diamagnetic and were characterized by a combination of ^{1}H, ^{13}C{^{1}H} and ^{31}P{^{1}H} NMR, IR spectroscopy, and elemental analysis. Additionally, the structure of these compounds was established by X-ray crystallography. Structural views are illustrated in Figures 3 and 4 with the main bond lengths and angles given in the captions.
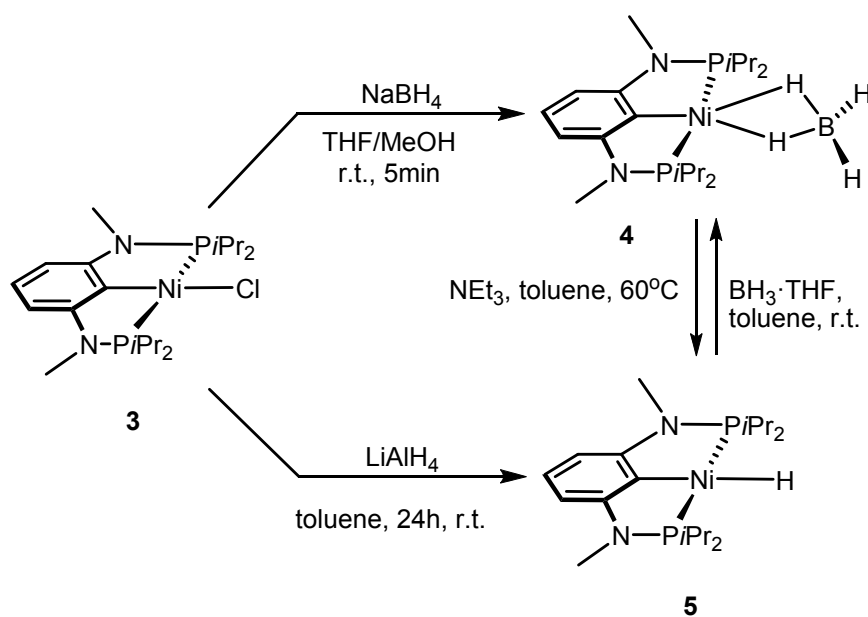
Scheme 3 Synthesis and reactivity of Ni(II) borohydride and hydride complexes [Ni(PCP^{Me}-iPr)(η^2-BH$_4$)] (**4**) and [Ni(PCP^{Me}-iPr)H] (**5**).

(a)   (b)
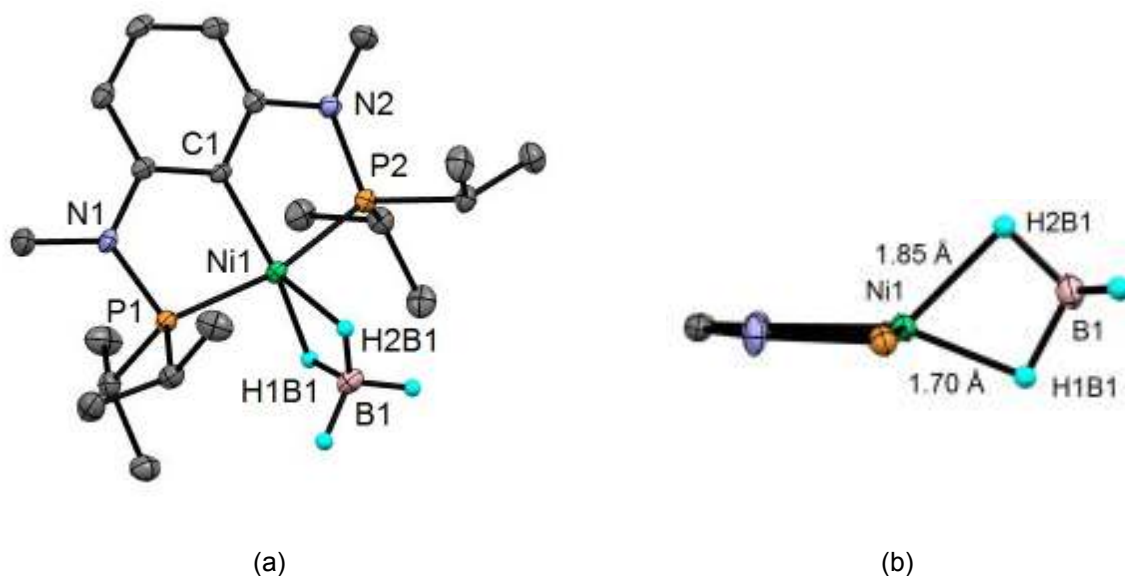
Figure 3. (a) Structural view of [Ni(PCP^{Me}-iPr)(η^2-BH$_4$)]·0.5C$_6$D$_6$ (**4**·0.5C$_6$D$_6$) showing 50% thermal ellipsoids (most H atoms, solvent molecule, and a second independent complex omitted for clarity). (b) Inner part of **5** showing the asymmetric bonding of the BH$_4^-$ ligand. Ni1-C1 1.906(2), Ni1-P1 2.1675(8), Ni1-P2 2.1691(8), Ni1···B1 2.218(3), Ni1-H1B1 1.70(3), Ni1-H2B1 1.85(2), P1-Ni1-P2 165.19(3),P1-Ni1-C1 83.67(6), P2-Ni1-C1 83.54(6), C1-Ni1-B1 167.4(1).
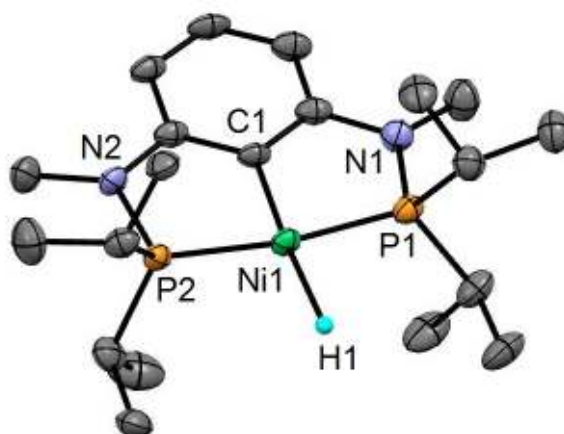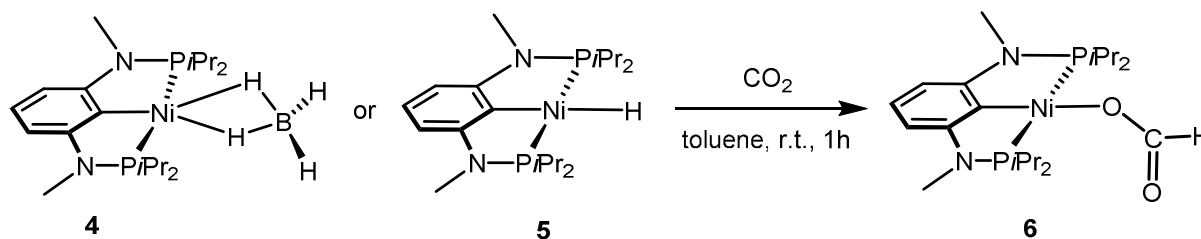
Figure 4. Structural view of [Ni(PCP^{Me}-iPr)H] (**5**) showing 50% thermal ellipsoids (most H atoms and a second independent complex omitted for clarity). Selected bond lengths (Å) and bond angles (°): Ni1-P1 2.115(1), Ni1-P2 2.122(1), Ni1-C1 1.908(3), P1-Ni1-P2 169.97(3), P1-Ni1-C1 85.3(1), P2-Ni1-C1 84.7(1), Ni1-H1 1.99(2).

The IR spectrum of **4** shows a strong intensity absorption in the terminal boron-hydrogen stretching region (2384 and 2321 cm^{-1}) and a broad medium vibration in the bridging borohydride stretching region (2107-1845 cm^{-1}) which support an η^2-bonding mode of the BH$_4^-$ ligand. In the ^{1}H NMR spectrum the BH$_4^-$ ligand gives rise to a broad low-field resonance quartet with an intensity ratio of approximately 1:1:1:1 centered at -0.75 ppm (J_{HB} = 75.0 Hz) (*cf* the free BH$_4^-$ anion gives rise to a sharp 1:1:1:1 quartet with a J_{HB} coupling constant of 50 Hz). The resonance integrates as four hydrogens with respect to one pincer unit. The magnetic equivalence of terminal and bridging hydrogens observed in the ^{1}H NMR spectra suggests that these hydrogens are fluxional on the NMR time scale possibly involving η^1- or η^3-BH$_4$ intermediates. The ^{1}H NMR spectrum of **5** confirmed the presence of one hydride ligand, which appeared at -8.26 ppm as a well-resolved triplet with a $^2J_{HP}$ coupling constant of about 55.8 Hz.[33,34] Complexes **4** and **5** exhibit a singlet at 136.0 and 144.5 ppm, respectively, in the ^{31}P{^{1}H} NMR spectrum.

The structural features of complex **4** are similar to those of complexes **2a** and **2b**. The τ value for **4** is 0.11 in agreement with a distorted square pyramidal geometry The nickel atom coordinates the BH$_4$-group in an η^2-fashion but in a slightly asymmetrical fashion with Ni-H$_b$ distances of 1.70(3) and 1.85(2) Å. Similar Ni-H$_b$ distances were found in several other Ni(II) borohydride complexes as shown in Table 1. Despite the similar covalent radii of Co and Ni, the Ni$\cdots$B distance of 2.218(3) Å in **4** is larger than in the corresponding paramagnetic Co(II) complexes **2a** and **2b**, but is comparable to those of related Ni(II) PCP complexes.[5] The opposite trend is observed for the metal-carbon bond distances. The Co-C distances in **2a** and **2b** are 1.945(2) and 1.933(1) Å, respectively, whereas in **4** the Ni-C distance is shorter being 1.906 Å. Similar Ni-C distances are found in [Ni(POCOP-iPr)(η^2-BH$_4$)] (1.901(2) Å), [Ni(POCOP-tBu)(η^2-BH$_4$)] (1.898(4) Å), and [Ni(POCOP-C$_5$H$_9$)(η^2-BH$_4$)] (1.892(2) Å).[5] It is interesting to note that in a related Pd PCP pincer complex based on ferrocene, the BH$_4^-$ moiety is coordinated in an unidentate mode with a Pd$\cdots$B distance of 2.614(7) Å.[35]

Guan and co-workers have recently shown[5] that both nickel hydride and borohydride PCP pincer complexes are able to reduce CO_2 to give formate complexes. Given the fact that **4** is also capable of liberating "BH_3" as amine adduct to form a nickel hydride, we also explored the possibility of reducing CO_2 with complexes **4** and **5**. When exposed to 1 bar of CO_2 at room temperature for 1h, **4** and **5** are fully converted to the nickel formate complex **6** (Scheme 4). This complex was again fully characterized by a combination of ^1H, $^{13}C\{^1H\}$ and $^{31}P\{^1H\}$ NMR, IR spectroscopy, and elemental analysis. Additionally, the solid state structure of **6** was determined by single-crystal X-ray diffraction. A structural view is depicted in Figure 5 with selected bond distances given in the caption.

Scheme 4 Reaction of $[Ni(PCP^{Me}\text{-}iPr)(\eta^2\text{-}BH_4)]$ (**4**) and $[Ni(PCP^{Me}\text{-}iPr)H]$ (**5**) with CO_2 giving the formate complex $[Ni(PCP^{Me}\text{-}iPr)(OC(=O)H)]$ (**7**).
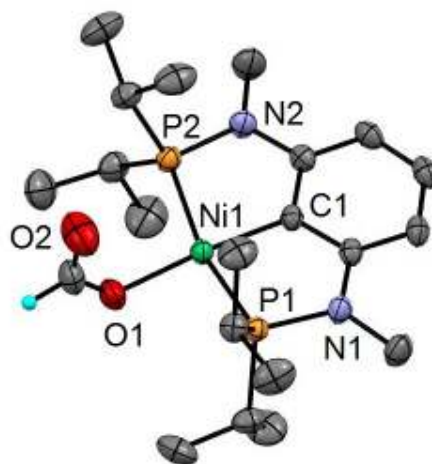

Figure 5. Structural view of $[Ni(PCP^{Me}\text{-}iPr)(OC(=O)H)]$ (**6**) showing 50% thermal ellipsoids (most H atoms and a second independent complex omitted for clarity). Selected bond lengths (Å) and bond angles (°): Ni1-P1 2.1712(7), Ni1-P2 2.1701(7), Ni1-O1 1.923(2), Ni1-C1 1.897(2), P1-Ni1-P2 166.49(2), P1-Ni1-O1 95.06(6), P1-Ni1-C1 84.05(7), P2-Ni1-O1 97.47(5), P2-Ni1-C1 84.12(7), O1-Ni1-C1 172.93(8).

Based on the above results with $[Ni(PCP^{Me}\text{-}iPr)(\eta^2\text{-}BH_4)]$ (**4**) and $[Ni(PCP^{Me}\text{-}iPr)H]$ (**5**), we also attempted to obtain Co(II) hydride as well as Co(II) formate complexes. It has to be mentioned that monomeric Co(II) hydride complexes are rather rare.[22,36,37] Unfortunately, the reaction of $[Co(PCP^{Me}\text{-}iPr)Cl]$ (**1b**) with $LiAlH_4$ resulted in the formation of intractable materials together with the free

protonated PCP^{Me}-*i*Pr ligand. Likewise, treatment of **1b** with Na[HBEt$_3$] or *n*BuLi led to recovery of the starting material or decomposition with no evidence for the formation of a hydride complex (Scheme 5). Moreover, **1b** did neither react with NEt$_3$ to give [Co(PCP^{Me}-*i*Pr)H] nor with CO$_2$ to afford the formate complex [Co(PCP^{Me}-*i*Pr)(OC(=O)H)] even at 80°C for 24h (Scheme 2). For comparison, it was shown[38] that BH$_3$ liberation from a Rh(I) *bis*-iminopyridine pincer borohydride with quinuclidine was strongly endothermic and attempts to obtain a Rh(I) hydride complex were unsuccessful.
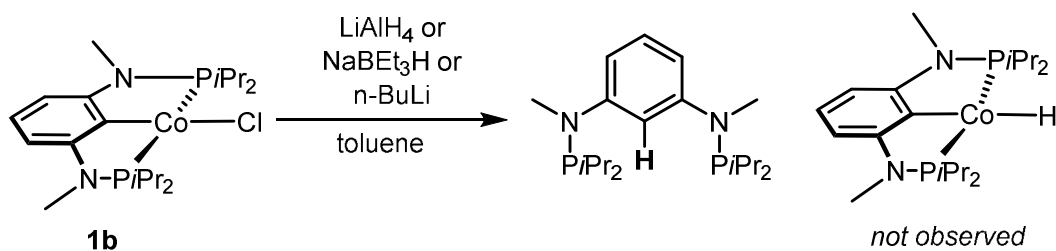
Scheme 5 Reaction of [Co(PCP^{Me}-*i*Pr)(Cl)] (**1b**) with various hydride sources

DFT Calculations

To address the binding mode of the BH$_4$ unit and the thermodynamics for the reaction of NH$_3$ with the Co-BH$_4$ and Ni-BH$_4$ moieties, we performed DFT calculations[39] on complexes **2b** and **4** (B3LYP functional, for details see the Experimental Section). This revealed that extrusion of BH$_3$ with NH$_3$ (as model for amines) from the cobalt complex **2b** is an endergonic process (2.2 kcal/mol), while in the case of **4** the process is exergonic by -6.0 kcal/mol (Scheme 6). These results, although taken with due care giving the simplicity of the amine used (NH$_3$) and the relatively small ΔG values obtained, indicate a clear trend and help explaining why attempts to obtain the corresponding Co hydride complex from **2b** by removal of BH$_3$ as an amine adduct were unsuccessful.

M = Co, ΔG = 2.2 kJ/mol
ΔH = 4.4 kJ/mol
M = Ni, ΔG = -6.0 kJ/mol
ΔH = -4.2 kJ/mol
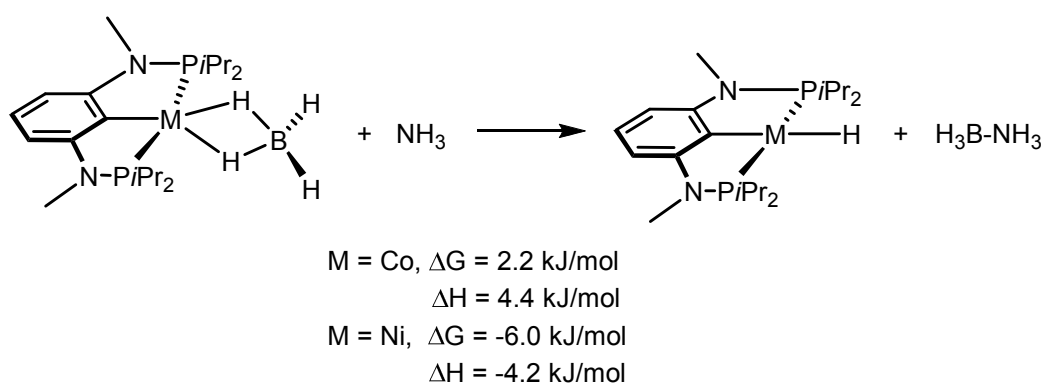
Scheme 6 DFT calculated thermodynamics of the reaction of [Co(PCP^{Me}-*i*Pr)(η^2-BH$_4$)] (**2b**) and [Ni(PCP^{Me}-*i*Pr)(η^2-BH$_4$)] (**4**) with NH$_3$.

The electronic structures of complexes **2b** and **4** was evaluated by DFT calculations and the relevant frontier orbitals (metal *d*-splitting), as well as the spin density of complex **2b**, are presented in in Figure 6. The orbitals are the expected ones for pseudo-square pyramidal molecules, and the spin density of complex **2b** is centered in the metal atom. Moreover, the calculations indicate a clear
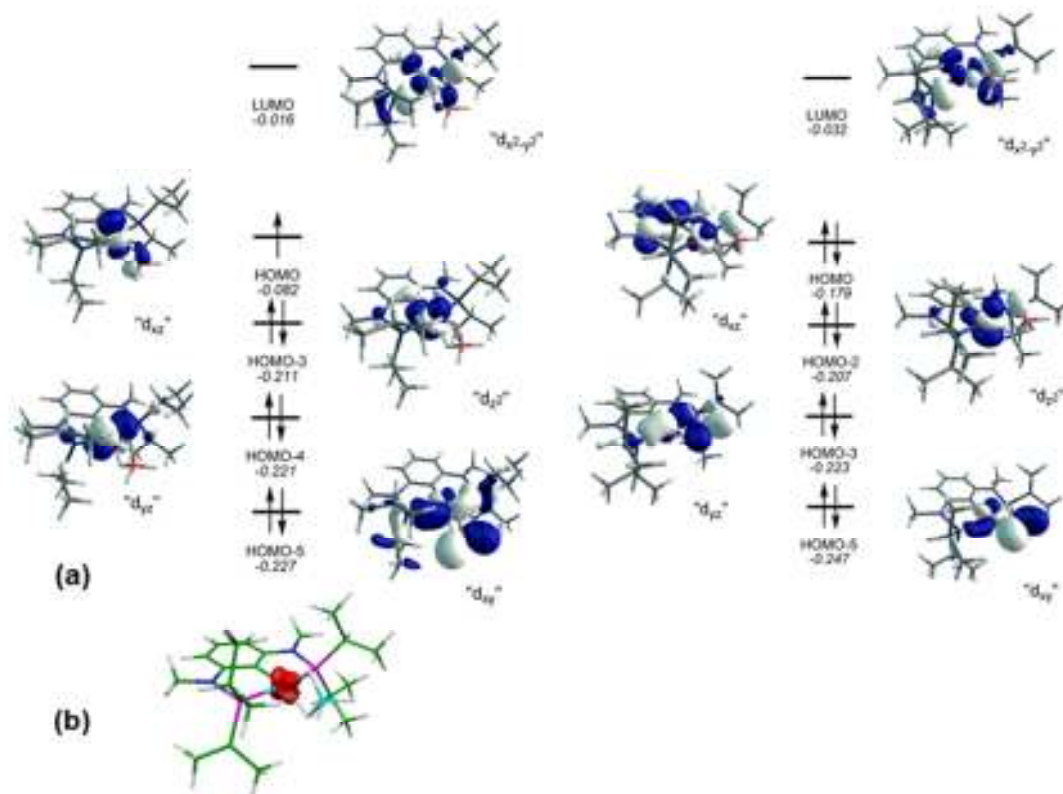

Figure 6. (a) DFT-computed frontier orbitals (*d*-splitting) for [Co(PCP^{Me}-*i*Pr)(η^2-BH$_4$)] (**2b**) (left) and for [Ni(PCP^{Me}-*i*Pr)(η^2-BH$_4$)] (**4**) (right) and (b) spin density of [Co(PCP^{Me}-*i*Pr)(η^2-BH$_4$)] (**2b**). Energy values in italics (atomic units).

difference in the coordination of the BH$_4^-$ ligand in the two complexes. In the Co species **2b** two comparable Co-H bonds exist, with distances of 1.84 and 1.72 Å. The corresponding Wiberg indices (WI) [40] of 0.09 and 0.13 also indicate interactions of similar magnitude. On the other hand, for the Ni complex **4** there is a clear asymmetry in the two Ni–H interactions, with a normal bond (d = 1.65 Å, WI = 0.15) and a much weaker interaction (d = 2.06 Å, WI = 0.02). In other words, for the Co complexes the BH$_4^-$ coordination is closer to η^2, and the overall geometry can be envisaged as in between square planar and square pyramidal. In complex **4**, the borohydride ligand coordination is closer to η^1, and the molecule overall geometry is nearer a normal square planar, reflecting the tendency of Ni(II) to form complexes with that geometry, as expected for a d^8 metal. Interestingly, the overall electron donation from the ligands to the metal is stronger in the case of the Co species as shown by the ligand charges (NPA,[41] see Computational details): C_{PCP} = 0.26 (**2b**) and 0.24 (**4**), C_{BH4} = -0.67 (**2b**) and -0.73 (**4**). This is reflected in an electron richer Co-atom in **2b** (C_{Co} = 0.42, compared with the Ni-atom in **4** (C_{Ni} = 0.49) and indicates stronger coordination of the ligands in the case of the Co complex, in particular a

stronger M–BH$_4$ bond, in good accordance with the reactivity pattern observed for the reaction with NH$_3$ (see Scheme 5). Notably, the cobalt borohydride complex **2b** does not react with the strong donor ligands PMe$_3$ and P(OMe)$_3$ (Scheme 7).
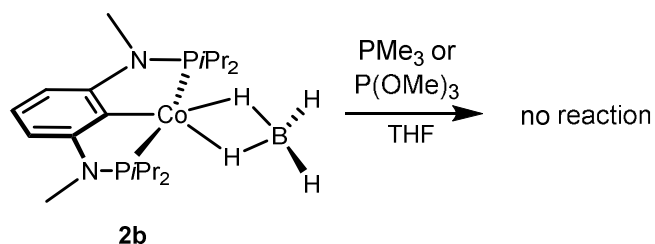
Scheme 7 Stable complex [Co(PCP^{Me}-iPr)(η^2-BH$_4$)] (**2b**) with PMe$_3$ or P(OMe)$_3$

When [Co(PCP^{Me}-iPr)(η^2-BH$_4$)] (**2b**) complex is treated with an excess of sodium nitrite in MeOH at 60°C the diamagnetic Co(III) complex [Co(PCP^{Me}-iPr)(NO)(κ^2O,O-NO$_2$)] (**7**) was formed. This complex is furnished by a combination of tridentate pincer ligand, bidentate nitrite ligand and a bent nitrogen oxide ligand in the arrangement of a distorted octahedral geometry (Scheme 8). The nitrite ligand is asymmetrically coordinated to the Co(III) center with Co1–O2 and Co1-O3 distances of 2.050(3) and 2.448(3) Å, respectively. The O2–N3–O3 angle is 123.0(3)° and the N3–O2 and N3-O3 distances are 1.189(4) and 1.134 (4) Å, which is comparable with the free nitrite ion being 114.9(5)° and 1.240(3) Å (Figure 7).
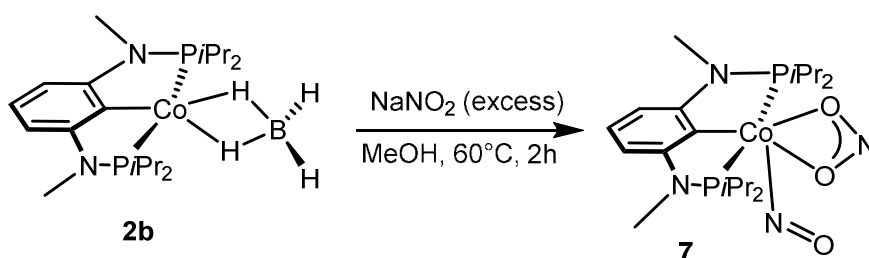
Scheme 8 Synthesis of [Co(PCP^{Me}-iPr)(NO)(κ^2O,O-NO$_2$)] (**7**)

The complexes [Co(PCP^{Me}-iPr)(CO)$_2$] (**8**) and [Co(PCP^{Me}-iPr)(CNtBu)$_2$] (**9**) were obtained by the reaction of [Co(PCP^{Me}-iPr)(η^2-BH$_4$)] with CO and CNtBu in 94 and 91% isolated yields, respectively (Scheme 9). While the reactivity of **2a** with CO and tBuNC were not given pure form of the complexes **10** and **11**, respectively. Complex **9** was already prepared *via* a different route by stirring [Co(PCP^{Me}-iPr)Cl] in toluene with KC$_8$ in the presence of CO (Scheme 5, Chapter 2). It should be noted that the complex **9** is stable in pentane or ether solvents like Et$_2$O and THF, with other solvents like CH$_2$Cl$_2$,
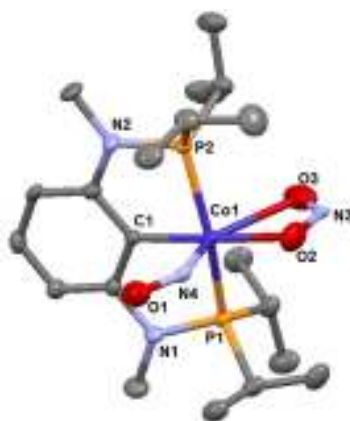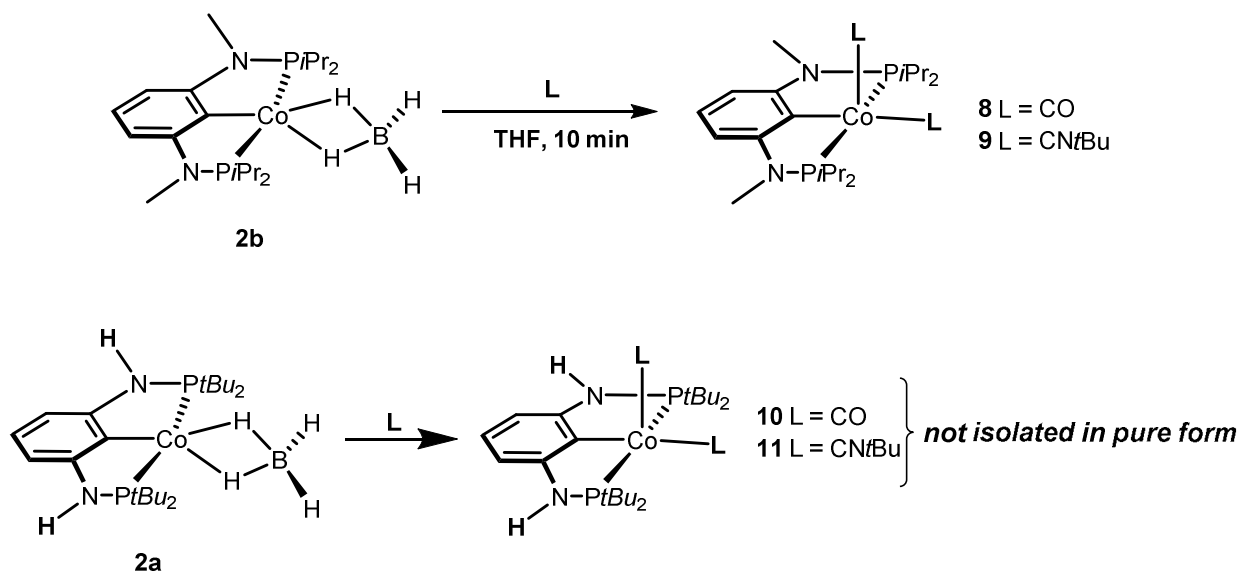
Figure 7 Structural view of [Co(PCP^{Me}-*i*Pr)(NO)(κ^2*O,O*-NO$_2$)] (**7**) showing 50% thermal ellipsoids (H atoms omitted for clarity). Selected bond lengths (Å) and bond angles (°): Co1-C1 1.965(3), Co1-P1 2.2318(9), Co1-P2 2.2357(9), Co1-N4 1.746(3), Co1-O2 2.050(3), Co1-O3 2.448(3). C1-Co1-N4 94.5(1), C1-Co1-P1 81.8(1), C1-Co1-P2 82.0(1), P1-Co1-P2 156.54(4), O2-Co1-O3 53.1(1), O2-N3-O3 123.0(3).

MeOH and acetone led to be slow undetermined product. The solid state structure of **9** was determined by X-ray diffraction. A structural view is presented in Figure 8. This complex **9** adopts a square pyramidal geometry around the cobalt centre.

Scheme 9 Synthesis of the Co(I) PCP carbonyl and isocyanide complexes [Co(PCP^{Me}-*i*Pr)(CO)$_2$] (**8**) and [Co(PCP^{Me}-*i*Pr)(CN*t*Bu)$_2$] (**9**)
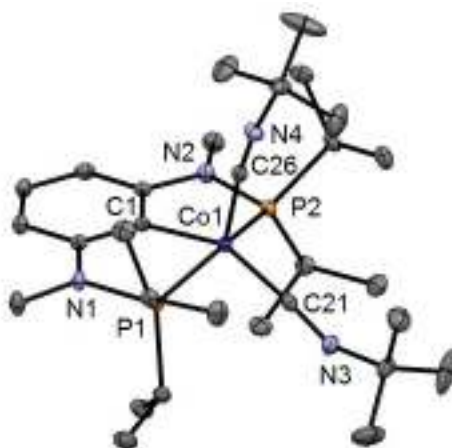
Figure 8. Structural view of [Co(PCP^{Me}-*i*Pr)(CN*t*Bu)₂] (**2**) showing 50% thermal ellipsoids (H atoms omitted for clarity). Selected bond lengths (Å) and bond angles (°): Co1-P1 2.1561(4), Co1-P2 2.1540(4), Co1-C1 1.9947(9), Co1-C21 1.781(1), Co1-C26 1.865(1), P1-Co1-P2 153.82(1), C1-Co1-C21 146.06(4), C1-Co1-C26 106.77(4), C21-Co1-C26 107.15(4), Co1-C26-N4 173.75(9), Co1-C21-N3 174.84(9), C21-N3-C22 144.5(1), C26-N4-C27 172.1(1).

3.3 Conclusion

We have shown that the 15e square planar complexes [Co(PCP-*t*Bu)Cl] (**1a**) and [Co(PCP^{Me}-*i*Pr)Cl] (**1b**), respectively, react readily with NaBH$_4$ to afford complexes [Co(PCP-*t*Bu)(η^2-BH$_4$)] (**2a**) and [Co(PCP^{Me}-*i*Pr)(η^2-BH$_4$)] (**2b**) in high yields. The η^2-bonding mode of the borohydride ligand was confirmed by IR spectroscopy and X-ray crystallography. These compounds are paramagnetic with effective magnetic moments of 2.1(1) and 2.0(1)μ_B consistent with a d^7 low spin system corresponding to one unpaired electron. None of these complexes reacts with CO$_2$ to give formate complexes. For structural and reactivity comparisons, we prepared the analogous Ni(II) borohydride complex [Ni(PCP^{Me}-*i*Pr)(η^2-BH$_4$)] (**4**) *via* two different routes. One utilizes [Ni(PCP^{Me}-*i*Pr)Cl] (**3**) and NaBH$_4$, the second one makes use of the hydride complex [Ni(PCP^{Me}-*i*Pr)H] (**5**) and BH$_3$·THF. In both cases, **5** was obtained in high yields. While [Ni(PCP^{Me}-*i*Pr)(η^2-BH$_4$)] (**4**) loses readily BH$_3$ at elevated temperatures in the presence of NEt$_3$ to form **5**, the Co(II) complex [Co(PCP^{Me}-*i*Pr)(η^2-BH$_4$)] (**2b**) did not react with NH$_3$ to give a hydride complex. Complexes **4** and **5** react with CO$_2$ to give the formate complex [Ni(PCP^{Me}-*i*Pr)(OC(C=O)H] (**6**). DFT calculations revealed that the formation of the Ni hydride is thermodynamically favorable, while the formation of the Co(II) hydride, in agreement with the experiment, is unfavorable. From the calculations it is apparent that for the Co complexes the BH$_4^-$ coordination is closer to η^2, and the overall geometry can be envisaged as in between square planar and square pyramidal. In complex **4**, the borohydride ligand coordination is closer to η^1, and the overall geometry of the molecule is closer to normal square planar, reflecting the tendency of Ni(II) to form complexes with that geometry, as expected for a d^8 metal. A very rare bidentate and tridentate ligand containing pincer complex [Co(PCP^{Me}-*i*Pr)(NO)(κ^2O,O-NO$_2$)] (**7**) synthesized by the reacting

substrate **2b** and NaNO$_2$. The cobalt borohydride complex [Co(PCP^{Me}-iPr)(η^2-BH$_4$)] (**2b**) is readily reacted with CO and tBuNC to produce the Co(I) complexes [Co(PCP^{Me}-iPr)(CO)$_2$] (**8**) and [Co(PCP^{Me}-iPr)(CNtBu)$_2$] (**9**), respectively.

3.4 Experimental Section

All manipulations were performed under an inert atmosphere of argon by using Schlenk techniques or in an MBraun inert-gas glovebox. The solvents were purified according to standard procedures.[42] The deuterated solvents were purchased from Aldrich and dried over 4 Å molecular sieves. [Co(PCP-tBu)Cl] (**1a**),[14b] [Co(PCP^{Me}-iPr)Cl] (**1b**),[14a] and [Ni(PCP^{Me}-iPr)Cl] (**3**),[14a] were reported in chapter 2. ^{1}H, ^{13}C{^{1}H}, and ^{31}P{^{1}H} NMR spectra were recorded on Bruker AVANCE-250, AVANCE-300 DPX, and AVANCE-400 spectrometers. ^{1}H and ^{13}C{^{1}H} NMR spectra were referenced internally to residual protio-solvent, and solvent resonances, respectively, and are reported relative to tetramethylsilane (δ = 0 ppm). ^{31}P{^{1}H} NMR spectra were referenced externally to H$_3$PO$_4$ (85%) (δ = 0 ppm).

[Co(PCP-tBu)(η^2-BH$_4$)] (2a). To suspension of **1a** (100 mg, 0.204 mmol) and NaBH$_4$ (17 mg, 0.408 mmol) in THF/MeOH (1:1) (10 mL) was added and the reaction mixture was stirred for 5 min. The solvent was then removed under reduced pressure and the crude product was dissolved in toluene. Insoluble materials were removed by filtration, and the solvent was evaporated under vacuum to afford **2a**. Yield: 87 mg (91%). Anal. Calcd. for C$_{22}$H$_{45}$BCoN$_2$P$_2$ (469.31): C, 56.30; H, 9.67; N, 5.97. Found: C, 56.34; H, 9.73; N, 5.89. IR (ATR, cm^{-1}): 1909 (br, ν_{B-Hb}), 1975 (br, ν_{B-Hb}), 2415 (s, ν_{B-Ht}), 2339 (s, ν_{B-Ht}). μ_{eff} = 2.1(1) μ_B (CH$_2$Cl$_2$, Evans method).

[Co(PCP^{Me}-iPr)(η^2-BH$_4$)] (2b). This complex was prepared in analogous fashion to **2a** with **1b** (200 mg, 0.43 mmol) and NaBH$_4$ (34 mg, 0.87 mmol) as starting materials. Yield: 180 mg (94%). Anal. Calcd. for C$_{20}$H$_{41}$BCoN$_2$P$_2$ (441.25): C, 54.44; H, 9.37; N, 6.35. Found: C, 54.34; H, 9.41; N, 6.45. IR (ATR, cm^{-1}): 1948-1825 (br, ν_{B-Hb}), 2387 (s, ν_{B-Ht}), 2312 (s, ν_{B-Ht}). μ_{eff} = 2.0(1)μ_B (CH$_2$Cl$_2$, Evans method).

[Ni(PCP^{Me}-iPr)(η^2-BH$_4$)] (4). Method A. A suspension of [Ni(PCP^{Me}-iPr)Cl] (**3**) (200 mg, 0.435 mmol) and NaBH$_4$ (38 mg, 0.87 mmol) in THF/MeOH (1:1) (10mL) was stirred at room temperature for 5 min. The solvent was then removed under vacuum. The crude product was dissolved in toluene and filtered through a short plug of Celite to give an orange-yellow solution. After removal of the solvent under vacuum, the desired complex was isolated as an orange-yellow solid. Yield: 91% (175 mg). **Method B.** To a suspension of **5** (200 mg, 0.469 mmol) in pentane (20mL) the BH$_3$·THF adduct (469 µl, 0.469 mmol, 1.0 M solution in THF) was added and stirred at room temperature for 30 min. The solvent was then evaporated under vacuum, and **5** was obtained as an orange-yellow solid. Yield: 192 mg (93%). Anal. Calcd. for C$_{20}$H$_{41}$BN$_2$NiP$_2$ (441.03): C, 54.47; H, 9.37; N, 6.35. Found: C, 54.45; H, 9.26; N, 6.41. ^{1}H NMR (δ, C$_6$D$_6$, 20°C): 7.26 (t, $^3J_{HH}$ = 7.8 Hz, 1H), 6.09 (d, $^3J_{HH}$ = 8.0 Hz, 2H), 2.53 (vt, $^{3,5}J_{HP}$ = 2.6 Hz, 6H, NCH$_3$), 2.37 (m, 4H, CH), 1.40 (vq, J_{HH} = 6.8 Hz, J_{HP} = 7.5 Hz, 12H, CH$_3$), 1.06 (vq, J_{HH} = 5.1 Hz, $^{3,5}J_{HP}$ = 7.5 Hz, 12H, CH$_3$), -0.75 (q, J_{HB} = 75.0 Hz, 4H, BH$_4$). ^{1}H{^{31}P} NMR (δ, C$_6$D$_6$, 20°C): 7.15 (t, $^3J_{HH}$ = 7.5 Hz, 1H), 6.00 (d, $^3J_{HH}$ = 8.0 Hz, 2H), 2.43 (s, 6H, NCH$_3$), 2.37 (m, 4H, CH), 1.40 (d, J_{HH} = 6.8 Hz, 12H, CH$_3$), 1.06 (d, J_{HH} = 5.1 Hz, 12H, CH$_3$), -0.75 (q, J_{HB} = 75.0 Hz, 4H, BH$_4$).

^{13}C{^{1}H} NMR (δ, C$_6$D$_6$, 20°C): 160.7 (t, $^2J_{CP}$ = 16.2 Hz, Ph), 126.5 (Ph), 100.8 (t, $^3J_{CP}$ = 6.2 Hz, Ph), 31.7 (NCH$_3$), 25.3 (t, $^2J_{CP}$ = 11.8 Hz, CH(CH$_3$)$_2$), 17.6 (CH(CH_3)$_2$), 17.4 (CH(CH_3)$_2$), the resonance of C$_{ipso}$ was obscured by the solvent peak. ^{31}P{^{1}H} NMR (δ, C$_6$D$_6$, 20°C): 136.0. IR (ATR, cm^{-1}): 1845-2107 (br, ν_{B-Hb}), 2321 (s, ν_{B-Ht}), 2384 (s, ν_{B-Ht}).

[Ni(PCP^{Me}-*i*Pr)H] (5): Method A. A suspension of [Ni(PCP^{Me}-*i*Pr)Cl] (**3**) (200 mg, 0.435 mmol) and LiAlH$_4$ (330 mg, 8.7 mmol) in toluene (25 mL) was stirred at room temperature for 24 h. The mixture was then filtered through a short plug of Celite to give a clear yellow solution. After the solvent was evaporated under vacuum, the desired complex was isolated as an orange-yellow solid. Yield: 90% (156 mg). **Method B.** A suspension of **4** (200 mg, 0.453 mmol) and NEt$_3$ (1.26 mL, 9.06 mmol) in toluene (10mL) was stirred at 80°C for 24h. After that the solvent was removed under vacuum, and **6** was obtained as an orange-yellow solid. Yield: 180 mg (93%). Anal. Calcd. for C$_{20}$H$_{38}$N$_2$NiP$_2$ (427.19): C, 56.23; H, 8.97; N, 6.56. Found: C, 56.15; H, 9.03; N, 6.50. ^{1}H NMR (δ, C$_6$D$_6$, 20°C): 7.31 (t, $^3J_{HH}$ = 7.9 Hz, 1H), 6.23 (d, $^3J_{HH}$ = 8.0 Hz, 2H), 2.65 (vt, $^{3,5}J_{HP}$ = 2.7 Hz, 6H, NCH$_3$), 2.06 (m, 4H, CH), 1.28 (m, 12H, CH$_3$), 0.95 (m, 12H, CH$_3$), -8.26 (t, $^2J_{HP}$ = 55.8 Hz, 1H, Ni-H). ^{13}C{^{1}H} NMR (δ, C$_6$D$_6$, 20°C): 160.6 (t, $^2J_{CP}$ = 16.8 Hz, Ph), 139.3 (t, $^2J_{CP}$ = 15.6 Hz, C$_{ipso}$ Ph), 127.0 (Ph), 100.2 (t, $^3J_{CP}$ = 6.2 Hz, Ph), 31.5 (NCH$_3$), 26.5 (CH(CH$_3$)$_2$), 19.9 (CH(CH_3)$_2$), 17.9 (CH(CH_3)$_2$). ^{31}P{^{1}H} NMR (δ, C$_6$D$_6$, 20°C): 144.5.

[Ni(PCP^{Me}-*i*Pr)(OC(=O)H)] (6): To a suspension of **5** (100 mg, 0.23 mmol) in pentane; the solution was stirred under 1 atm of CO$_2$, and resulting the solution immediately turned from orange-yellow to bright yellow. After 30 min. the solvent was removed under vacuum, and the bright yellow solid was obtained in good yield 90% (98 mg). Anal. Calcd. for C$_{21}$H$_{38}$N$_2$NiO$_2$P$_2$ (471.19): C, 55.53; H, 8.13; N, 5.95. Found: C, 55.65; H, 8.23; N, 5.88. ^{1}H NMR (δ, C$_6$D$_6$, 20°C): 8.61 (t, $^4J_{HP}$ = 2.5 Hz, 1H, Ni formate) 7.18 (t, $^3J_{HH}$ = 7.5 Hz, 1H), 5.96 (d, $^3J_{HH}$ = 7.5 Hz, 2H), 2.44 (vt, $^{3,5}J_{HP}$ = 2.5 Hz, 6H, NCH$_3$), 2.26 (m, 4H, CH), 1.45 (m, 12H, CH$_3$), 1.14 (m, 12H, CH$_3$). ^{13}C{^{1}H} NMR (δ, C$_6$D$_6$, 20°C): 167.1 (O(C=O)H), 161.7 (t, $^2J_{CP}$ = 16.2 Hz, Ph), 127.2 (Ph), 117.1 (t, $^2J_{CP}$ = 20.1 Hz, C$_{ipso}$ Ph), 100.7 (t, $^3J_{CP}$ = 6.2 Hz, Ph), 31.5 (t, $^2J_{CP}$ = 1.8 Hz, NCH$_3$), 25.7 (t, $^1J_{CP}$ = 10.0 Hz, CH(CH$_3$)$_2$), 17.6 (m, CH(CH_3)$_3$). ^{31}P{^{1}H} NMR (δ, C$_6$D$_6$, 20°C): 117.1. IR (ATR, cm^{-1}): 1614(s, ν_{CO}).

[Co(PCP^{Me}-*i*Pr)(NO)(κ^2O,O-NO$_2$)] (7). To a suspension of **2b** (100 mg, 0.204 mmol) and NaNO$_2$ (58 mg, 0.814 mmol) in MeOH (10 mL) was added and the reaction mixture was stirred at 60°C for 2 min. The solvent was then removed under reduced pressure and the crude product was dissolved in toluene. Insoluble materials were removed by filtration, and the solvent was evaporated under vacuum to afford **7**. This complex **7** could not be isolated in analytically pure form.

Alternative synthesis of [Co(PCP^{Me}-*i*Pr)(CO)$_2$] (8). A suspension of **2b** (300 mg, 0.68 mmol) in THF (10 mL) was stirred under a CO atmosphere for 10 min. The solvent was then removed under reduced pressure yielding **8** as analytically pure yellow solid. Yield: 318 mg (97%). The spectroscopic identification of **8** was confirmed by using an authentic sample generated *via* a different method reported recently.[13]

[Co(PCP^{Me}-*i*Pr)(CN*t*Bu)$_2$] (9). To a suspension of **2b** (300 mg, 0.68 mmol) and (300 mg, 0.68 mmol) *tert*-butyl isocyanide (154 µL, 1.36 mmol) in THF (10 mL) was added at room temperature and was stirred for 10 min. The solvent was then removed under reduced pressure yielding **9** as an

analytically pure yellow solid. Yield: 390 mg (97%). Anal. Calcd. for $C_{60}H_{55}CoN_4P_2$ (592.68): C, 60.80; H, 9.35; N, 9.45. Found: C, 59.84; H, 9.74; N, 9.27. ^{1}H NMR (δ, C_6D_6, 20°C): 7.10 (t, $^3J_{HH}$ = 7.5 Hz, 1H, Ph^4), 6.12 (d, $^3J_{HH}$ = 7.5 Hz, 2H, Ph^{3,5}), 2.85 (s, 6H, NCH$_3$), 2.37 (m, 4H, CH), 1.38 (vq, J = 7.5 Hz, 12H, CH$_3$), 1.24 (vq, J = 7.5 Hz, 12H, CH$_3$), 1.00 (s, 18H, CH$_3$). ^{31}P{^{1}H} NMR (δ, C_6D_6, 20°C): 164.6. IR (ATR, cm^{-1}): 2037 (ν_{CN}), 1990 (ν_{CN}).

X-ray Structure Determination. X-ray diffraction data of **2a**, **2b**, **4**, **5, 7** and **9** were collected at T = 100 K in a dry stream of nitrogen on a Bruker Kappa APEX II diffractometer system using graphite-monochromatized Mo-$K\alpha$ radiation (λ = 0.71073 Å) and fine sliced φ- and ω-scans. Data of **6** were collected on a Bruker SMART APEX diffractometer at 190 K. Crystals of **5** were systematically twinned by twofold rotation around [001]. The reflections of both domains were separated using RLATT.[43] Data were reduced to intensity values with SAINT and an absorption correction was applied with the multi-scan approach implemented in SADABS and TWINABS.[35] The structures were solved by charge flipping using SUPERFLIP[44] and refined against F with JANA2006.[45] The structure of **2b** was solved by direct methods and refined against F^2 with the SHELX suite.[46] Non-hydrogen atoms were refined anisotropically. The H atoms connected to C atoms were placed in calculated positions and thereafter refined as riding on the parent atoms. H atoms connected to N and B were located in difference Fourier maps and their positions refined without restraints. Molecular graphics were generated with the program MERCURY.[47] Crystal data and experimental details are given in Tables S1, S1 and S2.

Table S1. Details for the crystal structure determinations of **2a** and **2b**.

	2a	**2b**
formula	$C_{20}H_{41}BCoN_2P_2$	$C_{22}H_{45}BCoN_2P_2$
fw	441.2	469.3
cryst.size, mm	0.26 x 0.13 x 0.08	0.78 x 0.27 x 0.10
color, shape	red plate	red rhombic prism
crystal system	triclinic	orthorhombic
space group	P-1 (no. 2)	$Pna2_1$ (no. 33)
a, Å	7.8255(13)	22.7682(5)
b, Å	8.5372(15)	8.0685(8)
c, Å	17.914(3)	13.9631(15)
α, °	87.162(3)	90
β, °	81.981(3)	90
γ, °	80.160(3)	90
V, Å^3	1167.3(3)	2565.1(4)
T, K	100	100
Z,Z'	2,1	4,1
ρ_{calc}, g cm^{-3}	1.255	1.2148
μ, mm^{-1} (MoKα)	0.879	0.804
F(000)	474	1012
absorption corrections, T_{min}-T_{max}	multi-scan, 0.64–0.75	multi-scan, 0.77–0.2

θ range, deg	2.30–34.85	1.79–32.64
no. of rflns measd	45128	15456
R_{int}	0.0479	0.0374
no. of rflns unique	9458	8540
no. of observed rflns	7972	7256
no. of params / restraints	261 / 0	278 / 0
R (obs) [a]	0.0385	0.0342
R (all data)	0.0500	0.0438
wR (obs)	0.0829	0.0425
wR (all data)	0.0866	0.0443
GooF	1.127	1.19
Diff.Four.peaks min/max, eÅ^{-3}	-0.62 / 0.71	-0.46 / 0.78
Flack Parameter	-	0.039(10)
CCDC no.	1044984	1044985

[a] $R = \Sigma ||F_o|-|F_c|| / \Sigma|F_o|$, $wR = \Sigma w(|F_o| - |F_c|) / \Sigma w|F_o|$, $GooF = \{\Sigma[w(F_o^2 - F_c^2)^2] / (n-p)\}^{1/2}$

Table S2. Details for the crystal structure determinations of **4**·0.5C_6D_6, **5** and **6**.

	4·0.5C_6D_6	**5**	**6**
formula	$C_{23}H_{41}BD_3N_2NiP_2$	$C_{20}H_{38}N_2NiP_2$	$C_{21}H_{38}N_2NiO_2P_2$
fw	483.1	441.2	471.2
cryst.size, mm	0.70 x 0.22 x 0.18	0.75 x 0.44 x 0.21	0.41 x 0.17 x 0.12
color, shape	yellow rod	yellow rod	yellow rod
crystal system	triclinic	monoclinic	monoclinic
space group	P-1 (no. 2)	$C2/c$ (no. 15)	Pc (no. 7)
a, Å	8.1142(12)	42.645(3)	14.7792(2)
b, Å	17.466(3)	8.0359(5)	11.41410(10)
c, Å	18.659(3)	34.288(2)	14.7930(2)
α, °	80.991(4)	90	90
β, °	84.592(4)	128.157(2)	105.6859(6)
γ, °	84.341(4)	90	90
V, Å^3	2590.7(7)	9239.4(10)	2402.52(5)
T, K	100	100	100
Z,Z'	4,2	16,2	4,2
ρ_{calc}, g cm^{-3}	1.2382	1.228	1.3022
μ, mm^{-1} (MoKα)	0.884	0.984	0.959
F(000)	1036	3680	1008
absorption corrections, T_{min}-	multi-scan, 0.79–0.86	multi-scan, 0.60–0.81	multi-scan, 0.56–0.85
θ range, deg	1.11–32.70	1.21–30.16	1.78–32.49
no. of rflns measd	90328	182299	29799
R_{int}	0.0657	0.0403	0.0456
no. of rflns unique	18186	13654	13227
no. of observed rflns	11003	12567	10903
no. of params / restraints	555 / 0	460 / 0	278 / 0

R (obs) [a]	0.0524	0.0564	0.0323
R (all data)	0.1087	0.0617	0.0385
wR (obs)	0.0482	0.0617	0.0329
wR (all data)	0.0528	0.0630	0.0335
GooF	1.63	3.56	1.36
Diff.Four.peaks min/max. eÅ^{-3}	-1.03 / 0.96	-0.58 / 1.17	-0.24 / 0.45
Flack Parameter	-	-	-0.009(7)
Twin operation	-	twofold rotation around **c**	-
Twin volume fraction	-	0.7950:0.2050(6)	-
CCDC no.	1044986	1044987	1044988

Table S3. Details for the crystal structure determinations of **9**

	9
formula	$C_{30}H_{55}CoN_4P_2$
fw	592.7
cryst.size, mm	0.59 x 0.49 x 0.32
color, shape	dark red block
crystal system	triclinic
space group	$P\bar{1}$ (no. 2)
a, Å	10.8912(7)
b, Å	12.0810(7)
c, Å	14.7286(9)
α, °	80.2728(18)
β, °	69.8408(18)
γ, °	64.0797(16)
V, Å^3	1635.83(18)
T, K	100
Z,Z'	2,1
ρ_{calc}, g cm^{-3}	1.2033
μ, mm^{-1} (MoKα)	0.646
F(000)	640
absorption corrections, T_{min}-T_{max}	multi-scan, 0.69–0.81
θ range, deg	2.2–32.2
no. of rflns measd	42947
R_{int}	0.0224
no. of rflns unique	11934
no. of rflns $I>3\sigma(I)$	10062

no. of params / restraints	334 / 0
R ($I > 3\sigma(I)$) [a]	0.0284
R (all data)	0.0374
wR ($I > 3\sigma(I)$)	0.0375
wR (all data)	0.0381
GooF	2.04
Diff.Four.peaks min/max, eÅ^{-3}	-0.25 / 0.43
Flack Parameter	-
CCDC no.	1049854

[a] $R = \Sigma||F_o|-|F_c|| / \Sigma|F_o|$, $wR = \Sigma w(|F_o| - |F_c|) / \Sigma w|F_o|$, GooF = $\{\Sigma[w(F_o^2 - F_c^2)^2] / (n-p)\}^{1/2}$

Computational Details. All calculations were performed using the GAUSSIAN 09 software package[48] on the Phoenix Linux Cluster of the Vienna University of Technology. The optimized geometries were obtained with the B3LYP functional,[49] without symmetry constraints. That functional includes a mixture of Hartree-Fock[50] exchange with DFT[35] exchange-correlation, given by Becke's three parameter functional with the Lee, Yang and Parr correlation functional, which includes both local and non-local terms. The basis set used for the geometry optimizations consisted of the Stuttgart/Dresden ECP (SDD) basis set[51] to describe the electrons of the metal atoms, and a standard 6-31G(d,p) basis set[52] for all other atoms. A Natural Population Analysis (NPA)[37] and the resulting Wiberg indices[36] were used to study the electronic structure and bonding of the optimized species. The molecular orbitals of the Co complex presented in Figure 6 result from single point restricted open shell calculations performed on the optimized structure. Three-dimensional representations of the orbitals were obtained with the program Chemcraft.[53]

References

1   For reviews on borohydride complexes see: (a) Marks, T. J.; Kolb, J. R. *Chem. Rev.* **1977**, *77*, 263. (b) Ephritikhine, M. *Chem. Rev.* **1997**, *97*, 2193. (c) Xu, Z.; Lin, Z. *Coord. Chem. Rev.* **1996**, *156*, 139. (d) Edelstein, N. *Inorg. Chem.* **1981**, *20*, 297. (e) Makhaev, V. D. *Russ. Chem. Rev.* **2000**, *69*, 727. (f) Besora, M.; Lledos, A. *Struct. Bonding (Berlin)* **2008**, *130*, 149. (a) Ariafard, A.; Amini, M. M. *J. Organomet. Chem.* **2005**, *690*, 84.

2   Tamm, M.; Dreßel, B.; Bannenberg, T.; Grunenberg, J.; Herdtweck, E. *Z. Naturforsch.* **2006**, *61b*, 896.

3   Ohkuma, T.; Koizumi, M.; Muniz, K.; Hilt, G.; Kabuto, C.; Noyori, R. *J. Am. Chem. Soc.* **2002**, *124*, 6508. (b) Sandoval, C. A.; Ohkuma, T.; Muniz, K.; Noyori, R. *J. Am. Chem. Soc.* **2003**, *125*, 13490.

4   Guo, R.; Chen, X.; Elpelt, C.; Song, D.; Morris, R. *Org. Lett.* **2005**, *7*, 1757.

5   Chakraborty, S.; Zhang, J.; Patel, Y. J.; Krause, J. A.; Guan, H. *Inorg. Chem.* **2013**, *52*, 37.

6   Dudle, B.; Blacque, O.; Berke, H. *Organometallics* **2012**, 31, 1832.

7   Chakraborty, S. M.; Paraskevi O. Lagaditis, P.; Förster, M.; Bielinski, E. A.; Hazari, N.; Holthausen, M. C.; William D. Jones, W. D.; Schneider, S. *ACS Catal.* **2014**, 4, 3994.

8   Langer, R.; Iron, M. A.; Konstantinovski, L.; Diskin-Posner, Y.; Leitus, G.; Ben-David, Y.; Milstein, D. *Chem. Eur. J.* **2012**, *18*, 7196.

9   Zhang, J.; Balaraman, E.; Leitus, G.; Milstein, D. *Organometallics* **2011**, 30, 5716.

10   Chakraborty, S.; Dai, H.; Bhattacharya, P.; Fairweather, N. T.; Gibson, M. S.; Krause, J. A.; Guan, H. *J. Am. Chem. Soc.* **2014**, *136*, 7869.

11   Werkmeister, S.; Junge, K.; Wendt, B.; Alberico, E.; Jiao, H.; Baumann, W.; Junge, H.; Gallou, F.; Beller, M. *Angew. Chem. Int. Ed.* **2014**, *53*, 8722.

12   (a) Makhaev, V. D. *Russ. Chem. Rev.* **2003**, *69*, 257. (b) Hall, C. Perutz, R. N. *Chem. Rev.* **1996**, *96*, 3125.

13   Kubas, G. J. *Metal Dihydrogen and σ-Bond Complexes*, Kluwer Academic/Plenum Publishers, New York **2001**.

14   a) Murugesan, S.; Stöger, B.; Carvalho, M. D.; Ferreira, L. P.; Pittenauer, E.; Allmaier, G.; Veiros, L. F.; Kirchner, K. *Organometallics.* **2014**, *33*, 6132. b) S. Murugesan, B. Stöger, L. F. Veiros, K. Kirchner, *Organometallics*, **2015**, *34*, 1364.

15   Xu, G. Q.; Sun, H. J.; Li, X. Y. *Organometallics* **2009**, *28*, 6090.

16   Lian, Z.; Xu, G.; Li, X. *Acta Crystallogr., Sect. E:* Struct. Rep. Online **2010**, *E66*, m636.

17   Hebden, T. J.; St. John, A. J.; Gusev, D. G.; Kaminsky, W.; Goldberg, K. I.; Heinekey, D. M. *Angew. Chem. Int. Ed.* **2011,** *50,* 1873.

18   Zhu, G.; Li, X.; Xu, G.; Wang, L.; Sun, H. *Dalton Trans.* **2014**, *43*, 8595.

19   Kent, M. A.; Woodall, C. H.; Haddow, M. F.; McMullin, C. L.; Pringle, P. G.; Wass, D. F. *Organometallics* **2014**, *33*, 5686.

20   Holah, D. G.; Hughes, A. N.; Hui, B. C.; Wright, K. *Can. J. Chem.* **1974**, *52*, 2990.

21   (a) Dapporto, P.; Midollini, S.; Orlandini, A.; Sacconi, L. *Inorg. Chem.* **1976**, *15*, 2768. (b) Dapporto, P.; Midollini, S.; Orlandini, A.; Sacconi, L. *Cryst. Struct. Commun.* **1976**, *5*, 163.

22   (a) Nakajima, M.; Morivama, H.; Kobayashi, A.; Saito, T.; Sasaki, *Y. J. Chem. Soc., Chem. Commun.* **1975**, 80. (b) M. Nakajima. T. Saito. A. Kobayashi, Y. Sasaki. *J. Chem. Soc., Dalton Trans.* **1977**, 385.

23   Lin, T.-Z., Peters, J. C. *J. Am. Chem. Soc.* **2013**, *135*, 15310.

24   Corey, E. J.; Cooper, N. J.; Canning, W. M.; Lipscomb, W. N.; Koetzle, T. F. *Inorg Chem.* **1982**, *21*, 192.

25   Holah, D. G.; Hughes, A. N.; Maciaszek, S.; Magnuson, V. R.; Parker K. O. *Inorg. Chem.* **1985**, 24, 2956.

26   Sur, S. K. *J. Magn. Reson.* **1989**, *82*, 169.

27   (a) Carlin, R. L. *Magnetochemistry*; Springer-Verlag: Heidelberg, **1986**. (b) Orchard, A. F. *Magnetochemistry*; Oxford University Press, **2003**.

28   Addison, A. W.; Rao, T. N.; Reedijk, J.; van Rijn J.; Verschoor, G. C. *J. Chem. Soc., Dalton Trans.* **1984**, 1349.

29   Kandiah, M.; McGrady, G. S.; Decken, A.; Sirsch, P. *Inorg. Chem.* **2005**, *44*, 8650.

30   Churchard, A. J.; Cyranski, M. K.; Dobrzycki, L.; Budzianowski, A.; Grochala, W. *Energy Environ. Sci.* **2010**, *3*, 1973.

31   Saito, T.; Nakajima, M.; Kobayashi, A.; Sasaki, Y. *J. Chem. Soc., Dalton Trans*. **1978**, 482.

32   Desrochers, P. J.; LeLievre, S.; Johnson, R. J.; Lamb, B. T.; Phelps, A. L.; Cordes, A. W.; Gu, W.; Cramer, S. P. *Inorg. Chem.* **2003**, *42*, 7945.

33   Rossin, A.; Peruzzini, M.; Zanobini, F. *Dalton Trans.* **2011**, *40*, 4447.

34   Chakraborty, S.; Krause, J. A.; Guan, H. *Organometallics* **2009**, *28*, 582.

35   Koridze, A. A.; Kuklin, S. A.; Sheloumov, A. M.; Dolgushin, F. M.; Lagunova, V. Y.; Petukhova, I. I.; Ezernitskaya, M. G.; Peregudov, A. S.; Petrovskii, P. V.; Vorontsov, E. V.; Baya, M.; Poli, R. *Organometallics* **2004**, *23,* 4585.

36   Bianchini, C.; Laschi, F.; Peruzzini, M.; Ottaviani, F. M. ;Vacca, A.; Zanellot, P. *Inorg. Chem.* **1990**, *29*, 3394.

37   Semproni, S. P.; Milsmann, C.; Paul J. Chirik, P. J. *J. Am. Chem. Soc*. **2014**, *136*, 9211.

38   Nückel, S.; Burger, P. *Organometallics* **2001,** *20,* 4345.

39   Parr, R. G.; Yang, W. *Density Functional Theory of Atoms and Molecules*, Oxford University Press, New York, **1989**.

40   (a) WI represents the Wiberg index. Wiberg indices are electronic parameters related with the electron density between two atoms, which scale as bond strength indicators. They can be obtained from a Natural Population Analysis. (b) Wiberg, K. B. *Tetrahedron* **1968**, *24*, 1083.

41   (a) Carpenter, J. E.; Weinhold, F. *J. Mol. Struct. (Theochem)*, **1988,** *169*, 41. (b) Carpenter, J. E. *PhD. Thesis*. University of Wisconsin, Madison, WI, **1987**. (c) Foster, J. P.; Weinhold, F. *J. Am. Chem. Soc.*, **1980,** *102*, 7211. (d) Reed, A. E.; Weinhold, F. *J. Chem. Phys.*, **1983,** *78*, 4066. (e) Reed, A. E.; Weinhold, F. *J. Chem. Phys.*, **1985,** *83*, 1736. (f) Reed, A. E.; Weinstock, R. B.; Weinhold, F. *J. Chem. Phys.*, **1985,** *83*, 735. (g) Reed, A. E.; Curtiss, L. A.; Weinhold, F. *Chem. Rev.*, **1988,** *88*, 899. (h) Weinhold, F.; Carpenter, J. E., *The Structure of Small Molecules and Ions*. Plenum, New York, **1988**; p 227.

42   Perrin, D. D.; Armarego, W. L. F. *Purification of Laboratory Chemicals*, 3rd ed.; Pergamon: New York, **1988**.

43   Bruker computer programs: APEX2, SAINT, SADABS and TWINABS (Bruker AXS Inc., Madison, WI, 2012).

44   Palatinus, L.; Chapuis. G. *J. Appl. Cryst.* **2007,** *40*, 786.

45   Petříček, V.; Dušek, M.; Palatinus, L. *Z. Kristallogr*. **2014**, *229*, 345.

46   Sheldrick. G. M. *Acta Cryst.* **2008**, *A64*, 112.

47   Macrae, C. F.; Edgington, P. R.; McCabe, P.; Pidcock, E.; Shields, G. P.; Taylor, R.; Towler, M.; van de Streek, J. *J. Appl. Cryst.* **2006**, *39*, 453.

48   Gaussian 09, Revision A.02, Frisch, M. J.; Trucks, G. W.; Schlegel, H. B.; Scuseria, G. E.; Robb, M. A.; Cheeseman, J. R.; Scalmani, G.; Barone, V.; Mennucci, B.; Petersson, G. A.; Nakatsuji, H.; Caricato, M.; Li, X.; Hratchian, H. P.; Izmaylov, A. F.; Bloino, J.; Zheng, G.; Sonnenberg, J. L.; Hada, M.; Ehara, M.; Toyota, K.; Fukuda, R.; Hasegawa, J.; Ishida, M.; Nakajima, T.; Honda, Y.; Kitao, O.; Nakai, H.; Vreven, T.; Montgomery, Jr., J. A.; Peralta, J. E.; Ogliaro, F.; Bearpark, M.; Heyd, J. J.; Brothers, E.; Kudin, K. N.; Staroverov, V. N.; Kobayashi, R.; Normand, J.; Raghavachari, K.; Rendell, A.; Burant, J. C.; Iyengar, S. S.; Tomasi, J.; Cossi, M.; Rega, N.; Millam, J. M.; Klene, M.; Knox, J. E.; Cross, J. B.; Bakken, V.; Adamo, C.; Jaramillo, J.; Gomperts, R.; Stratmann, R. E.; Yazyev, O.; Austin, A. J.; Cammi, R.; Pomelli, C.; Ochterski, J. W.; Martin, R. L.; Morokuma, K.; Zakrzewski, V. G.; Voth, G. A.; Salvador, P.; Dannenberg, J. J.; Dapprich, S.; Daniels, A. D.; Farkas, Ö.; Foresman, J. B.; Ortiz, J. V.; Cioslowski, J.; Fox, D. J. Gaussian, Inc., Wallingford CT, **2009**.

49   (a) Becke, A. D. *J. Chem. Phys.* **1993**, *98*, 5648. (b) Miehlich, B.; Savin, A.; Stoll, H.; Preuss, H. *Chem. Phys. Lett* **1989**, *157*, 200. (c) Lee, C.; Yang, W.; Parr, G. *Phys. Rev. B* **1988**, *37*, 785.

50   Hehre, W. J.; Radom, L.; Schleyer, P. v. R.; Pople, J. A., *Ab Initio Molecular Orbital Theory*. John Wiley & Sons, New York, **1986**.

51   (a) Haeusermann, U.; Dolg, M.; Stoll, H.; Preuss, H. *Mol. Phys.* **1993**, *78*, 1211. (b) Kuechle, W.; Dolg, M.; Stoll, H.; Preuss, H. *J. Chem. Phys.* **1994**, *100*, 7535. (c) Leininger, T.; Nicklass, A.; Stoll, H.; Dolg, M.; Schwerdtfeger, P. *J. Chem. Phys.* **1996**, *105*, 1052.

52   (a) McLean, A. D.; Chandler, G. S. *J. Chem. Phys.* **1980**, *72*, 5639. (b) Krishnan, R.; Binkley, J. S.; Seeger, R.; Pople, J. A. *J. Chem. Phys.* **1980**, *72*, 650. (c) Wachters, A. J. H. *J. Chem. Phys.* **1970**, *52*, 1033. (d) Hay, P. J. *J. Chem. Phys.* **1977**, *66*, 4377. (e) Raghavachari, K.; Trucks, G. W. *J. Chem. Phys.* **1989**, *91*, 1062. (f) Binning Jr., R. C.; Curtiss, L. A. *J. Comp. Chem.,* **1990**, *11*, 1206. (g) McGrath, M. P.; Radom, L. *J. Chem. Phys.* **1991**, *94*, 511.

53   http://www.chemcraftprog.com/

A Co(I) Pincer Complex with an η^2-C-H Agostic Arene Bond - Facile C-H Bond Cleavage *via* Deprotonation, Radical Abstraction, and Oxidative Addition

The synthesis and reactivity of a Co(I) pincer complex [Co($\eta^3 P,CH,P$-P(CH)P^{Me}-*i*Pr)(CO)$_2$]$^+$ featuring an η^2-C$_{aryl}$-H agostic bond is described. This complex was obtained via protonation of the Co(I) complex [Co(PCP^{Me}-*i*Pr)(CO)$_2$]. The Co(III) hydride complex [Co(PCP^{Me}-*i*Pr)(CNtBu)$_2$(H)]$^+$ was obtained upon protonation of [Co(PCP^{Me}-*i*Pr)(CNtBu)$_2$]. Three ways to cleave the agostic C-H bond are presented. Due to the acidity of the agostic proton treatment with pyridine results in facile deprotonation (C-H bond cleavage), and reformation of [Co(PCP^{Me}-*i*Pr)(CO)$_2$]. Secondly, C-H bond cleavage is achieved upon exposure of [Co($\eta^3 P,CH,P$-P(CH)P^{Me}-*i*Pr)(CO)$_2$]$^+$ to oxygen or TEMPO to yield the paramagnetic Co(II) PCP complex [Co(PCP^{Me}-*i*Pr)(CO)$_2$]$^+$. Finally, replacement of one CO ligand in [Co($\eta^3 P,CH,P$-P(CH)P^{Me}-*i*Pr)(CO)$_2$]$^+$ by CNtBu promotes the rapid oxidative addition of the agostic η^2-C$_{aryl}$-H bond to give two isomeric hydride complexes of the type [Co(PCP^{Me}-*i*Pr)(CNtBu)(CO)(H)]$^+$.

4.1 Introduction

The selective activation and breaking of strong C-H bonds by transition metal complexes is of great importance in chemistry. Much research is devoted to fundamentally understand such processes which are key steps in many organic and organometallic reactions. In recent years, particularly catalytic C-H bond activation reactions emerged as powerful synthetic tool in organic synthesis.[1] There are reasonably well-established mechanistic pathways for C-H bond activation reported over the years including σ-bond metathesis in early transition metal complexes, electrophilic activation in electron-deficient late transition metal complexes, or Lewis-base assisted metalation.[2] As electron rich late transition metal complexes are concerned oxidative addition, which leads to alkyl or aryl hydride complexes, is the typical pathway. This process is associated with a formal two electron oxidation of the metal center. Oxidative addition requires apparently pre-coordination of the C-H bond, *i.e.*, the formation of an agostic intermediate or, at least, transition state.[3,4] In this respect, intramolecular and directed C-H activation reactions of Ru, Rh, and Ir PCP pincer complexes led to the formation of stable complexes which contain η^2-C-H agostic arene bonds.[5,6,7,8,9,10,11] Particularly intriguing are agostic square-planar Rh(I) pincer complexes reported by Milstein and coworkers.[5] These four-coordinate species were unable to cleave the C-H bond and no oxidative addition to form Rh(III) hydride complexes took place. However, addition of CO, despite of being a weak σ-donor, sufficiently increased the electron density at the metal center and triggered the oxidative addition process (Scheme 1). Based on DFT calculations, the aromatic C-H cyclometalation process was suggested to procced *via* an elusive agostic-like trigonal bipyramidal dicarbonyl Rh(I) intermediate.
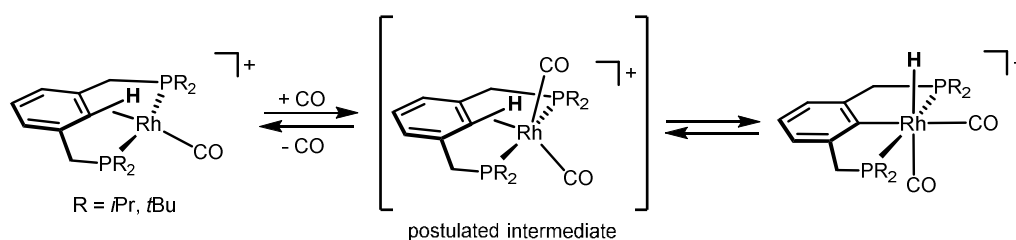
Scheme 1. Reaction pathway for the CO induced agostic/aryl hydride equilibrium of rhodium PCP pincer complexes proceeding *via* a postulated agostic dicarbonyl species.

Herein we report the synthesis and reactivity of a five-coordinate Co(I) PCP pincer complex which features an agostic η^2-C-H arene bond. This is the first agostic pincer complex of a non-precious transition metal and underlines the strikingly different coordination chemistry of low-spin Co(I) and Rh(I) complexes. The first favor typically five-coordinate square pyramidal of trigonal bipyramidal geometries,[12] while the latter favor four-coordinate square planar arrangements. Accordingly, the key complex described here may be viewed as "missing link" on the pathway to Rh(III) hydride complexes (Scheme 1).

4.2 Results and discussion

The starting materials for the study, $[Co(PCP^{Me}\text{-}i Pr)(CO)_2]$ (**1**) and $[Co(PCP^{Me}\text{-}i Pr)(CN t Bu)_2]$ (**2**), were obtained by the reaction of $[Co(PCP^{Me}\text{-}i Pr)(\eta^2\text{-}BH_4)]$ with CO and CN*t*Bu, respectively (Scheme 9, Chapter 3). Complex **1** was already prepared *via* a different route by stirring $[Co(PCP^{Me}\text{-}i Pr)Cl]$ in toluene with KC_8 in the presence of CO (Scheme 5, Chapter 2). It should be noted that the complex **2** is stable in pentane or ether solvents like Et_2O and THF, with other solvents like CH_2Cl_2, MeOH and acetone decomposed gradually (Scheme 2).
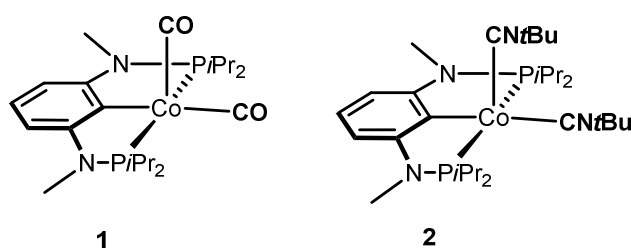
Scheme 2 Co(I) PCP carbonyl $[Co(PCP^{Me}\text{-}i Pr)(CO)_2]$ (**1**) and isocyanide $[Co(PCP^{Me}\text{-}i Pr)(CN t Bu)_2]$ (**2**) Complexes.

Protonation of $[Co(PCP^{Me}\text{-}i Pr)(CO)_2]$ (**1**)[13] with $HBF_4 \cdot Et_2O$ leads to the formation of the cationic Co(I) complex $[Co(\eta^3 P,CH,P\text{-}P(CH)P^{Me}\text{-}i Pr)(CO)_2]^+$ (**3**) in 94% isolated yield (Scheme 3). Interestingly, this complex features not only an $\eta^2\text{-}C_{aryl}$-H agostic bond but also contains two CO ligands which contrasts the

behavior of related Rh complexes were exclusively square-planar mono CO complexes are formed (Scheme 1).
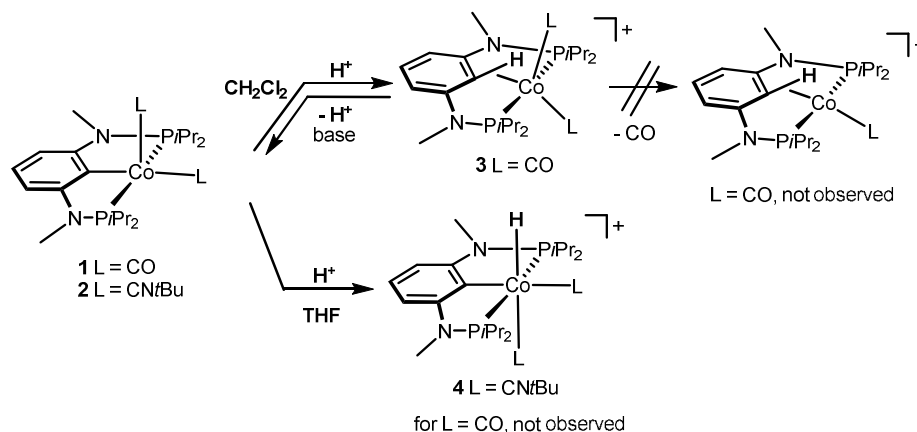
Scheme 3. Synthesis of **3** and **4** upon reaction of **1** with HBF$_4$·Et$_2$O - ligand *versus* metal protonation.

There was no evidence for the formation of the monocarbonyl complex [Co($\eta^3 P,CH,P$-P(CH)P^{Me}-iPr)(CO)]$^+$ or the Co(III) hydride complex [Co(PCP^{Me}-iPr)(CO)$_2$(H)]$^+$. Complex **3** was fully characterized by a combination of ^{1}H, ^{13}C{^{1}H}, and ^{31}P{^{1}H} NMR spectroscopy, IR, ESI MS, elemental analysis and X-ray crystallography. An important feature of the ^{1}H NMR spectrum is the high-field shift of the proton attached to the *ipso*-carbon giving rise to a triplet at 2.23 ppm ($^4 J_{HP}$ = 7.5 Hz). In the ^{13}C{^{1}H} NMR spectrum the ipso-carbon atom exhibits a signal at 67.0 ppm (105.3 ppm in the free PCP ligand) (Figure 2), the two CO ligands give rise to two low-field resonances as poorly resolved triplets centered at 197.9 and 197.5 ppm. The relatively low $^1 J_{HC}$ coupling constant of 102.0 Hz, as compared to 160.5 and 163.5 Hz for the other two aromatic C-H bonds, is also characteristic for a strong C-H metal interaction.[Complex **3** exhibits two bands at 1950 and 2009 cm^{-1} in the IR spectrum for the mutually *cis* CO ligands assignable to the symmetric and asymmetric CO stretching frequencies, respectively (*cf.* 1906 and 1963 cm^{-1} in the more electron rich complex **1**).
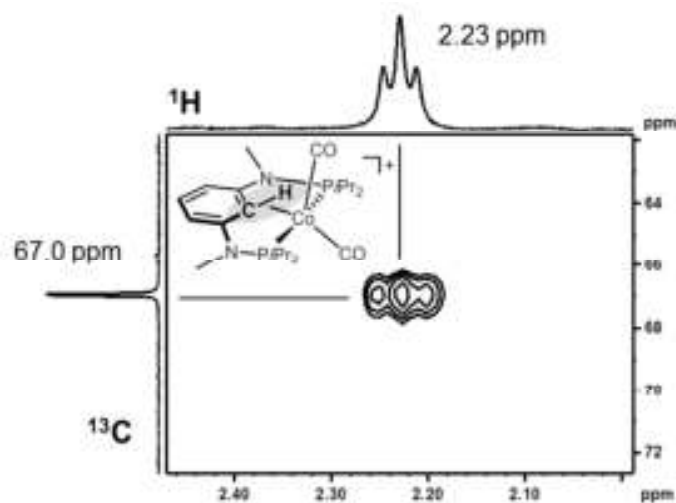
Figure 2. Section of the ^{1}H-^{13}C HSQC spectrum of **3** in CD$_2$Cl$_2$ indicating a cross-peak between the agostic H1 and C1 atoms.

A structural view of **3** is depicted in Figure 3 with selected bond distances and angles reported in the caption. The overall geometry about the cobalt center is best described as distorted trigonal bipyramidal where the two carbonyl ligands and the agostic η^2-C$_{aryl}$-H bond define the equatorial plane and the phosphine moieties the axial positions. The distance between the ipso-carbon and the Co atom is
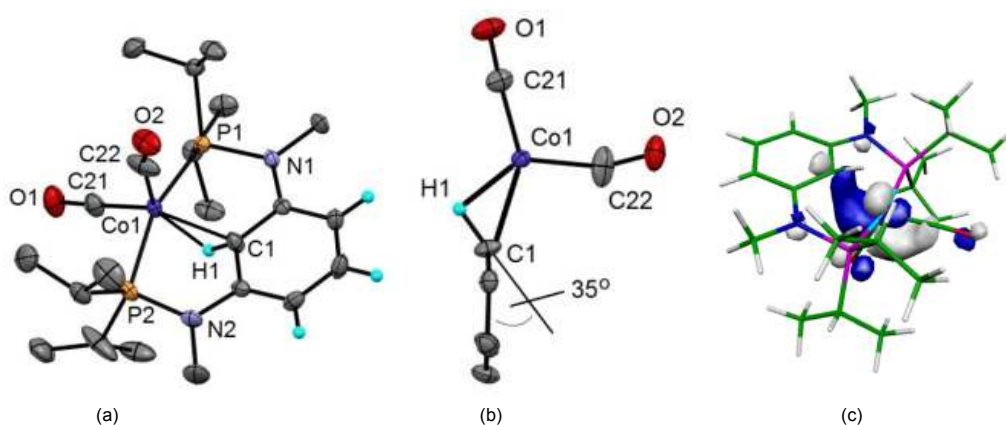
Figure 3. (a) Structural view of **3** showing 50% thermal ellipsoids (most H atoms and BF$_4^-$ counterion omitted for clarity). (b) Positioning of H1 in relation to the Co center and to the benzene ring. (c) HOMO-2 of complex **3** (1.2 eV below the HOMO).

extremely long (2.2197(6) Å) relative to regular cobalt-carbon σ-bonds. For instance the Co-C$_{ipso}$ bond distances in the Co(I) and Co(II) PCP complexes [Co(PCP^{Me}-iPr)(CO)$_2$] (**1**) and [Co(PCP^{Me}-iPr)(CO)$_2$]$^+$ (**5**) are substantially shorter being 1.998(2) and 1.953(2) Å, respectively. The H(1) atom (which was located in

difference Fourier maps and refined freely) strongly interacts with the cobalt center (1.72(2) Å) which was also evident from the ^{1}H NMR spectrum of **3**. It is noteworthy that this hydrogen is severely removed from the aromatic plane by ca. 35° (*cf* in related Ru, Rh, and Os complexes this angle is in the range of 14-30°).[5,7,10,14] The C1-H1 bond length of 1.05(3) Å is in the range observed in X-ray diffraction measurements for unactivated hydrocarbons (e.g., 1.08 Å in C_6H_6).

The nature of the interaction between the C1-H1 bond and the Co-atom in complex **3** was investigated by means of DFT/PBE0 calculations. The relevant Wiberg indices (WI)[15] indicate the formation of weak Co-C and Co-H bonds, with WI = 0.17 and 0.05, respectively, suggesting the existence of an agostic C-H···Co bond. As a consequence, there is a clear weakening of the C–H bond, much longer (1.14 Å) and weak (WI = 0.76) than the remaining C_{aryl}-H bonds (1.08 Å and WI = 0.90), justifying the H-acidity revealed by complex **3** (see above). Moreover, the HOMO-2 of complex **3** (Figure 3) represents π-back donation from a Co d-orbital to the C-H σ* orbital, being characteristic of an agostic bond and corroborating the experimental results. Positive-ion mass spectrum of oxidized (Co^+ to Co^{2+}) compound MS1 lacking an ion related to the agostic Co(I) complex **3** but forming a ($[M(Co^{2+})$-H–CO$]^+$ = 454.2) species during ionization by in-source decay. A second loss of CO of low abundance is detected at m/z 426.2. The inset corresponds to the measured isotope pattern of the selected signal $[M(Co^{2+})$-H-CO$]^+$ (blue line) in comparison to its calculated isotope pattern (red line) (Figure 4).
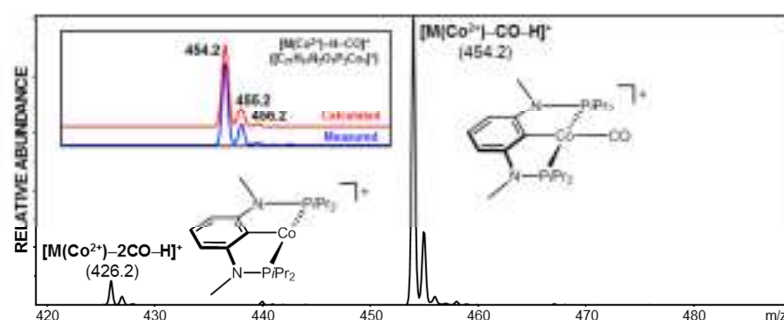
Figure 4. ESI MS spectrum of **3**

If, on the other hand, [Co(PCP^{Me}-*i*Pr)(CN*t*Bu)$_2$] (**2**)[16,17] (isocyanides are stronger electron donating ligands than CO) is treated with HBF$_4$·Et$_2$O, the metal center is now protonated affording exclusively the octahedral cationic Co(III) hydride complex [Co(PCP^{Me}-*i*Pr)(CN*t*Bu)$_2$(H)]$^+$ (**4**) in 94% isolated yield (Scheme 3). The ^{1}H NMR spectrum confirmed the presence of one hydride ligand, which appeared at -13.76 ppm as a well-resolved triplet with a $^2J_{HP}$ coupling constant of 50.0 Hz. In the ^{13}C{^{1}H} NMR spectrum the ipso carbon atom gives rise to a triplet centered at 101.1 ppm (J_{HP} = 5.6 Hz). Moreover, in the ESI MS spectrum of **4** the intact complex [M]$^+$ was observed as a major fragment m/z 593.3. (**A**) Positive-ion mass spectrum of oxidized (Co^{2+} to Co^{3+}) compound MS2 ([M(Co^{3+})]$^+$ = 593.3) as occurring during ionization and exhibiting strong in-source decay by loss of a hydrogen atom plus CN*t*Bu forming a

$[M(Co^{2+})-H-C_5H_9N_1]^+$ species (m/z 509.1). The small unassigned signal at m/z 592.3 most likely corresponds to an unoxidized $[M(Co^{2+})-H]^+$ species. Panel (**B**) shows the low-energy CID-MS^2 spectrum of the $[M(Co^{3+})]^+$ precursor ion exhibiting predominantly neutral loss of CN*t*Bu keeping the +III oxidation state of cobalt forming a $[M(Co^{3+})-C_5H_9N_1]^+$ product ion (m/z 510.1) and to a lesser extent a $[M(Co^{2+})-H-C_5H_9N_1]^+$ product ion (m/z 509.1). The isolation width and activation width for this tandem mass spectrometric experiment were 6 Dalton in order to cover the entire isotope cluster of the precursor ion. The insets in both panels correspond to the measured isotope pattern of selected signals (blue line) in comparison to their calculated isotope pattern (red line). Minor differences between measured and calculated pattern are due to different oxidation states of the central cobalt cation plus/minus one hydrogen atom (Figure 5).
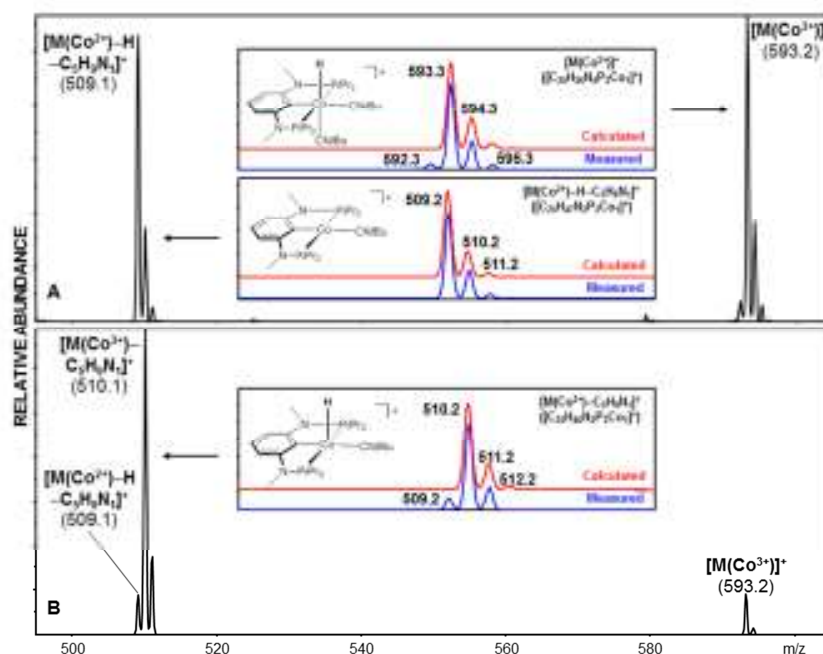
Figure 5. ESI MS spectrum of **4**

The agostic C-H arene bond in $[Co(\eta^3P,CH,P-P(CH)P^{Me}-iPr)(CO)_2]^+$ (**3**) is activated and can be cleaved in various ways. First, the agostic proton is comparatively acidic and thus even relatively weak bases, such as pyridine, deprotonate this bond to reform the starting material **1**. Secondly, cleavage of the agostic C-H arene bond is also achieved upon exposure of **3** to air (oxygen) or TEMPO which results in the immediate formation of the cationic paramagnetic Co(II) PCP complex $[Co(PCP^{Me}-iPr)(CO)_2]^+$ (**5**) (Scheme 4). This process involves hydrogen abstraction with concomitant oxidation of the metal center from Co(I) to Co(II). The fate of the hydrogen atom is unclear as yet. The solid state structure of **5** was

determined by X-ray diffraction. This complex **5** adopts a distorted square pyramidal geometry around the cobalt centre (Figure 6).
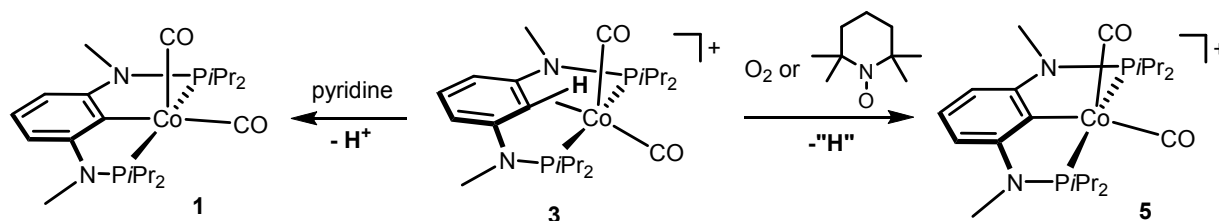
Scheme 4. Reaction of **3** with pyridine and oxygen or TEMPO.
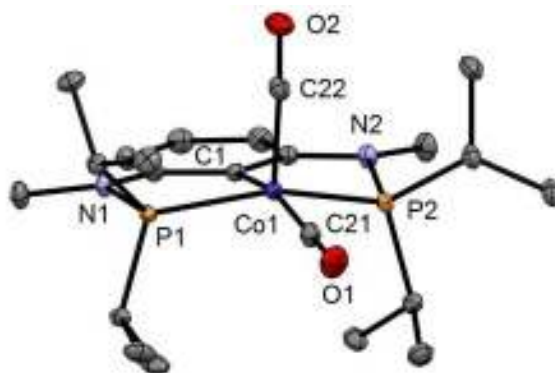
Figure 6. Structural view of $[Co(PCP^{Me}\text{-}iPr)(CO)_2]BF_4$ (**5**) showing 50% thermal ellipsoids (H atoms and BF_4^- counterion omitted for clarity). Selected bond lengths (Å) and bond angles (°): Co1-P1 2.2134(4), Co1-P2 2.2212(4), Co1-C1 1.9500(8), Co1-C21 1.8223(9), Co1-C22 1.8359(9), P1-Co1-P2 155.214(1), C1-Co1-C21 164.56(4), C1-Co1-C22 97.99(4), C21-Co1-C22 97.36(4).

Finally, replacement of one CO ligand in **3** by CN*t*Bu actually promotes the rapid oxidative addition of the agostic C-H arene bond (Scheme 5). Treatment of **3** in CD_2Cl_2 with 2.4 equivs of CN*t*Bu results in the quantitative formation of two isomeric Co(III) hydride complexes of the type $[Co(PCP^{Me}\text{-}iPr)(CN{t}Bu)(CO)(H)]^+$ (**6a, 6b**) in an about 1:2 ratio together with small amounts of $[Co(PCP^{Me}\text{-}iPr)(CN{t}Bu)_2(H)]^+$ (**4**). The hydride ligands of the two isomers **6a** (hydride *trans* to CO) and **6b** (hydride *trans* to CN*t*Bu) exhibit well-resolved triplet resonances at -10.81 and -12.86 ppm with $^2J_{HP}$ coupling constants of 40.7 and 44.9 Hz, respectively. After about 16h, **6a** and **6b** were quantitatively converted to **4** (Figure 7).
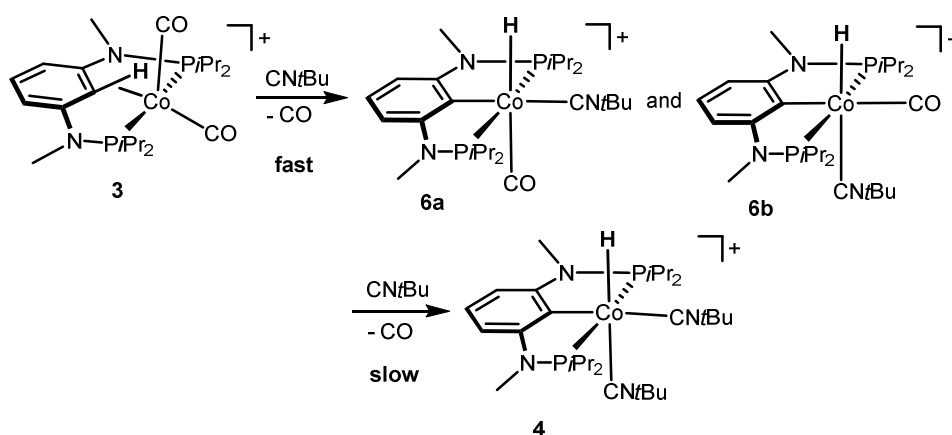
Scheme 5. Stepwise replacement of CO from **3** upon addition of CN*t*Bu in CD$_2$Cl$_2$.
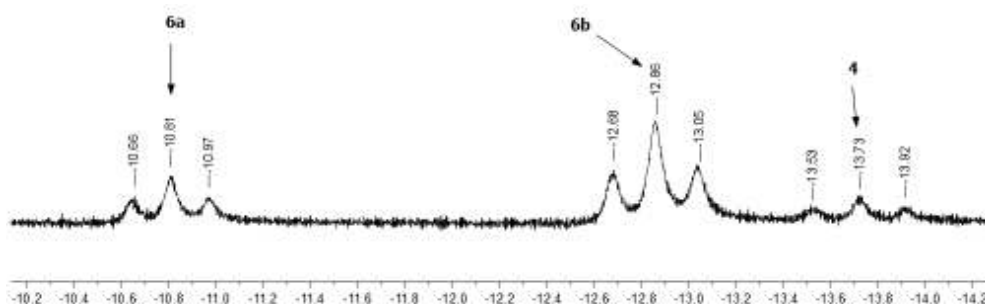
Figure 7. Hydride region of the ^{1}H NMR spectrum of **3** after addition of 2.4 equivs of CN*t*Bu and a reaction time of 10 min in CD$_2$Cl$_2$.

The free energy balances calculated for the CO addition reactions reproduce the differences observed for the Co and the Rh complexes (Scheme 6). While for the Co species the trigonal bipyramidal complex **3** is the most stable one, in the case of Rh, both CO loss with formation of the square planar complex, as well as C-H oxidative addition, are thermodynamic favourable processes.
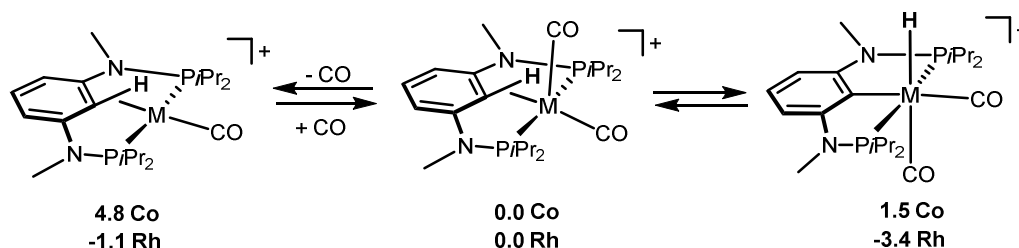
Scheme 6. Thermodynamic comparisons between Co and Rh complexes based on DFT/PBE0 calculations (Free energies in kcal/mol).

4.3 Conclusion

We described the synthesis and reactivity of the first Co(I) pincer complex [Co($\eta^3 P,CH,P$-P(CH)P^{Me}-iPr)(CO)$_2$]$^+$ featuring an agostic η^2-C$_{aryl}$-H bond. This complex was obtained via protonation of the Co(I) complex [Co(PCP^{Me}-iPr)(CO)$_2$]. In contrast to related Rh(I) agostic pincer complexes, this complex is five coordinate and adopts a trigonal bipyramidal geometry. Since the CO ligands are not sufficiently electron rich to promote an oxidative addition of the C-H bond, a Co(III) hydride complex is not formed. A Co(III) hydride complex [Co(PCP^{Me}-iPr)(CNtBu)$_2$(H)]$^+$ was obtained upon protonation of the more electron rich Co(I) complex [Co(PCP^{Me}-iPr)(CNtBu)$_2$]. Three ways to cleave the agostic C-H arene bond are presented. First, the agostic proton in [Co($\eta^3 P,CH,P$-P(CH)P^{Me}-iPr)(CO)$_2$]$^+$ is acidic and pyridine deprotonates the C-H bond to reform the starting material. Another way to cleave the agostic C-H bond is hydrogen abstraction upon exposure of [Co($\eta^3 P,CH,P$-P(CH)P^{Me}-iPr)(CO)$_2$]$^+$ to oxygen) or TEMPO which results in the formation of the paramagnetic Co(II) PCP complex [Co(PCP^{Me}-iPr)(CO)$_2$]$^+$. This process involves oxidation of the metal center from Co(I) to Co(II). Finally, replacement of one CO ligand in [Co($\eta^3 P,CH,P$-P(CH)P^{Me}-iPr)(CO)$_2$]$^+$ by CNtBu promotes the oxidative addition of the agostic C-H arene bond. This yields two isomeric hydride complexes of the type [Co(PCP^{Me}-iPr)(CNtBu)(CO)(H)]$^+$. DFT calculations support the existence of the agostic bond in complex [Co($\eta^3 P,CH,P$-P(CH)P^{Me}-iPr)(CO)$_2$]$^+$ and corroborate the differences observed between the Co and the Rh species.

4.5 Experimental Section

All manipulations were performed under an inert atmosphere of argon by using Schlenk techniques or in a MBraun inert-gas glovebox. The solvents were purified according to standard procedures.[18] The deuterated solvents were purchased from Aldrich and dried over 4 Å molecular sieves. [Co(PCP^{Me}-iPr)(CO)$_2$] (**1**) and [Co(PCP^{Me}-iPr)(CNtBu)$_2$] (**2**), were prepared according in chapter 3.[13,17] ^{1}H, ^{13}C{^{1}H}, and ^{31}P{^{1}H} NMR spectra were recorded on Bruker AVANCE-250, 400 and 600 spectrometers. ^{1}H and ^{13}C{^{1}H} NMR spectra were referenced internally to residual protio-solvent, and

solvent resonances, respectively, and are reported relative to tetramethylsilane (δ = 0 ppm). ^{31}P{^{1}H} NMR spectra were referenced externally to H_3PO_4 (85%) (δ = 0 ppm). ^{1}H, ^{13}C{^{1}H}, ^{31}P{^{1}H} NMR signal assignments were confirmed by ^{1}H{^{31}P}, 135-DEPT, and HMQC(^{1}H-^{13}C) experiments.

All mass spectrometric measurements were performed on an Esquire 3000^{plus} 3D-quadrupole ion trap mass spectrometer (Bruker Daltonics, Bremen, Germany) in positive-ion mode by means of electrospray ionization (ESI). Mass calibration was done with a commercial mixture of perfluorinated trialkyl-triazines (ES Tuning Mix, Agilent Technologies, Santa Clara, CA, USA). All analytes were dissolved in acetonitrile "hypergrade for LC-MS Lichrosolv" quality (Merck, Darmstadt, Germany) to form a concentration of roughly 1 mg/mL. Direct infusion experiments were carried out using a Cole Parmer model 74900 syringe pump (Cole Parmer Instruments, Vernon Hills, IL, USA) at a flow rate of 2 μL/min. Full scan and MS/MS (low energy CID)-scans were measured in the range m/z 100-1100 with the target mass set to m/z 1000. Further experimental conditions include: drying gas temperature: 150°C; capillary voltage: -4 kV; skimmer voltage: 40 V; octapole and lens voltages: according to the target mass set. Helium was used as buffer gas for full scans and as collision gas for MS/MS-scans in the low energy CID mode. The activation and fragmentation width for tandem mass spectrometric (CID-MS/MS) experiments was set to 6 Da to cover the main isotope cluster for fragmentation. The corresponding fragmentation amplitude ranged from 0.4 to 0.6 V in order to keep a precursor ion intensity of low abundance in the resulting MS/MS spectrum. All mass calculations are based on the lowest mass cobalt isotope (^{59}Co-isotope). Mass spectra and CID spectra were averaged during data acquisition time of 1 to 2 min and one analytical scan consisted of five successive micro scans resulting in 50 and 100 analytical scans, respectively, for the final full scan mass spectrum or MS/MS spectrum.

[Co(η^3P,CH,P-P(CH)P^{Me}-*i*Pr)(CO)$_2$]BF$_4$ (3). To a suspension of **1** (100 mg, 0.206 mmol) in CH_2Cl_2 (10 mL) a solution of HBF$_4$·Et$_2$O (34 μL, 0.247 mmol) was added at room temperature and the reaction mixture was stirred for 10 min. The solvent was then removed under reduced pressure and the remaining solid was washed twice with diethyl ether (10 mL) to afford analytically pure **2** as a dark red solid. Yield: 110 mg (94%). Anal. Calcd. for $C_{22}H_{38}BCoF_4N_2O_2P_2$ (570.24): C, 46.34; H, 6.72; N, 4.91. Found: C, 46.37; H, 6.61; N, 4.76. ^{1}H NMR (δ, CD_2Cl_2, 20°C): 7.51 (t, $^3J_{HH}$ = 6.0 Hz, 1H, Ph), 6.23 (d, $^3J_{HH}$ = 6.0 Hz, 2H, Ph), 3.14 (s, 6H, NC*H$_3$*), 2.77 (m, 4H, C*H*), 2.23 (t, $^2J_{HP}$ = 7.5 Hz, 1H, agostic C*H*), 1.34 (m, 24H, C*H$_3$*). ^{13}C{^{1}H} NMR (δ, CD_2Cl_2, 20°C): 197.9 (t, $^2J_{CP}$ = 20.0 Hz, CO), 197.5 (t, $^2J_{CP}$ = 18.0 Hz, CO), 164.3 (vt, $^2J_{CP}$ = 10.0 Hz, Ph), 137.5 (Ph), 104.9 (vt, $^3J_{CP}$ = 4.0 Hz, Ph), 67.0 (C$_{ipso}$, C*H*), 33.6 (NCH$_3$), 30.4 (vt, $^1J_{CP}$ = 14 Hz, C*H*), 30.1 (vt, $^1J_{CP}$ = 14.0 Hz, C*H*) 17.7 (C*H$_3$*), 17.1 (C*H$_3$*), 16.6 (C*H$_3$*), 16.5 (vt, $^2J_{CP}$ = 3.0 Hz, C*H$_3$*). ^{31}P{^{1}H} NMR (δ, CD_2Cl_2, 20°C): 148.4. IR (ATR, cm^{-1}): 2009 (ν_{CO}), 1950 (ν_{CO}). ESI-MS (*m/z,* CH_3CN) positive ion: 454.2 [M-CO-H]$^+$, 426.2 [M-2CO-H]$^+$.

[Co(PCP^{Me}-*i*Pr)(CN*t*Bu)$_2$(H)]BF$_4$ (4). To a suspension of **2** (300 mg, 0.507 mmol) in THF (10 mL) a solution of HBF$_4$·Et$_2$O (83 μL, 0.608 mmol) was added at room temperature and the reaction mixture was stirred for 10 min. The solvent was then removed under vacuum, and then crude product washed twice with Et$_2$O (10 mL) to afford **4** as a dark violet solid. Yield: 325 mg (94%). Anal. Calcd. for

$C_{30}H_{56}BCoF_4N_4P_2$ (680.49): C, 52.95; H, 8.30; N, 8.23. Found: C, 53.14; H, 8.28; N, 8.35. ^{1}H NMR (δ, CD_2Cl_2, 20°C): 6.88 (t, $^3J_{HH}$ = 7.5 Hz, 1H, Ph), 5.99 (d, $^3J_{HH}$ = 7.5 Hz, 2H, Ph), 2.95 (vt, $^3J_{HP}$ = 2.5 Hz, 6H, NCH_3), 2.75 (m, 2H, CH), 2.55 (m, 2H, CH), 1.54 (vq, 6H, CH_3), 1.45 (s, 9H, CH_3), 1.19 (vq, 6H, CH_3), 1.17 (s, 9H, CH_3), 0.96 (vq, 6H, CH_3), -13.76 (t, $^2J_{HP}$ = 50.0 Hz, 1H, Co-H). ^{13}C{^{1}H} NMR (δ, CD_2Cl_2, 20°C): 156.0 (t, $^2J_{CP}$ = 13.5 Hz, Ph), 150.4 (CN), 148.1 (CN), 125.7 (Ph), 123.7 (t, $^2J_{CP}$ = 6.0 Hz, Ph), 101.1 (t, $^3J_{CP}$ = 5.6 Hz, Ph), 58.7 (CNC(CH$_3$)$_3$), 58.3 (CNC(CH$_3$)$_3$), 32.0 (NCH$_3$), 31.7 (vt, $^1J_{CP}$ = 15.0 Hz, CH), 31.3 (vt, $^1J_{CP}$ = 13.5 Hz, CH), 31.39 (vt, $^1J_{CP}$ = 13.5 Hz CH), 19.4 (CH$_3$), 17.7 (CH$_3$). ^{31}P{^{1}H} NMR (δ, CD_2Cl_2, 20°C): 156.7. IR (ATR, cm^{-1}): 2149 (ν_{CN}), 2131 (ν_{CN}). ESI-MS (*m/z,* CH_3CN) positive ion: 593.3 [M]$^+$, 509.2 [M-CNtBu-H]$^+$.

[Co(PCP^{Me}-*i*Pr)(CO)$_2$]BF$_4$ (5). A solution of **3** (100 mg, 0.175 mmol) in CH_2Cl_2 (5 mL) was stirred for 10 min in the presence of air or in the presence of 2,2,6,6-tetramethylpiperidinyloxyl (TEMPO) (27.3 mg, 0.175 mmol) at room temperature. The solvent was then removed under vacuum. The remaining solid was washed with diethyl ether and dried under vacuum to afford **6** as a blue solid. Yield: 95 mg (95%). Anal. Calcd. for $C_{22}H_{37}BCoF_4N_2O_2P_2$ (569.23): C, 46.42; H, 6.55; N, 4.92. Found: C, 46.34; H, 6.47; N, 4.98. %. IR (ATR, cm^{-1}): 2041 (ν_{CO}), 2008 (ν_{CO}). μ_{eff} = 1.93 μ_B (CH_2Cl_2, Evans method[19]). ESI-MS (*m/z,* CH_3CN) positive ion: 454.2 [M-CO]$^+$, 426.2 [M-2CO]$^+$.

Reaction of 3 with CN*t*Bu. To a 5mm NMR tube containing a sample of **3** (15 mg, 0.026 mmol) in CD_2Cl_2, as slight excess of CN*t*Bu (7 µL, 0.063 mmol) was added by a syringe. The sample was transferred to a NMR probe and ^{1}H NMR spectra were recorded. After about 10 min the starting material was completely consumed and two isomeric complexes of the type [Co(PCP^{Me}-*i*Pr)(CN*t*Bu)(CO)(H)]$^+$ (**6a, 6b**) were formed in an about 1:2 ratio together with small amounts of [Co(PCP^{Me}-*i*Pr)(CN*t*Bu)$_2$(H)]$^+$ (**4**). The hydride ligands of the two isomers **6a** (hydride *trans* to CO) and **6b** (hydride *trans* to CN*t*Bu) exhibit well-resolved triplet resonances at -10.81 and -12.86 ppm with $^2J_{HP}$ coupling constants of 40.7 and 44.9 Hz, respectively. After about 16h, **6a** and **6b** were quantitatively converted to [Co(PCP^{Me}-*i*Pr)(CN*t*Bu)$_2$(H)]$^+$ (**4**).

X-ray Structure Determination. X-ray diffraction data of **3**, and **5** (1049857 (**3**), 1049856 (**5**)) were collected at *T* = 100 K in a dry stream of nitrogen on Bruker Kappa APEX II diffractometer systems using graphite-monochromatized Mo-*K*α radiation (λ = 0.71073 Å) and fine sliced *φ*- and *ω*-scans. Data were reduced to intensity values with SAINT and an absorption correction was applied with the multi-scan approach implemented in SADABS.[20] The structures were solved by charge flipping using SUPERFLIP[21] and refined against *F* with JANA2006.[22] Non-hydrogen atoms were refined anisotropically. The H atoms connected to C atoms were placed in calculated positions and thereafter refined as riding on the parent atoms. The agostic H atom in **3** was located in difference Fourier maps and freely refined. Molecular graphics were generated with the program MERCURY.[23] Crystal data and experimental details are given in Table S1.

Table 1. Details for the crystal structure determinations of **3**, and **5**.

	3	5
formula	$C_{22}H_{38}BCoF_4N_2O_2P_2$	$C_{22}H_{37}BCoF_4N_2O_2P_2$
fw	570.2	569.2
cryst.size, mm	0.70 x 0.30 x 0.03	0.65 x 0.33 x 0.25
color, shape	dark violet tabular	dark blue rod
crystal system	monoclinic	orthorhombic
space group	$P\bar{1}$ (no. 2)	$Pna2_1$ (no. 33)
a, Å	11.8384(8)	14.8793(7)
b, Å	7.9692(6)	8.7868(11)
c, Å	27.7945(18)	20.2644(15
α, °	90	90
β, °	91.2446(19)	90
γ, °	90	90
V, Å^3	2621.6(3)	2649.4(4)
T, K	100	100
Z,Z'	4,1	4,1
ρ_{calc}, g cm^{-3}	1.4443	1.4266
μ, mm^{-1}	0.828	0.819
$F(000)$	1192	1188
absorption	Multi-scan, 0.74–	multi-scan, 0.55–
θ range, deg	1.47–29.31	2.01–32.65
no. of rflns	68106	76074
R_{int}	0.0472	0.0340
no. of rflns	7158	9683
no. of rflns	5384	9380
no. of params /	347 / 0	307 / 0
R ($I > 3\sigma(I)$) [a]	0.0348	0.0174
R (all data)	0.0561	0.0182
wR ($I > 3\sigma(I)$)	0.0379	0.0232
wR (all data)	0.0399	0.0233
GooF	1.84	1.31
Diff.Four.peaks min/max, eÅ^{-3}	-0.31 / 0.41	-0.13 / 0.29
Flack Parameter	-	0.003(4)
CCDC no.	1049857	1049856

[a] $R = \Sigma||F_o|-|F_c|| / \Sigma|F_o|$, $wR = \Sigma w(|F_o| - |F_c|) / \Sigma w|F_o|$, GooF $= \{\Sigma[w(F_o^2 - F_c^2)^2] / (n-p)\}^{\frac{1}{2}}$

Computational Details. Calculations were performed using the GAUSSIAN 09 software package,[24] and the PBE0 functional without symmetry constraints. That functional uses a hybrid generalized gradient approximation (GGA), including 25 % mixture of Hartree-Fock[25] exchange with DFT[26] exchange-correlation, given by Perdew, Burke and Ernzerhof functional (PBE).[27] The optimized geometries were obtained with the Stuttgart/Dresden ECP (SDD) basis set[28] to describe the electrons of the metal atoms (Co and Rh). For all other atoms a standard 6-31G** basis set was employed.[29] Frequency calculations yielded no imaginary frequencies confirming the stationary points as minima. The free energy values reported were calculated at 298.15 K and 1 atm by using zero point energy and thermal energy corrections based on structural and vibration frequency data calculated at the same level. A Natural Population Analysis (NPA)[30] and the resulting Wiberg indices[31] were used to study the electronic structure and bonding of the optimized species. Three-dimensional representations of the orbitals were obtained with Molekel.[32]

References

1   For recent reviews on C-H activation and functionalization, see, a) C. Jia , T. Kitamura , Y. Fujiwara, *Acc. Chem. Res.* **2001,** *34*, 633-639. b) V. Ritleng, C. Sirlin, M. Pfeffer, *Chem. Rev.*, **2002**, *102*, 1731–1770. c) D. A. Colby, R. G. Bergman, J. A. Ellman, *Chem. Rev.*, **2010**, *110*, 624–655. d) P. B. Arockiam, C. Bruneau, P. H. Dixneuf, *Chem. Rev.*, **2012**, *112*, 5879–5918. e) J. C. Lewis, R. G. Bergman, J. A. Ellman, *Acc. Chem. Res.*, **2008**, *41*, 1013–1025. f) S. Gaillard, C. S. J. Cazin, S. P. Nolan *Acc. Chem. Res.*, **2012**, *45*, 778–787. g) B. Li, P. H. Dixneuf, *Chem. Soc. Rev.* **2013**, *42*, 5744-5767. h) J. Wencel-Delord, T. Dröge, F. Liu, F. Glorius, *Chem. Soc. Rev.* **2011**, *40*, 4740-4761.

2   a) A. E. Shilov, G. B. Shul'pin, *Chem. Rev.* **1997**, *97*, 2879-2932; b) J. A. Labinger, J. E. Bercaw, *Nature* **2002**, *417*, 507-514; c) S. Sakaki, *Top. Organomet. Chem.* **2005**, *12*, 31-78.

3   For the central role of agostic interactions in C-H activations, see, a) C. Hall, R. N. Perutz, *Chem. Rev.* **1996**, *96*, 3125-3146; b) R. H. Crabtree, *J. Organomet. Chem.* **2004**, *689*, 4083-4091. c) B. Rybtchinski, R. Cohen, Y. Ben-David, J. M. L. Martin, D. Milstein, *J. Am. Chem. Soc.* **2003**, *125*, 11041-11050; d) W. D. Jones, *Inorg. Chem.* **2005**, *44*, 4475-4484. e) W. H. Bernskoetter, C. K. Schauer, K. I. Goldberg, M. Brookhart, *Science* **2009**, *326*, 553-556.

4   C. Lepetit, J. Poater, M. E. Alikhani, B. Silvi, Y. Canac, J. Contreras-García, M. Sola, R. Chauvin, *Inorg. Chem.* **2015**, *54*, 2960-2969.

5   a) A. Vigalok, O. Uzan, L. J. W. Shimon, Y. Ben-David, J. L. Martin, D. Milstein, *J. Am. Chem. Soc.* **1998**, *120,* 12539-12544. b) A. Vigalok, B. Rybtchinski, L. J. W. Shimon, Y. Ben-David, D. Milstein, *Organometallics* **1999**, *18*, 895-905. c) M. Montag, L. Schwartsburd, R. Cohen, G. Leitus, Y. Ben-David, J. M. L. Martin, D. Milstein, *Angew. Chem. Int. Ed.* **2007**, *46*, 1901-1904. d) C. M. Frech, L. J. W. Shimon, D. Milstein, *Organometallics* **2009,** *28,* 1900-1908. e) M. Montag, I. Efremenko, R.

Cohen, L. J. W. Shimon, G. Leitus, Y. Diskin-Posner, Y. Ben-David, H. Salem, J. M. L. Martin, D. Milstein, *Chem. Eur. J.* **2010**, *16*, 328-353.

6   A. C. Albeniz, G. Schulte, R. H. Crabtree, *Organometallics* **1992**, *11*, 242-249.

7   a) P. Dani, T. Karlen, R. A. Gossage, W. J. J. Smeets, A. L. Spek, G. van Koten, *J. Am. Chem. Soc.* **1997**, *119*, 11317-11318. b) P. Dani, M. A. M. Toorneman, G. P. M. van Klink, G. van Koten, *Organometallics* **2000**, *19*, 5287-5296.

8   M. A. McLoughlin, R. J. Flesher, W. C. Kaska, H. A. Mayer, *Organometallics* **1994**, *13,* 3816-3822.

9   M. E. van der Boom, M. A. Iron, O. Atasoylu, L. J.W. Shimon, H. Rozenberg, Y. Ben-David, L. Konstantinovski, J. M.L. Martin, D. Milstein, *Inorg. Chim. Acta* **2004**, *357*, 1854-1864.

10 D. G. Gusev, M. Madott, F. M. Dolgushin, K. A. Lyssenko, M. Yu. Antipin, *Organometallics* **2000**, *19,* 1734-1739.

11 C. Barthes, C. Lepetit, Y. Canac, C. Duhayon, D. Zargarian, R. Chauvin, *Inorg. Chem.* **2013**, *52*, 48−58.

12 Diamagnetic square-planar d8-complexes of Co(I) are rare in comparison to Rh(I) and Ir(I) species. In most cases, Co(I) species tend slip away to the high-spin state or to higher oxidation states like Co(II) or Co(III), for examples see: a) Z. Mo, Y. Li, H. K. Lee, L. Deng, *Organometallics* **2011**, *30*, 4687- 4694. b) Q. Knijnenburg, D. Hetterscheid, T. M. Kooistra, P. H. M. Budzelaar, *Eur. J. Inorg. Chem.* **2004**, 1204-1211.

13 S. Murugesan, B. Stöger, M. D. Carvalho, L. P. Ferreira, E. Pittenauer, G. Allmaier, L. F. Veiros, K. Kirchner, *Organometallics* **2014***, 33*, 6132-6140.

14 R. Castro-Rodrigo, M. A. Esteruelas, A. M. Lopez, E. Oñate, *Organometallics* **2008**, *27*, 3547−3555.

15 a) K. B. Wiberg, *Tetrahedron* **1968**, *24*, 1083-1096; b) Wiberg indices are electronic parameters related with the electron density in between two atoms, which scale as bond strength indicators. They can be obtained from a Natural Population Analysis.

16 This complex was prepared by treatment of [Co(PCP^{Me}-*i*Pr)($\square^2$-BH$_4$)] (ref [16] with 2 equivs of CN*t*Bu.

17 S. Murugesan, B. Stöger, L. F. Veiros, K. Kirchner, *Organometallics*, **2015***, 34*, 1364-1372.

18 Perrin, D. D.; Armarego, W. L. F. *Purification of Laboratory Chemicals*, 3rd ed.; Pergamon: New York, **1988**.

19 S. K. Sur, *J. Magn. Reson.* **1989**, *82*, 169.

20 Bruker computer programs: APEX2, SAINT and SADABS (Bruker AXS Inc., Madison, WI, 2012).

21 L. Palatinus, G. Chapuis. *J. Appl. Cryst.* 2007**, 40**, 786-790.

22 V. Petříček, M. Dušek, L. Palatinus, JANA2006, the crystallographic computing system. (Institute of Physics, Praha, Czeck Republic, 2006)

23 C. F. Macrae, P. R. Edgington, P. McCabe, E. Pidcock, G. P. Shields, R. Taylor, M. Towler and J. van de Streek, *J. Appl. Cryst.* 2006, **39**, 453.

24 Gaussian 09, Revision A.01, M. J. Frisch, G. W. Trucks, H. B. Schlegel, G. E. Scuseria, M. A. Robb, J. R. Cheeseman, G. Scalmani, V. Barone, B. Mennucci, G. A. Petersson, H. Nakatsuji, M. Caricato,

X. Li, H. P. Hratchian, A. F. Izmaylov, J. Bloino, G. Zheng, J. L. Sonnenberg, M. Hada, M. Ehara, K. Toyota, R. Fukuda, J. Hasegawa, M. Ishida, T. Nakajima, Y. Honda, O. Kitao, H. Nakai, T. Vreven, J. A. Montgomery, Jr., J. E. Peralta, F. Ogliaro, M. Bearpark, J. J. Heyd, E. Brothers, K. N. Kudin, V. N. B. Staroverov, R. Kobayashi, J. Normand, K. Raghavachari, A. Rendell, J. C. Burant, S. S. Iyengar, J. Tomasi, M. Cossi, N. Rega, J. M. Millam, M. Klene, J. E. Knox, J. B. Cross, V. Bakken, C. Adamo, J. Jaramillo, R. Gomperts, R. E. Stratmann, O. Yazyev, A. J. Austin, R. Cammi, C. Pomelli, J. W. Ochterski, R. L. Martin, K. Morokuma, V. G. Zakrzewski, G. A. Voth, P. Salvador, J. J. Dannenberg, S. Dapprich, A. D. Daniels, Ö. Farkas, J. B. Foresman, J. V. Ortiz, J. Cioslowski, D. J. Fox, Gaussian, Inc., Wallingford CT, **2009**.

25 W. J. Hehre, L. Radom, P. v. R. Schleyer, J. A. Pople, Ab Initio Molecular Orbital Theory, Wiley, New York, 1986.

26 R. G. Parr, W. Yang, Density Functional Theory of Atoms and Molecules, Oxford University Press, New York, 1989.

27 a) U. Haeusermann, M. Dolg, H. Stoll, H. Preuss, *Mol. Phys.* **1993**, *78*, 1211; b) W. Kuechle, M. Dolg, H. Stoll, H. Preuss, *J. Chem. Phys.* **1994**, *100*, 7535; c) T. Leininger, A. Nicklass, H. Stoll, M. Dolg, P. Schwerdtfeger, *J. Chem. Phys.* **1996**, *105*, 1052.

28 a) U. Haeusermann, M. Dolg, H. Stoll, H. Preuss, *Mol. Phys.* **1993**, *78*, 1211; b) W. Kuechle, M. Dolg, H. Stoll, H. Preuss, *J. Chem. Phys.* **1994**, *100*, 7535; c) T. Leininger, A. Nicklass, H. Stoll, M. Dolg, P. Schwerdtfeger, *J. Chem. Phys.* **1996**, *105*, 1052.

29 a) A. D. McLean, G. S. Chandler, *J. Chem. Phys.* **1980**, *72*, 5639; b) R. Krishnan, J. S. Binkley, R. Seeger, J. A. Pople, *J. Chem. Phys.* **1980**, *72*, 650; c) P. J. Hay, *J. Chem. Phys.* 1977, 66, 4377; d) K. Raghavachari, G. W. Trucks, *J. Chem. Phys.* 1989, 91, 1062; e) R. C. Binning, L. A. Curtiss, *J. Comput. Chem.* 1995, 103, 6104; f) M. P. McGrath, L. Radom, *J. Chem. Phys.* **1991**, 94, 511.

30 a) J. E. Carpenter, F. Weinhold, *J. Mol. Struct. (Theochem)* **1988**, *169*, 41; b) J. E. Carpenter, *PhD thesis*, University of Wisconsin (Madison WI), 1987; c) J. P. Foster, F. Weinhold, *J. Am. Chem. Soc.* **1980**, *102*, 7211; d) A. E. Reed, F. Weinhold, *J. Chem. Phys.* **1983**, *78*, 4066; e) A. E. Reed, F. Weinhold, *J. Chem. Phys.* **1983**, *78*, 1736; f) A. E. Reed, R. B. Weinstock, F. Weinhold, *J. Chem. Phys.* **1985**, *83*, 735; g) A. E. Reed, L. A. Curtiss, F. Weinhold, *Chem. Rev.* **1988**, *88*, 899; h) F. Weinhold, J. E. Carpenter, *The Structure of Small Molecules and Ions*, Plenum, 1988, p. 227.

31 a) K. B. Wiberg, *Tetrahedron* **1968**, *24*, 1083; b) Wiberg indices are electronic parameters related with the electron density in between two atoms, which scale as bond strength indicators. They can be obtained from a Natural Population Analysis.

32 S. Portmann, H. P. Lüthi, *Chimia,* **2000**, *54*, 766.

Synthesis of novel Mo(II) and Mo(IV) PCP pincer complexes

We have synthesized two diamagnetic 16e molybdenum PCP pincer complexes of the types [Mo(PCP^{Me}-*i*Pr)(Br)(O)], and [Mo(PCP^{Me}-*i*Pr)(Br)(CO)$_2$] from the precursors [Mo(Br)$_3$(THF)$_3$] and [Mo(Br)$_2$(CO)$_4$]$_2$, respectively. The first one is a mono oxo Mo(IV) complex involving presumably dioxygen activation.

5.1 Introduction

The activation and cleavage of dinitrogen is an important reaction and is realized efficiently in biological processes with nitrogenase.[1] This enzyme catalyzes the conversion of dinitrogen into ammonia. The cluster form of the FeMo cofactor is involved in this process which involves various protonation and reduction steps.[2] Also molybdenum complexes play a major role in chemical reactions with dinitrogen.[3] Several high valent PNP based molybdenum halide complexes are able to form dinitrogen complexes in the presence of strong reducing agents under a dinitrogen atmosphere. Such reactions were also utilized in the catalytic formation ammonia.[4] Dinitrogen was also converted to ammonia when related PNN molybdenum complexes were used.[5] Moreover, oxidation and reduction reactions of PNP molybdenum carbonyl complexes have been studied,[6] while Veige *et al* reported the synthesis of trianionic OCO pincer molybdenum derivatives bearing nitride and oxo ligands.[7] In 2015, tridentate ONO pincer molybdenum complexes were found to be active catalysts for ring-opening metathesis polymerization of strained alkynes.[8] Tuczek and coworkers reported on a neutral tridentate PCP containing molybdenum complex which coordinates dinitrogen using reducing agents in the presence of phosphine co-ligands.[9] The first synthesized anionic PCP pincer molybdenum complexes (**1** and **2**) where the pincer ligand contains oxygen linkers between the aromatic ring and phosphine moieties, were reported by Schrock and coworkers (Scheme 1).[10] Reduction of complex **1** with NaHg in the presence of dinitrogen yielded the PCP molybdenum nitride complex **3** through dinitrogen splitting. This complex **3** was protonated with [Et$_3$NH][BAr'$_4$] to yield complex **4** (Scheme 2). Complex **3** was structurally characterized by X-ray crystallography.
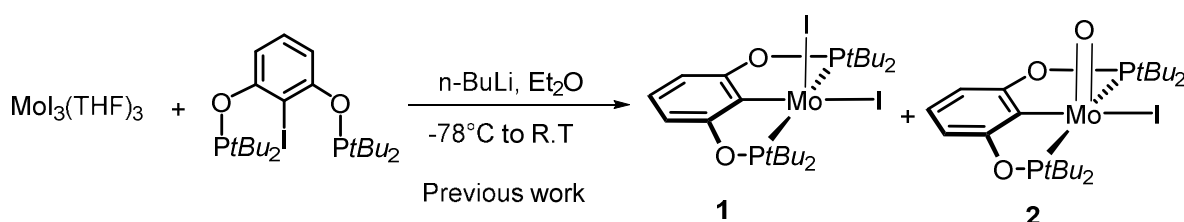
Scheme 1 Synthesis of PCP Molybdenum pincer complexes
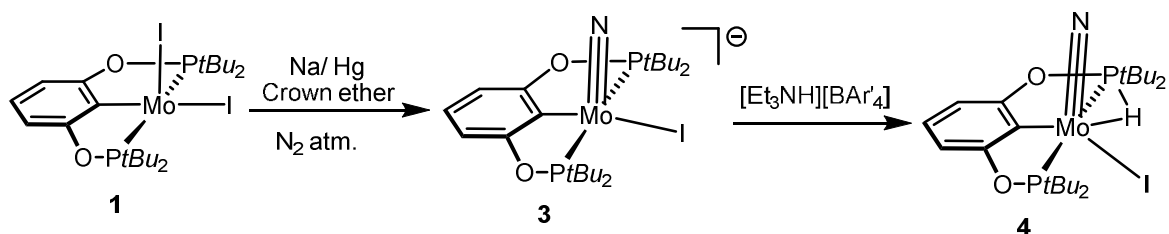
Scheme 2 Synthesis and reactivity of the anionic Mo(IV) nitride complex [Mo(PCsp^2P)(N)(I)]⁻ (**3**)

5.2 Results and discussion

Treatment of [Mo(Br)$_3$(THF)$_3$] with the PCP ligand in the presence of *n*BuLi in diethyl ether affords the diamagnetic molybdenum mono oxo complex [Mo(PCP^{Me}-*i*Pr)(Br)(O)] (**5**) in 75% isolated yield (Scheme 3). This complex is characterized by a combination of ^{1}H, ^{31}P{^{1}H}, and ^{13}C{^{1}H} NMR and X-ray crystallography. Complex **5** adopts a distorted square pyramidal geometry around the molybdenum center, where Mo oxo bond distance.
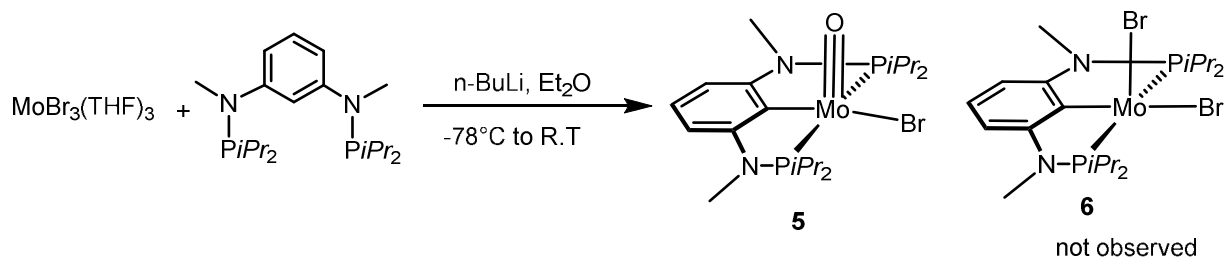
Scheme 3 Synthesis of the Mo(IV) PCP oxo complex (**5**)
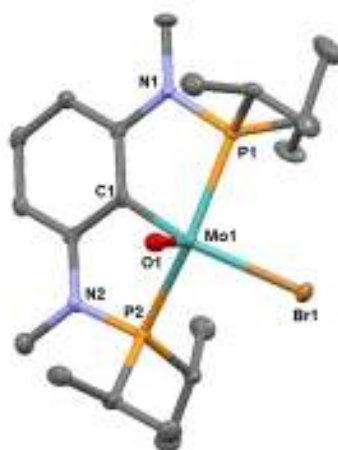
Figure 1. Structural view of [Mo(PCP^{Me}-*i*Pr)(O)(Br)] (**5**) showing 50% thermal ellipsoids (H atoms omitted for clarity). Selected bond lengths (Å) and bond angles (°): Mo1-P1 2.439(1), Mo-P2 2.437(1), Mo1-C1 2.145(3), Mo-Br1 2.5912(5), Mo1-O1 1.681(2), P1-Mo1-P2 143.88(3), C1-Mo1-Br1 136.54(9), C1-Mo1-O1 109.4(1), Br1-Mo1-O1 114.10(8).

At this stage the actual oxygen source (air or THF) to yield **5** remains unclear. In literature it was described[10] that molybdenum oxo complexes are formed upon decomposition of the molybdenum precursor [MoI$_3$(THF)$_3$] with THF being the source of oxygen. This was supported by the fact that 1,4-di-iodobutane was detected as decomposition product. In the course of our investigations, the molybdenum precursor [Mo(Br)$_3$(THF)$_3$] was freshly prepared, and characterized by X-ray crystallography and there was no evidence for an oxo species in the precursor. After treatment of the PC^{H}P ligand with *n*BuLi this solution was treated with [Mo(Br)$_3$(THF)$_3$] under an argon atmosphere and the molybdenum oxo complex **5** was formed. When the reaction was completed, the remaining solution was injected into an GC-MS, and no evidence of 1,4-di-bromobutane was found. We then performed this reaction inside a glove box (10 ppm oxygen) and again obtained the Mo(IV) oxo complex (**5**). An intermediate was not observed and the mechanism of this reaction remains unclear.

When the Mo(IV) oxo complex **5** was over oxidized formation of pincer ligand **8** was observed (Scheme 4). We then investigated the reaction of **8** with [MoBr$_3$(THF)$_3$] in presence of Et$_2$O at room temperature but unfortunately no reaction took place (Scheme 5).
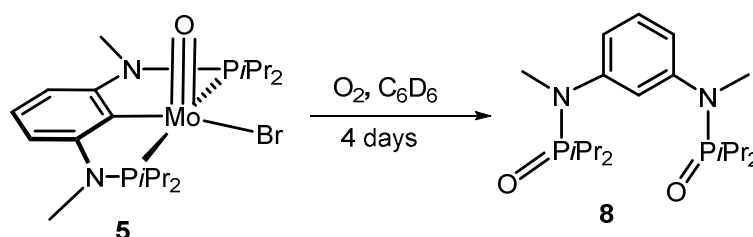
Scheme 4 Decomposition of the Mo(IV) oxo complex **5** in the presence of air
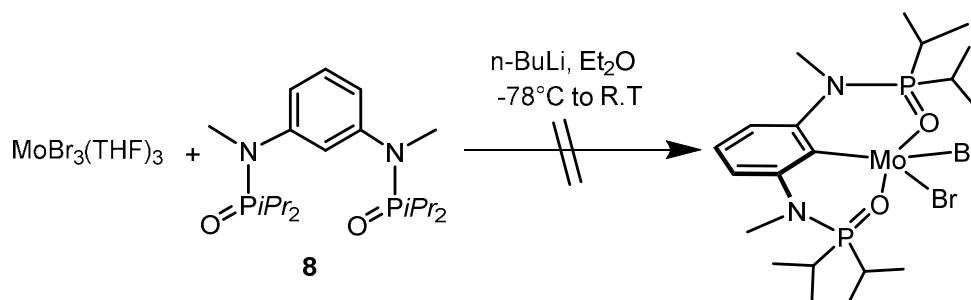
Scheme 5 Reaction of the Mo(III) precursor [MoBr$_3$(THF)$_3$] with **8**

Treatment of [Mo(Br)$_3$(THF)$_3$] with oxidized phosphine ligand **8** in presence of dichloromethane under air at room temperature for three days resulted in the formation of the air stable paramagnetic Mo(V) oxo complex. This complex displays large paramagnetic shifted and very broad ^{1}H NMR signals and were thus not very informative. ^{13}C{^{1}H} and ^{31}P{^{1}H} NMR spectra could not be detected at all. The solution magnetic moments of 1.7(4) μ_B is consistent with one unpaired electron. This value is lower than the one expected for the spin-only approximation.
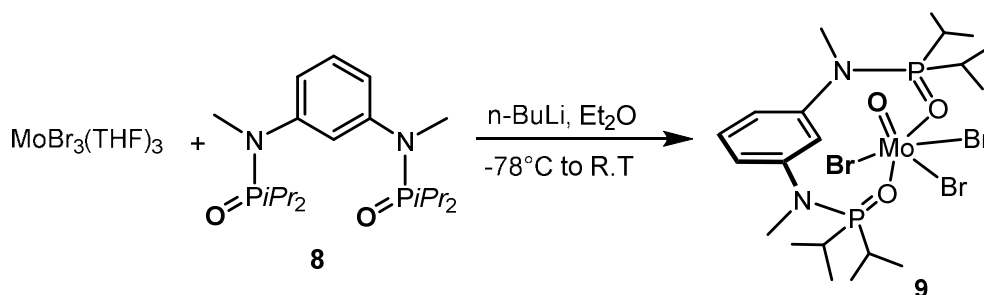
Scheme 6 Synthesis of Mo(V) oxo complex
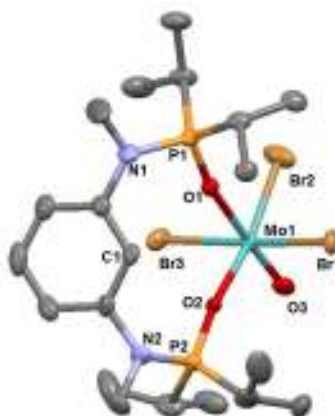
Figure 3. Structural view of [Mo(PCP^Me^-*i*Pr)(O)(Br)₃] (**9**) showing 50% thermal ellipsoids (H atoms omitted for clarity). Selected bond lengths (Å) and bond angles (°): Mo1-O1 2.152(3), Mo-O2 2.065(3), Mo1-O3 1.701(4), Mo-Br1 2.5506(7), Mo1-Br2 2.4955(8), Mo1-Br3 2.5273(7), O1-Mo1-O2 85.1(1), O2-Mo1-O3 94.8(2), O3-Mo1-Br2 94.2(1), Br2-Mo1-Br1 94.81(2), Br1-Mo1-O1 85.04(9), Br1-Mo1-Br3 170.69(3), O1-Mo1-O3 176.6(2).

The formation of the Mo(II) PCP pincer complex **10** was achieved by reacting [Mo(Br)₂(CO)₄]₂ and the PC^H^P ligand in the presence of *n*BuLi in diethyl ether at room temperature for 16 h (Scheme 7). This air stable 16e complex was obtained in only 20% isolated yield, and was characterized by a combination of ¹H, ¹³C{¹H} and ³¹P{¹H} NMR, IR, and X-ray diffraction. This complex adopts an octahedral geometry around the molybdenum center.
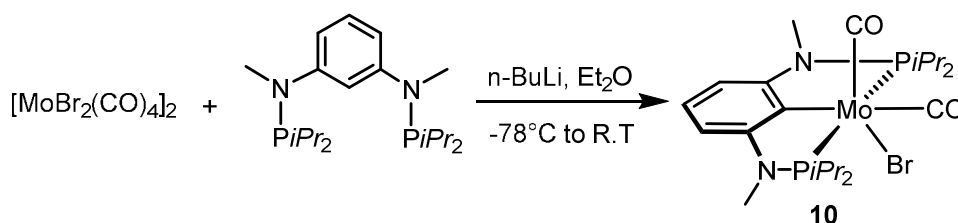
Scheme 7 Synthesis of Mo(II) PCP pincer complex (**10**)
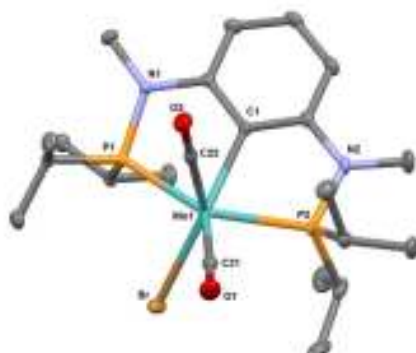
Figure 3. Structural view of [Mo(PCP^{Me}-*i*Pr)(CO)$_2$(Br)] (**10**) showing 50% thermal ellipsoids (H atoms omitted for clarity). Selected bond lengths (Å) and bond angles (°): Mo1-P1 2.5050(3), Mo-P2 2.4372(3), Mo1-C1 2.200(1), Mo-Br1 2.5837(2), Mo1-O1 3.127, Mo1-C21 1.978(1), Mo1-C22 1.924(1), P1-Mo1-P2 147.94(1), C1-Mo1-Br1 138.78(3), C1-Mo1-C21 136.78(5), C1-Mo1-C22 74.71(5).

5.3 Conclusion

We synthesized two diamagnetic molybdenum pincer complexes [Mo(PCP^{Me}-*i*Pr)(Br)(O)] and [Mo(PCP^{Me}-*i*Pr)(Br)(CO)$_2$] from molybdenum precursors [Mo(Br)$_3$(THF)$_3$] and [Mo(Br)$_2$(CO)$_4$]$_2$, respectively.

5.4 Experimental Section

All manipulations were performed under an inert atmosphere of argon by using Schlenk techniques or in a MBraun inert-gas glovebox. The solvents were purified according to standard procedures.[11] The molybdenum precursors such as [Mo(Br)$_2$(CO)$_4$] and [Mo(Br)$_3$(THF)$_3$] were prepared to according published literature.[12] The deuterated solvents were purchased from Aldrich and dried over 4 Å molecular sieves. ^{1}H, ^{13}C{^{1}H}, and ^{31}P{^{1}H} NMR spectra were recorded on Bruker AVANCE-250, 200, and 400 spectrometers. ^{1}H and ^{13}C{^{1}H} NMR spectra were referenced internally to residual protio-solvent, and solvent resonances, respectively, and are reported relative to tetramethylsilane (δ = 0 ppm). ^{31}P{^{1}H} NMR spectra were referenced externally to H$_3$PO$_4$ (85%) (δ = 0 ppm).

[Mo(PCP^{Me}-*i*Pr)(Br)(O)] (5): A suspension of **8** (350 mg, 0.95 mmol) in Et$_2$O (20 mL) was cooled to −78 °C, and n-BuLi (1.0 mmol, 399 µL of a 2.5 M solution in n-hexane) was added in a dropwise fashion. The mixture was then allowed to reach room temperature and stirred for 2 h. Again the reaction mixture was cooled to -30°C and this solution was transferred to another schlenk tube where was the 1.0 equiv of **7** (521 mg, 0.95 mmol), whereupon the solution slowly turned brown. After the mixture was stirred for 16 h, the solvent was removed under vacuum. The resulting crude product was redissolved in toluene, insoluble materials were removed by filtration, and the solvent was evaporated under vacuum to afford the product as a brown solid. Yield: 400 mg (75%). ^{1}H NMR (δ, CD$_2$Cl$_2$, 20°C): 7.22 (t, $^3J_{HH}$= 8 Hz, 1H), 6.21

(d, $^3J_{HH}$= 8 Hz, 2H), 3.04 (s, 6H, NCH$_3$), 2.90-2.73 (m, 4H, CH), 1.53-0.97 (m, 24H, CH$_3$). ^{13}C{^{1}H} NMR (δ, CD$_2$Cl$_2$, 20°C): 162.9 (t, $^2J_{CP}$= 13.5 Hz, Ph), 134.8 (s, Ph), 102.0 (t, $^3J_{CP}$= 5.5 Hz, Ph), 34.3 (t, $^2J_{CP}$= 1.8 Hz, NCH$_3$), 27.3 (t, $^1J_{CP}$= 10.5 Hz, CH(CH$_3$)$_2$), 23.1 (t, $^1J_{CP}$= 10.5 Hz, CH(CH$_3$)$_2$), 18.5-17.1 (m, CH(CH$_3$)$_2$). ^{31}P{^{1}H} NMR (δ, CD$_2$Cl$_2$, 20°C): 150.3

OPCPO Ligand (8): A suspension of **8** (400mg, 1.09 mmol) in dichloromethane was cooled to 0°C, and aqueous 30% H$_2$O$_2$ (6 equiv.) was added in dropwise fashion. The mixture was then allowed to room temperature. After 1 hour, the solvent was evaporated, and the crude product was washed with 5 mL diethyl ether in three times. The product was dried in over vacuum to yield colorless solid. Yield: 94% (410 mg). ^{1}H NMR (δ, C$_6$D$_6$, 20°C): 7.86 (s, 1H), 7.20 (t, $^3J_{HH}$= 7.5 Hz, 1H), 6.87 (d, $^3J_{HH}$ = 7.5 Hz, 2H), 2.93 (d, $^3J_{HP}$= 7.5 Hz, 6H, NCH$_3$), 2.28-2.14 (m, 4H), 1.26 (vq, $^2J_{HH}$ = 7.5 Hz, $^3J_{HP}$ = 7.5 Hz, 12H, CH$_3$), 1.11 (vq, $^2J_{HH}$ = 7.5 Hz, $^3J_{HP}$ = 7.5 Hz, 12H, CH$_3$). ^{31}P{^{1}H} NMR (δ, C$_6$D$_6$, 20°C): 56.1.

[Mo(OPCPO)(O)(Br)$_3$] (9): A suspension of MoBr$_3$(thf)$_3$ (298mg, 0.543 mmol), and **8** (217 mg, 0.543mmol) in dichloromethane was kept without stirring at room temperature under an air atmosphere. After the 3 days the reaction mixture colour was completely changed from brown to green. Then, the solvent was removed under vacuum. The resulting crude material was redissolved in toluene, insoluble materials were removed by filtration, and the solvent was evaporated under vacuum to afford the product as a green solid. Yield: 93% (380 mg). μ$_{eff}$ = 1.7(4) μB (CH$_2$Cl$_2$, Evans method).

[Mo(PCP^{Me}-*iPr*)(Br)(CO)$_2$] (10): A suspension of PCP ligand (100 mg, 0.272 mmol) in Et$_2$O (15 mL) was cooled to -78°C, and n-BuLi (0.286 mmol, 115 μL of a 2.5 M solution in n-hexane) was added in a dropwise fashion. The mixture was then allowed to reach room temperature and stirred for 2h. After that 0.5 equiv of [MoBr$_2$(CO)$_4$]$_2$ (100 mg, 0.136 mmol) was added. After the reaction mixture was stirred for 16h, the solvent was removed under vacuum. The resulting crude material was redissolved in toluene, insoluble materials were removed by filtration, and the solvent was evaporated under vacuum to afford the product as a yellow solid. Yield: 20% (32 mg). IR (C$_6$D$_6$ solution, cm^{-1}): 1855 (ν_{CO}), 1955 (ν_{CO}); (ATR, cm^{-1}): 1827 (ν_{CO}), 1933 (ν_{CO}). ^{1}H NMR (δ, C$_6$D$_6$, 20°C): 7.07 (t, $^3J_{HH}$= 7.5 Hz, 1H), 6.03 (d, $^3J_{HH}$= 7.5 Hz, 2H), 2.40 (t, $^3J_{HP}$= 2.5 Hz, 6H, NCH$_3$), 2.06-1.96 (m, 2H, CH), 1.92-1.82 (m, 2H, CH), 1.34-0.93 (m, 24H, CH$_3$). ^{13}C{^{1}H} NMR (δ, C$_6$D$_6$, 20°C): 219 (t, $^2J_{CP}$= 8.1 Hz, CO), 216 (t, $^2J_{CP}$= 8.1 Hz, CO), 163.9 (t, $^3J_{CP}$= 10.0 Hz, Ph), 132.9 (s, Ph), 104.4 (t, $^3J_{CP}$= 3.1 Hz), *ipso* C not detected, 33.4 (t, $^2J_{CP}$= 6.8 Hz, NCH$_3$), 32.6 (t, $^1J_{CP}$= 8.1 Hz, CH(CH$_3$)$_2$), 30.9 (t, $^1J_{CP}$= 10.6 Hz, CH(CH$_3$)$_2$), 19.1 (t, $^2J_{CP}$= 6.8 Hz, CH(CH$_3$)$_2$), 18.40-18.05 (m, CH(CH$_3$)$_2$). ^{31}P{^{1}H} NMR (δ, C$_6$D$_6$, 20°C): 150.85

References

1 Postgate, J. (1998). *Nitrogen Fixation, 3rd Edition*. Cambridge University Press, Cambridge UK.

2 Hoffman, B. M.; Lukoyanov, D.; Dean, D. R.; Seefeldt, L. C. *Acc. Chem. Res.* 2013, **46**, 587.

3 a) J. S. Anderson, J. Rittle, J. C. Peters, *Nature,* 2013, **501**, 84. b) S. E. Creutz, J. C. Peters, *J. Am. Chem. Soc.* 2014, **136**, 1105. c) G. Ung, J. C. Peters, *Angew. Chem. Int. Ed.* 2015, **54**, 532. d) D. V. Yandulov, R. R. Schrock, *Science,* 2003, **301**, 76. e) R. R. Schrock, *Acc. Chem.*

Res. 2005, **38**, 955. f) W. W. Weare, X. Dai, M. J. Byrnes, J. M. Chin, R. R. Schrock, P. Müller, *Proc. Natl. Acad. Sci. USA* 2006, **103**, 17099. g) R. R. Schrock, *Angew. Chem. Int. Ed.* 2008, **47**, 5512. h) K. Shiina, *J. Am. Chem.Soc.*1972, **94**, 9266. i) K. Komori, H. Oshita, Y. Mizobe, M. Hidai, *J. Am. Chem. Soc.* 1989, **111**, 1939. k) M. Mori, *J. Organomet. Chem.* 2004, **689**, 4210. l) H. Tanaka, A. Sasada, T. Kouno, M. Yuki, Y. Miyake, H. Nakanishi, Y. Nishibayashi, K. Yoshizawa, *J. Am. Chem. Soc.* 2011, **133**, 3498. m) M. Yuki, H. Tanaka, K. Sasaki, Y. Miyake, K. Yoshizawa, Y. Nishibayashi, *Nat. Commun.* 2012, **3**, 1254; n) Q. Liao, N. Saffon-Merceron, N. Mézailles, *Angew. Chem. Int. Ed.* 2014, **53**, 14206.

4   a) S. Kuriyama, K. Arashiba, K. Nakajima, H. Tanaka, K. Yoshizawa, Y. Nishibayashi, *Chem. Sci.,* 2015, **6**, 3940. c) K. Arashiba, Y. Miyake, Y. Nishibayashi, *Nat. Chem.* 2011, **3**, 120. d) E. Kinoshita, K. Arashiba, S. Kuriyama, A. Eizawa, K. Nakajima, Y. Nishibayashi, *Eur. J. Inorg. Chem.* 2015, 1789. e) E. Kinoshita, K. Arashiba, S. Kuriyama, Y. Miyake, R. Shimazaki, H. Nakanishi, Y. Nishibayashi, *Organometallics,* 2012, **31**, 8437. f) K. Arashiba, K. Sasaki, S. Kuriyama, Y. Miyake, H. Nakanishi, Y. Nishibayashi, *Organometallics* 2012, **31**, 2035. g) S. Kuriyama, K. Arashiba, K. Nakajima, H. Tanaka, N. Kamaru, K. Yoshizawa, Y. Nishibayashi, *J. Am. Chem. Soc.* 2014, **136**, 9719. h) H. Tanaka, K. Arashiba, S. Kuriyama, A. Sasada, K. Nakajima, K. Yoshizawa, Y. Nishibayashi, *Nat. Commun.* 2014, **5**, 3737.

5   K. Arashiba, K. Nakajima, Y. Nishibayashi, *Z. Anorg. Allg. Chem.* 2015, **641**, 100.

6   a) S. R. M. M. de Aguiar, B. Stöger, E. Pittenauer, M. Puchberger, G. Allmaier, L. F. Veiros, K. Kirchner, *J. Organomet. Chem.,* 2014, **760**, 74. a) D. Benito-Garagorri, E. Becker, J. Wiedermann, W. Lackner, M. Pollak, K. Mereiter, J. Kisala, K. Kirchner, *Organometallics* 2006, **25**, 1900. b) Ö. Öztopcu, C. Holzhacker, M. Puchberger, M. Weil, K. Mereiter, L. F. Veiros, K. Kirchner, *Organometallics* 2013, **32**, 3042. c) S. R. M. M. de Aguiar, Ö. Öztopcu, B. Stöger, K. Mereiter, L. F. Veiros, E. Pittenauer, G. Allmaier, K. Kirchner, *Dalton Trans.* 2014, **43**, 14669.

7   a) M. E. O'Reilly, A. S. Veige, *Chem. Soc. Rev.* 2014, **43**, 6325. b) S. Sarkar, K. A. Abboud, A. S. Veige, *J. Am. Chem. Soc.* 2008, **130**, 16128. c) M. T. Jan, S. Sarkar, S. Kuppuswamy, I. Ghiviriga, K. A. Abboud, A. S. Veige, *J. Organomet. Chem.* 2011, **696**, 4079.

8   D. E. Bellone, J. Bours, E. H. Menke, F. R. Fischer, *J. Am. Chem. Soc.* 2015, **137**, 850.

9   C. Gradert, N. Stucke, J. Krahmer, C. Nther, F. Tuczek, *Chem. Eur. J.* 2015, **21**, 1130.

10   a) T. J. Hebden, R. R. Schrock, M. K. Takase, P. Mueller, *Chem. Comm.,* 2012, **48,** 1851. b) F. A. Cotton, R. Poli, *Inorg. Chem.*, 1987, **26**, 1514.

11   D. D. Perrin, W. L. F. Armarego, *Purification of Laboratory Chemicals*, 3rd ed.; Pergamon: New York, **1988**.

12 B. E. Owens, R. Poli, A. L. Rheingold, *Inorg. Chem.*1989, **28**, 8.

Summary

In ***Chapter 1***, this chapter provides an overview of the advancements in the field of non-precious metal (Ni, Co and Mo) complexes featuring anionic PCP pincer ligands where the (CH_2, O and NH) linkers between aromatic ring and phosphine moieties. While the research in nickel PCP complexes is already quite extensive, the chemistry of cobalt and molybdenum PCP complexes is comparatively sparse. In the case of nickel PCP complexes already many catalytic applications such as Suzuki–Miyaura coupling, C-S cross coupling, Michael additions, Alcoholysis of acrylonitrile, hydrosilylation of aldehyde and cyanomethylation of aldehydes were reported. Cobalt and molybdenum PCP complexes were not applied to any catalytic reactions. Surprisingly, only one molybdenum PCP complex is reported, which was capable of cleaving dinitrogen to give a nitride complex. This literature survey is motivated us to find and develop the combination of cheap and abundant metals such as nickel, cobalt and molybdenum with PCP pincer ligands may result in the development of novel, versatile, and efficient catalysts for atom-efficient catalytic reactions. In ***Chapter 2***, we have shown here that a PCP pincer ligand based on 1,3-diaminobenzene acts as versatile supporting scaffold in cobalt chemistry. The PCP moiety provides access to a range of Co complexes in formal oxidation states +I, +II, and +III by utilizing the 15e square planar d^7 complex [Co(PCP^{Me}-*i*Pr)Cl] as synthetic precursor. In contrast to the analogous Ni(II) complex [Ni(PCP^{Me}-*i*Pr)Cl], [Co(PCP^{Me}-*i*Pr)Cl] is able to form stable pentacoordinate square pyramidal or trigonal bipyramidal 17e complexes. For instance, [Co(PCP^{Me}-*i*Pr)Cl] readily adds CO and pyridine to afford the five-coordinate square-pyramidal complexes [Co(PCP^{Me}-*i*Pr)(CO)Cl] and [Co(PCP^{Me}-*i*Pr)(py)Cl], respectively, while in the presence of Ag^+ and CO the cationic bipyramidal complex [Co(PCP^{Me}-*i*Pr)(CO)$_2$]$^+$ is formed. The effective magnetic moments μ_{eff} of all Co(II) complexes derived from the temperature dependence of the inverse molar magnetic susceptibility by SQUID measurements are in the range of 1.9 to 2.4μ_B. This is consistent with a d^7 low spin configuration with a contribution from the second-order spin orbit coupling. Oxidation of [Co(PCP^{Me}-*i*Pr)Cl] with $CuCl_2$ yields the Co(III) PCP complex [Co(PCP^{Me}-*i*Pr)Cl$_2$], while the synthesis of the Co(I) complex [Co(PCP^{Me}-*i*Pr)(CO)$_2$] was achieved by reducing [Co(PCP^{Me}-*i*Pr)Cl] with KC_8 in the presence of CO. Complex [Co(PCP^{Me}-*i*Pr)Cl$_2$] exhibits a solution magnetic moment of 3.1μ_B which is consistent with a d^6 intermediate spin system. The tendency of Co(I), Co(II) and Ni(II) PCP complexes of the type [M(PCP^{Me}-*i*Pr)(CO)]^n (n = +1, 0) to add CO was investigated by DFT calculations showing that the Co species readily form the five-coordinate complexes [Co(PCP^{Me}-*i*Pr)(CO)$_2$]$^+$ and [Co(PCP^{Me}-*i*Pr)(CO)$_2$] which are thermodynamically favorable, while Ni(II) maintains the 16e configuration since CO addition is thermodynamically unfavorable in this case. X-ray structures of most complexes are provided and discussed. A structural feature of interest is that the CO ligand in [Co(PCP^{Me}-*i*Pr)(CO)Cl] deviates significantly from linearity with a Co-C-O angle of 170.0(1)°. The DFT calculated value is 172° clearly showing that this is not a packing but an electronic effect. In ***Chapter 3***, we have shown that the 15e square-planar complexes [Co(PCP^{Me}-*i*Pr)Cl] and [Co(PCP-*t*Bu)Cl], respectively, react readily with $NaBH_4$ to afford complexes [Co-(PCP^{Me}-*i*Pr)(η^2-BH$_4$)] and [Co(PCP-*t*Bu)(η^2-BH$_4$)] in high yields. The η^2-bonding mode of the borohydride ligand was confirmed by IR

spectroscopy and X-ray crystallography. These compounds are paramagnetic with effective magnetic moments of 2.0(1) and 2.1(1) μ_B consistent with a d^7 low-spin system corresponding to one unpaired electron. None of these complexes react with CO_2 to give formate complexes. For structural and reactivity comparisons, we prepared the analogous Ni(II) borohydride complex [Ni(PCP^{Me}-*i*Pr)(η^2-BH$_4$)] via two different routes. One utilizes [Ni(PCP^{Me}-*i*Pr)Cl] and NaBH$_4$, the second one makes use of the hydride complex [Ni(PCP^{Me}-*i*Pr)H] and BH$_3 \cdot$THF. In both cases, [Ni(PCP^{Me}-*i*Pr)(η^2-BH$_4$)] was obtained in high yields. While [Ni(PCP^{Me}-*i*Pr)(η^2-BH$_4$)] loses readily BH$_3$ at elevated temperatures in the presence of NEt$_3$ to form [Ni(PCP^{Me}-*i*Pr)H], the Co(II) complex [Co(PCP^{Me}-*i*Pr)(η^2-BH$_4$)] did not react with NH$_3$ to give a hydride complex. Complexes [Ni(PCP^{Me}-*i*Pr)(η^2-BH$_4$)] and [Ni(PCP^{Me}-*i*Pr)H] react with CO_2 to give the formate complex [Ni(PCP^{Me}-*i*Pr)(OC(C=O)H]. DFT calculations revealed that the formation of the Ni hydride is thermodynamically favorable, whereas the formation of the Co(II) hydride, in agreement with the experiment, is unfavorable. From the calculations, it is apparent that, for the Co complexes, the BH$_4^-$ coordination is closer to η^2, and the overall geometry can be envisaged as in between square-planar and square-pyramidal. In complex [Ni(PCP^{Me}-*i*Pr)(η^2-BH$_4$)], the borohydride ligand coordination is closer to η^1, and the overall geometry of the molecule is closer to normal square-planar, reflecting the tendency of Ni(II) to form complexes with that geometry, as expected for a d^8 metal. A very rare bidentate and tridentate ligand containing pincer complex [Co(PCP^{Me}-*i*Pr)(NO)(NO$_2$)] is synthesized by the reacting substrate [Co(PCP^{Me}-*i*Pr)(η^2-BH$_4$)] and NaNO$_2$. The cobalt borohydride complex [Co(PCP^{Me}-*i*Pr)(η^2-BH$_4$)] is readily reacted with CO and *t*BuNC to produce the Co(I) complexes [Co(PCP^{Me}-*i*Pr)(CO)$_2$] and [Co(PCP^{Me}-*i*Pr)(CN*t*Bu)$_2$], respectively. In **Chapter 4**, we described the synthesis and reactivity of the first Co(I) pincer complex [Co($\eta^3 P,CH,P$-P(CH)P^{Me}-*i*Pr)(CO)$_2$]$^+$ featuring an agostic η^2-C$_{aryl}$-H bond. This complex was obtained via protonation of the Co(I) complex [Co(PCP^{Me}-*i*Pr)(CO)$_2$]. In contrast to related Rh(I) agostic pincer complexes, this complex is five coordinate and adopts a trigonal bipyramidal geometry. Since the CO ligands are not sufficiently electron rich to promote an oxidative addition of the C-H bond, a Co(III) hydride complex is not formed. A Co(III) hydride complex [Co(PCP^{Me}-*i*Pr)(CN*t*Bu)$_2$(H)]$^+$ was obtained upon protonation of the more electron rich Co(I) complex [Co(PCP^{Me}-*i*Pr)(CN*t*Bu)$_2$]. Three ways to cleave the agostic C-H arene bond are presented. First, the agostic proton in [Co($\eta^3 P,CH,P$-P(CH)P^{Me}-*i*Pr)(CO)$_2$]$^+$ is acidic and pyridine deprotonates the C-H bond to reform the starting material. Another way to cleave the agostic C-H bond is hydrogen abstraction upon exposure of [Co($\eta^3 P,CH,P$-P(CH)P^{Me}-*i*Pr)(CO)$_2$]$^+$ to oxygen) or TEMPO which results in the formation of the paramagnetic Co(II) PCP complex [Co(PCP^{Me}-*i*Pr)(CO)$_2$]$^+$. This process involves oxidation of the metal center from Co(I) to Co(II). Finally, replacement of one CO ligand in [Co($\eta^3 P,CH,P$-P(CH)P^{Me}-*i*Pr)(CO)$_2$]$^+$ by CN*t*Bu promotes the oxidative addition of the agostic C-H arene bond. This yields two isomeric hydride complexes of the type [Co(PCP^{Me}-*i*Pr)(CN*t*Bu)(CO)(H)]$^+$. DFT calculations support the existence of the agostic bond in complex [Co($\eta^3 P,CH,P$-P(CH)P^{Me}-*i*Pr)(CO)$_2$]$^+$ and corroborate the differences observed between the Co and the Rh species. In **Chapter 5**, We have synthesized two diamagnetic 16e molybdenum PCP pincer complexes of the types [Mo(PCP^{Me}-*i*Pr)(Br)(O)], and [Mo(PCP^{Me}-*i*Pr)(Br)(CO)$_2$] from the precursors [Mo(Br)$_3$(THF)$_3$] and

[Mo(Br)$_2$(CO)$_4$]$_2$, respectively. The first one is a mono oxo Mo(IV) complex involving presumably dioxygen activation.
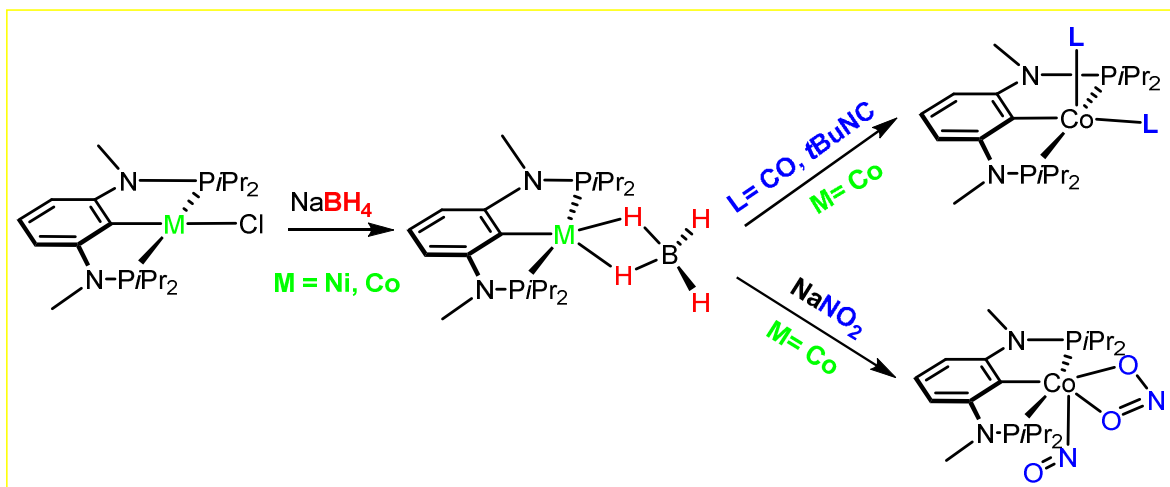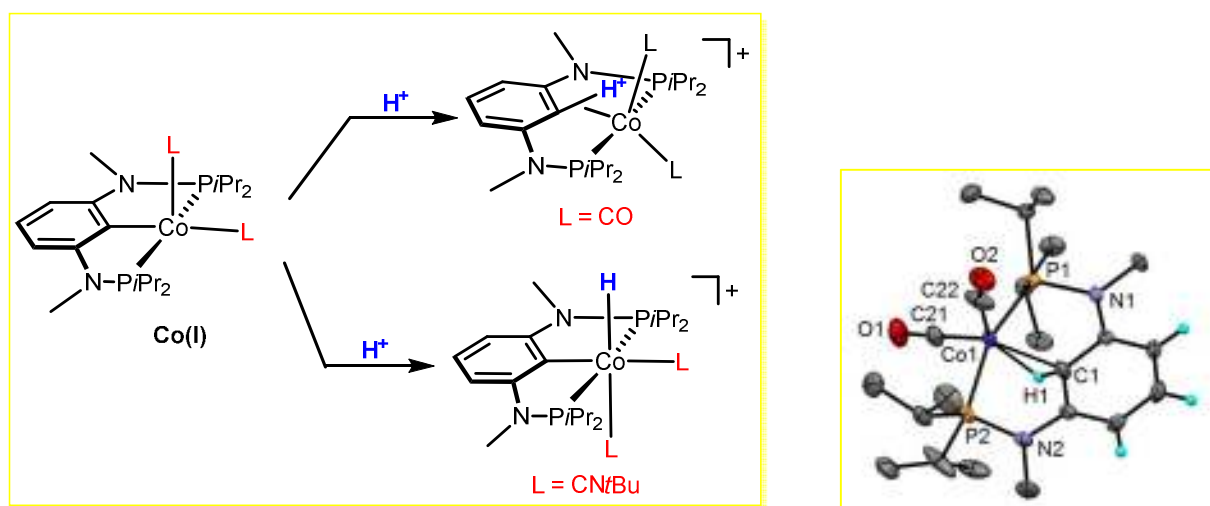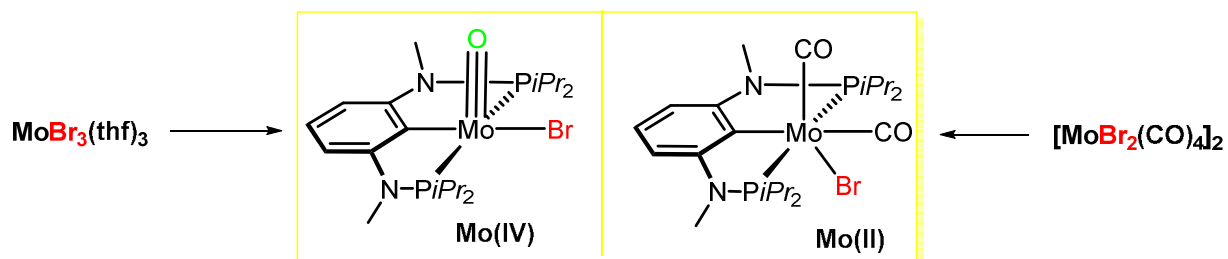
Graphical abstract
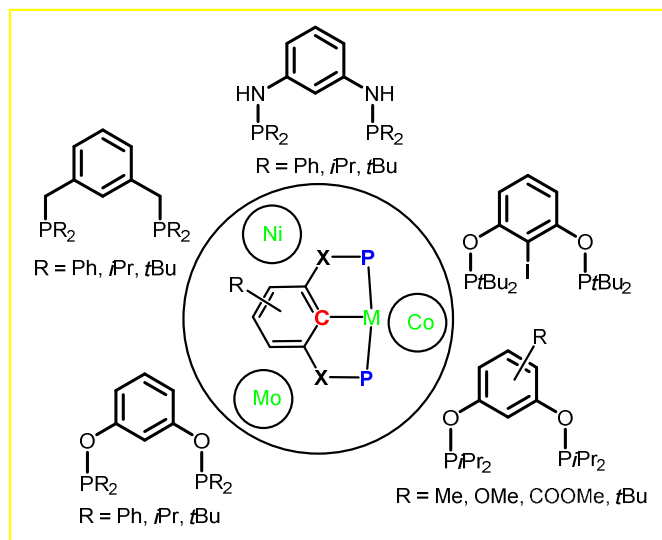
Chapter 1
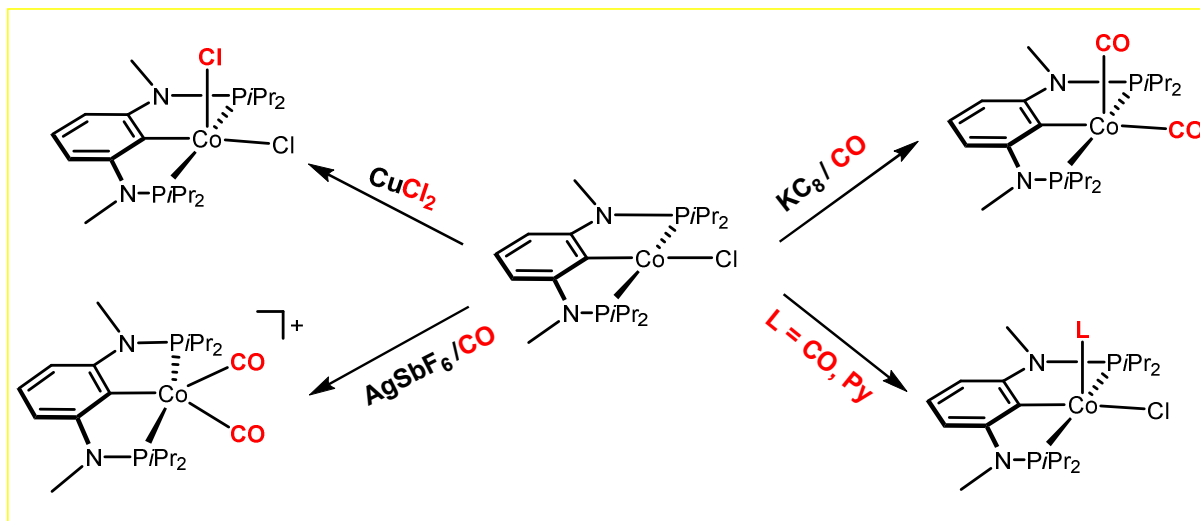
Chapter 2

Chapter 3

Chapter 4

Chapter 5

Acknowledgements

In three year enjoyable life in Vienna, It is just happened in short days that I now look back, I realize that those days are unforgettable forever. Most of the people have been involved in my personal life and scientific developments as well, without these people I would not have been made doctoral thesis.

First of all, I am very grateful to my promoter prof. Karl Kirchner, Dear **Karl**, thank you for your great motivation, guidance, teaching etc. throughout last three year period. You are very great keeping me motivated in doing experiments, played key role in me to learn scientific skills. Your passion, vision, enthusiasm to research and teaching were tremendously inspiring to me. I highly appreciate all your advice, guidance, and patience especially during my first year in pick up this field of research. Also, I enjoyed the generous financial support for attending the international conference. I was privileged to be part of your group and thank you so much for all your continuous support on my research career.

Berthold Stöger, you joined in my whole research period for measuring and solving the crystal structure analysis. I am happy with your quick appointment for the crystal measurement, and your output results were very curious in me to do further movement of research. I am very thankful to you for your involvement in my project. I would also thankful to **Matthias Weil** for measuring some crystals. **Ernst**, you have been very helpful in providing us the lab for measuring required ESI-MS samples. Dear **Kurt**, I am great thankful to you for your advice that how to organize the duration of completing this thesis at the end.

I was very lucky to have nice colleagues such **Özgür, Bernhard, Christian, Mathias, Matthias, Sara, Nikolaus,** and **Afrooz**. You all gave pleasant time in lab, group meetings etc. **Özgür**, you were very helpful to me for preparation of literature known ligands, and I learned some basic techniques in crystal growth. **Christian**, your deep knowledge in NMR software skills were handy in fulfilling my needs. **Glatz**, you are very cool, kind, patient, and close to me in all the way to show place of where the apparatus located in the lab, and also helping me out whenever I faced some problem with basic computer related issues. I enjoyed a lot whenever **Matthias**, and **Mathias** made typical Austrian food. **Matthias** and **Mathias** are very hospitality whenever made food and serving to our people in during the party. We enjoyed a lot whenever we go out for the party it was cheerful time, and had lot of fun in party in our social room, and also during the summer had bbq in terrace. We also enjoyed in our institute one-day trip with lot of fun, and it's unforgettable forever. **Sara**, you are very talkative person among the group people, you people **Sara**, **Dany**, **Christian**, **Afrooz** and **Karl** gave great accompany throughout the Japan international conference days. **Danny**, you have been very helpful in getting all the lab stuffs whenever I come to you and also useful discussions too. I also enjoyed talking with you guys **Mathias**, **Matthias**, **Bernhard**, **Sara**, **Ester**, **Roland**, **Danny**, **Christian** and **Marko** when we get together for drinking coffee or lunch in our social room. I would also remember our sincere bachelor students **Wolfgang**, **Gerald**, **Clara**, **Buket**, **Lukas**, and **Alex** who have been done good work for successful synthesis of ligand precursor. Mr. **Dazinger** and Mr. **Untersteiner**, both of you solved many times computer based on technical problems, software installations etc.

List of Publications

Sathiyamoorthy Murugesan, Fan Jiang, Mathieu Achard, Christian Bruneau and Sylvie Dérien, *Chem. Commun.,* **2012,** *48,* 6589.
'Regio- and Stereoselective Syntheses of Piperidine Derivatives via Ruthenium-Catalyzed Coupling of Propargylic Amides and Allylic Alcohols.'

Sathiyamoorthy Murugesan, Berthold Stöger, Maria Deus Carvalho, Liliana P. Ferreira, Ernst Pittenauer, Gunter Allmaier, Luis F. Veiros, and Karl Kirchner, *Organometallics,* **2014**, *33,* 6132. (Chapter 2 of this thesis).
'Synthesis and Reactivity of Four- and Five-Coordinate Low-Spin Cobalt(II) PCP Pincer Complexes and Some Nickel(II) Analogues.'

Sathiyamoorthy Murugesan, Berthold Stöger, Matthias Weil, Luis F. Veiros, and Karl, *Organometallics,* **2015,** *34,* 1364. (Chapter 3 of this thesis).
'Synthesis, Structure, and Reactivity of Co(II) and Ni(II) PCP Pincer Borohydride complexes.'

Sathiyamoorthy Murugesan, and Karl Kirchner, *Dalton Trans.,* **2016**, *45,* 416.
'Non-Precious Metal Complexes with an Anionic PCP Architecture.'

Sathiyamoorthy Murugesan, Berthold Stöger, Ernst Pittenauer, Günter Allmaier, Luis F. Veiros and Karl Kirchner, ***Angew. Chem. Int. Ed.*** **2016**., just accepted. (Chapter 4 of this thesis).
'A Co(I) Pincer Complex with an η^2-C-H Agostic Arene Bond - Facile C-H Bond Cleavage *via* Deprotonation, Radical Abstraction, and Oxidative Addition.'

Sathiyamoorthy Murugesan, Berthold Stöger, Luis F. Veiros and Karl Kirchner, *to be submitted* (Chapter 5 of this thesis).
'Synthesis of novel Mo(II) and Mo(IV) PCP pincer complexes.'

Curriculum Vitae

Sathiyamoorthy Murugesan was born on 17 March 1988 in Kadukkathurai Tiruchirappalli in Tamilnadu, India. After higher Secondary School Education in Thiruvasi, he started B.Sc. Chemistry in 2005 at St. Joseph's College (affiliated to Bharathidasan University), Tiruchirappalli. In 2008, he started M.Sc. in St. Joseph's College, Tiruchirappalli. In 2009, he did two-months internship at Bhaba Atomic Research Centre (BARC) with an Indian Academy of Sciences fellowship. In 2010, he additionally did master's program in Catalysis, Molecules, and Green Chemistry' at the University of Rennes 1, France. His master thesis was titled 'Regio- and Stereoselective Syntheses of Piperidine Derivatives via Ruthenium-Catalyzed Coupling of Propargylic Amides and Allylic Alcohols' and was supervised by both of dr. Sylvie Dérien, dr. Mathieu Achard in the group of prof. Christian Bruneau and prof. Pierre H. Dixneuf. In 2012, he was worked as project assistant with prof. Sambasivarao Kotha in Indian Institute of Technology, Bombay, India, and the project was titled 'Synthesis of modified furan peptides and oxabicyclo compounds by a diels– alder reaction as Key Steps.'

In 2013, he started his PhD studies at Technical University of Vienna, funded by Austrian Science Fund (FWF), under the supervision of prof. Karl Kirchner. His PhD works are described in this thesis, and was also presented in International Conference on Organometallic Chemistry (ICOMC 2014, Sapporo, Japan).